Fall 2010

Developing new probes of functionally relevant dynamics in NAD-dependent enzymes

Samrat Dutta
University of Iowa

DEVELOPING NEW PROBES OF FUNCTIONALLY RELEVANT DYNAMICS IN NAD-DEPENDENT ENZYMES

by

Samrat Dutta

An Abstract

Of a thesis submitted in partial fulfillment
of the requirements for the Doctor of
Philosophy degree in Chemistry
in the Graduate College of
The University of Iowa

December 2010

Thesis Supervisor: Assistant Professor Christopher M. Cheatum

ABSTRACT

Femtosecond to picosecond dynamics of enzyme active sites is relatively unknown. With the advent of two-dimension infrared spectroscopy, it is now possible to characterize thermally activated motions at this time scale in functionally relevant enzyme complexes. We present a series of measurements on complexes of formate dehydrogenase (FDH) using transitional-state analog inhibitor azide as a reporter. Our results show that for ternary complexes with NAD^+ and NADH, the frequency-frequency correlation function (FFCF) decays completely. This indicates that the active site at the transitional state is rigid and the azide completely samples the high frequency fluctuations within a couple of picoseconds. In contrast, the FFCF of binary complexes show significant static component to the overall decay. Such functionally relevant dynamics observed in FDH is difficult to investigate in other enzymatic system due to the lack of suitable probes. We have synthesized two new mid-IR active analogs of NAD^+ , azido-NAD^+ and picolyl azido adenine dinucleotide (PAAD), each of which have the potential to be a general probe for enzyme dynamics. These new probes were fully characterized as potential candidates for probing the active sites of NAD-dependent enzymes. As with FDH-azide complex, PAAD bound to FDH shows a significant static component. Our result with ternary complex of FDH with PAAD and azide shows that the active site of this enzyme still represents the transitional state of the system albeit with perturbations and both the reporter completely samples the fluctuations in the active site within 10 ps. This result indicates that the active site is rigid within the

immediate vicinity of the probes and that this rigidity might be a general characteristic of the entire active site at the transitional state.

Abstract Approved: _____
Thesis Supervisor

_____
Title and Department

_____
Date

DEVELOPING NEW PROBES OF FUNCTIONALLY RELEVANT DYNAMICS IN NAD-DEPENDENT ENZYMES

by

Samrat Dutta

A thesis submitted in partial fulfillment
of the requirements for the Doctor of
Philosophy degree in Chemistry
in the Graduate College of
The University of Iowa

December 2010

Thesis Supervisor: Assistant Professor Christopher Cheatum

Graduate College
The University of Iowa
Iowa City, Iowa

CERTIFICATE OF APPROVAL

PH.D. THESIS

This is to certify that the Ph.D. thesis of

Samrat Dutta

has been approved by the Examining Committee
for the thesis requirement for the Doctor of Philosophy
degree in Chemistry at the December 2010 graduation.

Thesis Committee: _____
Christopher Cheatum, Thesis Supervisor

_____
Amnon Kohen

_____
Alexei V. Tivanski

_____
Jon C.D. Houtmann

_____
Daniel M.Quinn

To my late father Dilip Dutta

Thou hast power only to act not over the result thereof. Act thou therefore without prospect of the result and without succumbing to inaction.

Karmani ave adhikars te,ma phalesu kadachana, ma karmaphal hetur bhoo, ma sangostu akramani

Bhagavat Gita

ACKNOWLEDGMENTS

This is one of the few occasions in life, where you can pen down your philosophy and expect someone to read it. Getting a degree in philosophy was not my intention; nonetheless I have an atavistic sense of glee in the kill. I believe that whatever you do you should do with a sense of pride and happiness and this event encompasses both.

I take this occasion to thank my advisor, Professor Chris Cheatum for giving me a happy, eventful and productive graduate career. Chris is a well read man, a good orator, an excellent writer, mathematician, a physicist to the core and above all a good human being. I warn you though that there is no short answer to a question that you can ask to him. He has either a 45-minute version or a 2-hour version. Nonetheless, it has been a pleasure to work with him and I promise that I will keep up his good work.

I am indebt to Professor Kohen for being sensitive and caring surrogate advisor. I would not be standing here if he did not let me use his laboratory and guided me in most difficult of times. I admit that sometimes I have no clue what he is talking about but I can assured myself that it was all for my benefit. I thank him sincerely for being such a wonderful mentor.

This is also an opportunity for me to thank Professor Jon Houtman for advising me and having the confidence of granting me full access to his laboratory. It was really pleasant to work for him. I also thank Professor Daniel Quinn and Professor Alexei Tivanski for being enthusiastic to evaluate my research.

A man is a bare tree without friends. So, yes I have huge motley of friends without whom I would be really not be what I am today. I acknowledge and thank, ‘my ole Seville Gang’, Salil , Mads, Dis, Sandeep,

Linda, Sushmita, Sunny, Viabhavi, ankur, Sriram , Ganesh and floaters (apologies), with whom I really spent most cherished times on my graduate life, the 'Chicago Gang'; Prags, Hari, Vivek, Sriram and Sangs , who took the every opportunity to explore downtown Chicago, my own 'Chemistry ole School Gang' ; Adil, Ram, Dis, Rashmi, Poonam, Mayuri, Harsha, Gopee, Sai and Jigar, whom I consider a part of my family and last but not the least, the wonderful collage of people I met in recent years, Pradeep, Puja, Yogesh, Suman , Abvinab, Lokesh (Nivedita Akshit), Ami, Sheru, Asish, Nisarg and others (apologise) (I am old and losing memory), who made me feel what a wonderful life to live with friends. I thank for you all for believing in me and giving me their unwavering support in my time of need.

I would like to acknowledge my colleagues, who are just wonderful people and created for me such a nice work environment. Jigar, who is a great friend, an erudite person and level headed gentleman. Kenan, the cheerful fat Turk, who was always there to share his experience and knowledge, in the most pleasant way. Mike, who is a friend, well wisher and a man with absolute impeccable work ethics. Willam ("rocks"),who apart from being scientifically sound, taught me to appreciate music and mix music with science. Thank you, all for being my friend and colleague. I would also thank the newbies, Jameson, Gail, Dom, Joe and Post Doc (Yan liang) for making me enjoy their company.

I would thank my mother, Malati Dutta for being such a wonderful person. Supporting me 20000 miles away, with long uncertain visits is not a task for the weak hearted. I thank you for teaching me everything I am today. I also dedicate this work to my departed father, who would have been delighted to see me achieve this goal. My dear Sister, who is just enchanted by Ph.D, I thank you for being always on my side.

Finally, my wife Mary, whom I would not insult by penning down words of praise. Thank you, for being my better part and I know now why wife is called the “better” part.

ABSTRACT

Femtosecond to picosecond dynamics of enzyme active sites is relatively unknown. With the advent of two-dimension infrared spectroscopy, it is now possible to characterize thermally activated motions at this time scale in functionally relevant enzyme complexes. We present a series of measurements on complexes of formate dehydrogenase (FDH) using transitional-state analog inhibitor azide as a reporter. Our results show that for ternary complexes with NAD^+ and NADH, the frequency-frequency correlation function (FFCF) decays completely. This indicates that the active site at the transitional state is rigid and the azide completely samples the high frequency fluctuations within a couple of picoseconds. In contrast, the FFCF of binary complexes show a significant static component to the overall decay. Such functionally relevant dynamics observed in FDH is difficult to investigate in other enzymatic system due to the lack of suitable probes. We have synthesized two new mid-IR active analogs of NAD^+ , azido-NAD^+ and picolyl azido adenine dinucleotide (PAAD), each of which have the potential to be a general probe for enzyme dynamics. These new probes were fully characterized as potential candidates for probing the active sites of NAD-dependent enzymes. As with FDH-azide complex, PAAD bound to FDH shows a significant static component. Our result with ternary complex of FDH with PAAD and azide shows that the active site of this enzyme still represents the transitional state of the system albeit with perturbations and both the reporter completely samples the fluctuations in the active site within 10 ps. This result indicates that the active site is rigid within the immediate vicinity of the probes and that this rigidity might be a general characteristic of the entire active site at the transitional state.

TABLE OF CONTENT

LIST OF TABLES

Table

LIST OF FIGURES

Figures

LIST OF EQUATIONS

Equations

CHAPTER 1

INTRODUCTION

1.1 Scope of research

Enzymes are biocatalyst that plays a very crucial role in many life processes. It is well known that enzymes, which are essentially proteins, can accelerate reactions by as many orders of magnitude. The factors, that enable enzymes to provide the large enhancement of reaction rates, exquisite substrate specificity and selectivity; however, still remain a matter of discussion. The quest for gaining molecular insight into the origins of the catalytic power possessed by the enzymes has been a topic of intense exploration for a long time.[1-8] In spite of progress both theoretically and experimental techniques, we still lack a complete description of enzyme catalysis.

Over the years many theories have been proposed to explain enzyme catalysis. In past, enzymes were viewed as static entities and their function has been explained on the basis of direct structural interactions between the enzyme and the substrate. Earlier hypothesis, which include "lock and key" model and "induced fit",[9, 10] suggests that the enzyme is designed to bind the substrate, which results in its activation and formation of a reactive conformation. Such veiws are contested as it fails to explain coopetartive and allosteric effects as well as the large rate enhancement in enzymes. In recent years an integrated view of protein structure, dynamics and function is emerging, where proteins internal motions are closely related to its function.

A number of features of the enzymes are now well accepted. In enzyme, the catalyzed process involves covalent bond breaking and bond making (chemical step),which is also accompanied by processes such as substrate

binding, protein rearrangement and product release, many of which can be rate determining. It is also known that the chemical step, which in most process is rate limiting, might not be necessarily rate limiting in enzymatic catalysis. The catalytic pathway can be seen a complicated energy landscape with multiple global minimum. The multistep process, involved in catalysis, results in a decrease in the free energy of activation[11] and stabilization of the transition state for the chemical step by proper orientation of the active site residues. This results in specific interactions between the enzyme and the substrate, i.e., general acid/base, electrostatic, steric, hydrogen bonding or preferential solvation effects and can influence the rate enhancement. Although the earlier notion of enzyme catalysis largely based on the static structure, it is logical that any structural change in the enzyme can modify its interaction with substrate and affect the catalytic efficiency of the enzyme. Hence apart from these facts an essential requirement for the enzymes is to have conformational flexibility.

The conformational flexibility is essential for enzyme to accommodate events like substrate binding, product formation and subsequent release[12]. These enzyme motions can span over time scales over many magnitude. Enzyme motions include bond vibrations on the femtosecond (fs) timescale, rotations of the side chains, hinge bending, loop movements on picosecond (ps) to nanosecond (ns) timescale, and secondary structural or specific domain movements that happen on microsecond (μs) to millisecond (ms) timescale. As there is varying time scales, not all enzyme motions are accessible by a single technique. Techniques like nuclear magnetic resonance (NMR) can explore the dynamics of proteins upto microsecond time resolution. However, motions on the timescales of femtosecond to picosecond are relatively unexplored.

There is gathering evidence that motion at these time scales is relevant to understand the nature of enzymes.

Investigation of many enzyme systems, which are involved in hydride transfer reactions, points to the importance of fast dynamics. For hydride-transfer reaction involving these enzymes, there is evidence of hydrogen tunneling,[13] from anomalous primary kinetic isotope effect (K.I.E) that exceeds the semiclassical limit.[3, 14, 15] Apart for this, many of these enzymes, show temperature independent KIE and have a significant energy of activation. These results cannot be explained by simple correction to transitional state theory (TST) and a more suitable "Marcus-like" model[16, 17] with environmental motions has to be invoked explain these observations. These types of environmental motions can modulate the tunneling barrier, typically by modulating the driving force of the reaction, the reorganization energy and the degeneracy of the reactant and product energy levels. Terms that describe such motions include ""vibrationally enhanced ground-state quantum tunneling", "rate promoting tunneling" and "environmentally tunneled coupling".

The importance of fast motions at the active site is also evident from several computational studies. Theoretical studies show that protein promoted vibration can modulate the height and width of the activation barrier and hence influence the rate of the reaction.[18-20] These theoretical investigations are based on transitional state theory and generalization of free energy profile as a function of suitable reaction coordinates, which includes Marcus like model. In the TST model, protein dynamics can influence the reaction rate in two possible way; by altering the height of the activation barrier or by altering the active site conditions such that more reactive trajectories are converted to product successfully.[21, 22] In other

studies with enzymes like Cyclophilin A, DHFR and lactate dehydrogenase, it has been shown that network of protein vibrations has a promoting effect on activity and is therefore a factor contributing to rate enhancement. It is suggested that certain protein vibrational modes alter the reaction by changing the active site environment such that more reaction trajectories can cross the product side.

Although there are indirect experimental evidences and computational methods to indicate the importance of fast enzyme motions, there was until recently no direct experimental means to probe the dynamics of the active site of enzymes. However with the advent of non-linear techniques like 2D-IR, it is now possible to investigate the dynamical landscape of the enzyme[23, 24] active site. We choose to investigate these motions with chromophore bound to the active site using heterodyned 2D-IR technique. These chromophores both natural and synthesized allow us to investigate the enzyme active site in a timescales ranging from hundreds of femtosecond to couple of picoseconds. The synthesized chromophores sets up ground for future works, where site specific mutations, temperature dependence and substrate dependent dynamics can be tested across a wide gamut of enzyme.

1.2 Thesis Overveiw

Our aim is to characterize the fast time scale motions at the active site of the enzyme and to investigate their functional relevance to kinetics. Initially we perform 2D-IR on the ternary complex of formate dehydrogenase from *Candida Bodinii* with cofactor NAD^+ and azide. This complex, which represents the transitional state reveals the dynamics as probe by azide at the active site of the enzyme and sheds light on the structural distribution and the timescale for its sampling. We also measure the dynamics for ternary complex of the enzyme with reduced form of the cofactor NADH and azide,

and for the binary complex of the enzyme with azide. These measurements demonstrate the difference in the active-site dynamics when the system is far away from the transition state and when it is near the transition state. The work supports the hypothesis put forth by Marcus-like model, which suggests that enzymes are evolved to optimize the conformation of the transition state for tunneling and lays ground for can be more rigorously testing the hypothesis. This led us to synthesis two new NAD-dependent analogs, azido-NAD^+ and picolyl azide nicotinamide adenine dinucleotide (PAAD), to characterize the dynamics of the active site. The characteristics of these two probes are extensively studied as viable general probes for enzyme dynamics. The dynamics of PAAD bound to formate dehydrogenase is studied and compared to our previous studies. The active site dynamics reported by PAAD shows that rigidity of active site at transitional state is not a local to azide but extends around the immediate vicinity of the active site. These studies open the door for using PAAD and similar analogs as infrared markers to study the enzyme active site.

CHAPTER 2

MATERIALS AND METHODS

2.1 Background on Materials

The starting materials 3-amino pyridine, sodium nirite, sodium formate, picolyl chloride, glucose, sodium azide, sodium hydroxide, phenylmethanesulphonylfluoride (PMSF), glucose, trypsin, glucono-δ-lactone, malic acid, NADase and NAD^+ are obtained from Aldrich and used as received. All solvents namely chloroform, methelene chloride, ethyl acetate, acetone, methanol , hexane, 2-propanol and ethanol are obtained from commercial sources and used without further purification. Phosphate salts were procured from Acros Organics. Silica Gel is purchased from Fisher scientific. C-18 silica gel is obtained from Analtech, Newark. Thin layer chromatographic (TLC) plates were obtained from Sorbent Technologies. Centrifuge filter units are procured from Millipore with molecular cut-offs of 10000 Da.

Solvent: Chloroform, methelene chloride, ethyl acetate, acetone, methanol, hexane, 2-propanol and ethanol are common organic solvents used for chromatographic separations and extraction in this research. As these are low boiling point inflammable solvents, they are handled with care. Precautions using these solvents include working in a well ventilated fume hood and wearing solvent resistant gloves. Strong acids, HCl and H_2SO_4, are diluted before use in a fume hood in this work.

3-amino pyridine: This brown solid (molar mass 94.1 g/mol) is soluble in water and is the starting material for our synthesis. It is a common intermediate for agrochemical, pharmaceuticals and colorants. This compound is stable under ordinary conditions.

Sodium Azide: Sodium azide is an ionic solid with molar mass of 65 g/mol. It is soluble in water and alcohol. It is extremely toxic and prone to explosion. This reagent is used to introduce azido functional group in our research

Sodium Nitrite: Sodium nitrite (molar mass 68.9 g/mol) is a food additive and highly soluble in water. All solutions of sodium nitrate in this research are freshly prepared as sodium nitrite has a tendency to slowly oxidize to $NaNO_3$.

Sodium hydroxide: Sodium hydroxide (molar mass 39.9 g/mol) is a strong base and corrosive. It is soluble in water and is hygroscopic. This base is used in this work to maintain pH in buffer solutions.

Phenylmethanesulphonylfluoride (PMSF): It is a serine protease inhibitor with molar mass of 174.1 g/mol. It degrades rapidly in water and as such its solution is prepared in isopropanol or ethanol. It is toxic and targets nerves.

Sodium Formate: Sodium formate (molar mass 68.01) is a white deliquescent powder. It is soluble in water (97 g/100 mL) and have a tendency to form bubbles. It is used as a substrate in our work.

Glucose: It is a monosaccharide and a chief source of energy for the cells. It is highly soluble in water (91g/100 mL) and has a molar mass of 180.16 g/mol. Glucose shows optical activity and rotates the plane polarized light to right (dextro-rotatory). In solution, it can exist both in cyclic and acyclic forms. Like formate, it is primarily used as a substrate in our research.

Malic acid: It is a biologically relevant organic molecule with molar mass 134.09 g/mol with a molecular formula of $C_4H_6O_5$. In our research, we convert it into sodium malate by adding sodium hydroxide.

Trypsin: Trypsin is a digestive enzyme which cleaves peptide chains. It very specific in cleaving peptide chains and do not cleave proline if it is on the carboxylic side of the chain. Its optimum pH range is 7.5-8.5. Trysin powder (1:250) grade is used in this research.

Glucono-δ-lactone: Glucono-δ-lactone is a cyclic ester of gluconic acid and is a common food additive. It water it hydrolyses to gluconic acid. The rate of hydrolysis increases in high pH. All solutions of this compound for this work is prepared fresh, and used within an hour of preparation.

3-Picolyl chloride hydrochloride : It is a solid of molecular weight of 164, with melting point 137-143 ^{o}C. This compound is soluble in water, and forms a solution with reddish tinge. It is a starting material for our work, as it is for many organic synthesis as chlorine can be readily replaced with other functionalities.

Nicotinamide adenine dinucleotide (NAD^+): NAD^+ shown below is a coenzyme

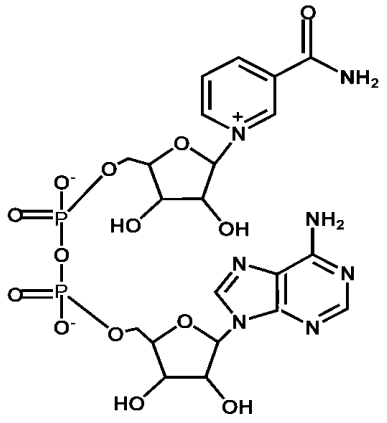

Figure 1 Nicotinamide adenine Dinucleotide (NAD^+)

for a class of enzyme called dehydrogenases and plays a vital role in many metabolic processes. As coenzyme, NAD^+ is involved in many redox reactions. In addition, it is now know that this coenzyme participates in many nonredox reactions. NAD^+ plays a role in DNA repair and replication, chromatin structure and protein biosynthesis. It is also involved in phagocytosis and the

protection of organism by means of generating cytotoxic compounds. Recent studies have shown that apart from being a coenzyme it also contributes to cell signaling. [25-28]

NAD^+ is the first of the broad class of pyridine coenzyme discovered in 1904. It was isolated in laboratory by von Euler and its structure was elucidated by O.Warburg in 1936. The moiety consists of two nucleotide, adenine and nicotinamide, joined by a pair of phosphate groups. [29]

NAD^+ is key energy carrier in numerous metabolic reactions. In metabolic reaction, a hydride ion is transferred to the C4 position of the nicotinamide to form a reducing agent, 1,4-dihydronicotinamide dinucleotide (NADH). This conversion of NAD^+ to NADH is reversible and is one of the most common biological redox reaction. In general, the organic metabolite (SH_2) is stripped of it hydrogen atoms to form reduced NADH.

$$SH_2 + NAD^+ \leftrightarrow NADH + H^+ + S$$

In enzymes-coenzyme complexes, NAD^+ must position close to the substrate so that hydride transfer can occur. As such, the coenzyme makes a part of the active site. NAD^+ in most of the enzymes bind in a characteristic structural unit called the Rossmann fold. The common features of this domain in dehydrogenases consist of four strands of parallel pleated sheet with stand order β-C, β–B, β-A and β-D plus one helix α-B. NAD^+ always binds with the pyrophosphate bridge across the carboxylic edge of the parallel strand between β-A and β-D. The geometry of this backbone moiety (pyrophosphate) is indispensible for the function of the coenzyme. The nicotinamide binds in a cleft in interior of all enzymes. One side of the nicotinamide part of NAD^+ interacts with the binding domain of the enzyme whereas the other side faces the active site. In ternary complexes of enzymes,

there are interactions between the substrate or inhibitor and nicotinamide ring that stabilizes the enzyme.

The ordinary β–anomeric forms of NAD^+ and NADH have characteristic ultraviolet (UV) absorption. The spectra (Figure 2) are dominated by the properties of three chromophores: adenine, nicotinamide and 1,4-dihydronicotinamide. The absorption band of NAD^+ at 260 nm (ε = 17800 M^{-1} cm^{-1}) contains contribution of both adenine and nicotinamide. The NAD^+ spectra have further shortwave absorption at 206 nm and 189 nm as a result of overlapping bands of the two chromophores. On the other hand, the first absorption band of NADH around 340 nm is entirely due to dihydronicotinamide system and the second absorption at around 260 nm contains major contribution of adenine.[29] At shorter wavelengths, NADH shows absorption maxima at 208 nm resulting from additional transitions of

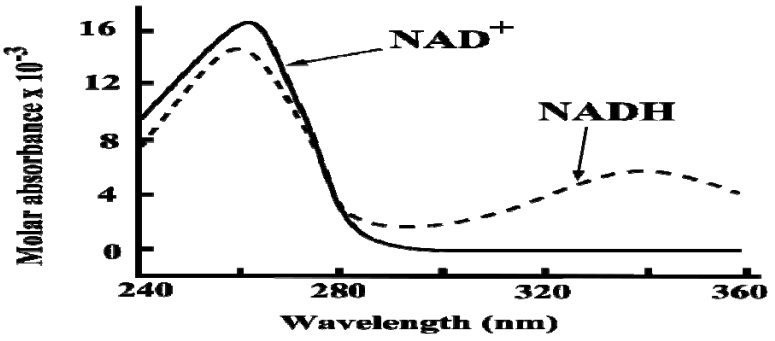

Figure 2 UV absorbance profile of NAD^+ and NADH.

both chromophores.

In our research, NAD is the primary precursor for most of our synthetic scheme, to convert it into an mid-IR active analog. NAD analogs with various

substituent's on the base have been known for the last fifty years.[29-32] NAD^+ is known to form adducts with small molecules under suitable conditions. These molecules such as cyanide ions, hydroxylamine and so on generally covalently bounds to the C-4 atom of nicotinamide with consequent loss of aromaticity and formation of a substituted 1,4- dihydronicotinamide, which displays absorption band above 300 nm. Most substitution on the pyridine ring is known to retain activity of the natural coenzyme if the pyrophosphate is unaltered. Analogs with 3-substituted pyridine of NAD^+ have widely been studied as they represent natural NAD^+ where amide in position 3 is replaced by different functional groups. These functional groups include nicotinic acid, 3-cyanopyridine, 3-acylpyridine, 3-hydroxymethyl pyridine and 3-pyridlacetone analogs. Such substituted analogs are used to understand structure function relationship and as affinity ligands.[29] Non carbon substituents, 3-amino pyridine and pyridine analogs have also been reported. 3-amino pyridine analog is a versatile analog and acts as a competitive inhibitory to a wide variety of pyridine nucleotide dependent enzymes. A number of heterocyclics in position 3 of pyridinium ring have also been reported.[29] As substitution in position 3 of pyridinium ring in NAD^+ yields analogs which are active, we devised strategies to replace amide in position 3 with mid-IR chromophores. A general method of preparing analogs mentioned above is by using NADase (glycohydrolase) from various species by base exchange reaction. This technique is used in this research.

NADase : The term NADase refers to enzymes that hydrolyzes the nicotinamide-ribose bond of NAD^+ and $NADP^+$. There are several NADase extracted from animal tissue which are sensitive to nicotinamide concentration except for *Neurospora crassa*. The NADase (EC 3.2.2.5) from pig brain has been used to prepare a number of analogs of NAD^+. The

material can be solubilized with trypsin and has a molecular weight of 26000. This NADase is catalyst for preparing many analogs as it is insensitive to most bases.

2.2 Preparative method for azido-NAD^+

2.2.1 Synthesis of 3-azidopyridine

Azidopyridine is synthesized as described by Sawanishi[33] *et al.* We start out by taking 30 mL of water in a round bottom flask (250 mL). To this 5-6 mL of concentrated HCL, is added and allowed to cool ($\leq 5^{\circ}C$) in an ice bath for at least half an hour. In this solution, 3-amino pyridine (8g, 0.08 mols) is added with constant stirring at $\leq 5^{\circ}C$ for 10-15 min. A solution of sodium nitrate (10g, 0.15 mols) is prepared in water in a separate beaker and allowed to cool for 10 min in an ice bath. This solution is added drop wise to the acidic 3-aminopyridine solution. The reaction of 3-aminopyridine with nitrate is vigorous. So, the next drop is added after the evanescence of the preceding drop subsides. A solution of sodium azide (13g, 0.15 mols) is prepared analogous to the method of preparation of sodium nitrite. As with the previous addition, each drop of sodium azide reacted violently with the mixture (Caution; Sodium azide is explosive). Hence, the mixture is often gently shaken apart from constant stirring. This reaction is allowed to react for 10-15 minutes, whereby it changes to a dark reddish-brown solution. The solution is removed from the ice bath and the mixture is reacted for another 30 minutes at room temperature. It is then quenched with Na_2CO_3 till alkaline, which is checked by pH test paper. The oily liquid is filtered and extracted with CH_2Cl_2 (3 x 200 mL).The extract is filtered and washed with water. The mixture is tested by TLC with various organic solvent mixtures. The results indicate that the best separation with of the product can be achieved with 1 : 1 CH_2Cl_2–EtAc solvent mixture. The R_f for the product is

0.78. In this mixture, the product is mobile whereas the starting material is nearly stationary (Rf 0.12). No other side products are observed. The product is rotoevaporated and is purified using Silica-Gel chromatography with CH_2Cl_2–EtAc (1:1). Each fraction collected in test tube is tested on TLC plates with CH_2Cl_2–EtAc. The correct fractions showing only the product peak is collected and rotovaped. The final product is oily yellow liquid with a pungent smell.

Yeild = 5.57g (68.7%, overall yield).

The characterization of this compound is given below

UV spectroscopy : In a silica cuvette , 1 ml of compound 3-azidopyridine is

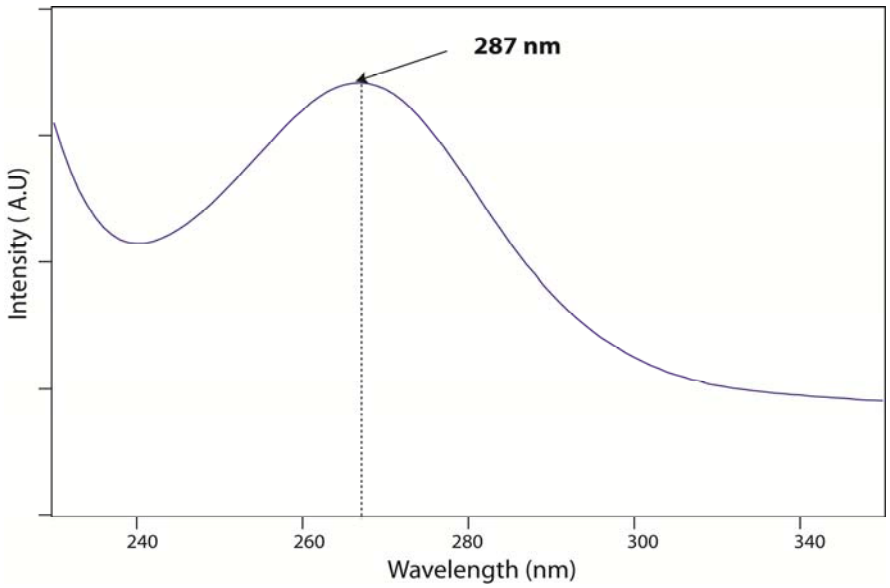

Figure 3 UV profile of 3-azidopyridine

dissolved in buffer was taken and its spectrum was taken on Cary 300 UV-The spectrum (Figure 3) shows a peak position at 287 nm.

^{1}H-NMR: The compound is dissolved in deuterated chloroform and scanned on Bruker Avance 300. 16 scans were acquired for this spectrum. The software Topspin is used to collect, analyze and process the data. The peak shifts position of 3-azido pyridine are : 7.2-7.4 (2H, m), 8.3-8.4 (2H, m). The same solution is used to take C-13 spectra. The carbon peak shifts were found to be at 124.0,125.8,137.0,141.2 and 145.9.

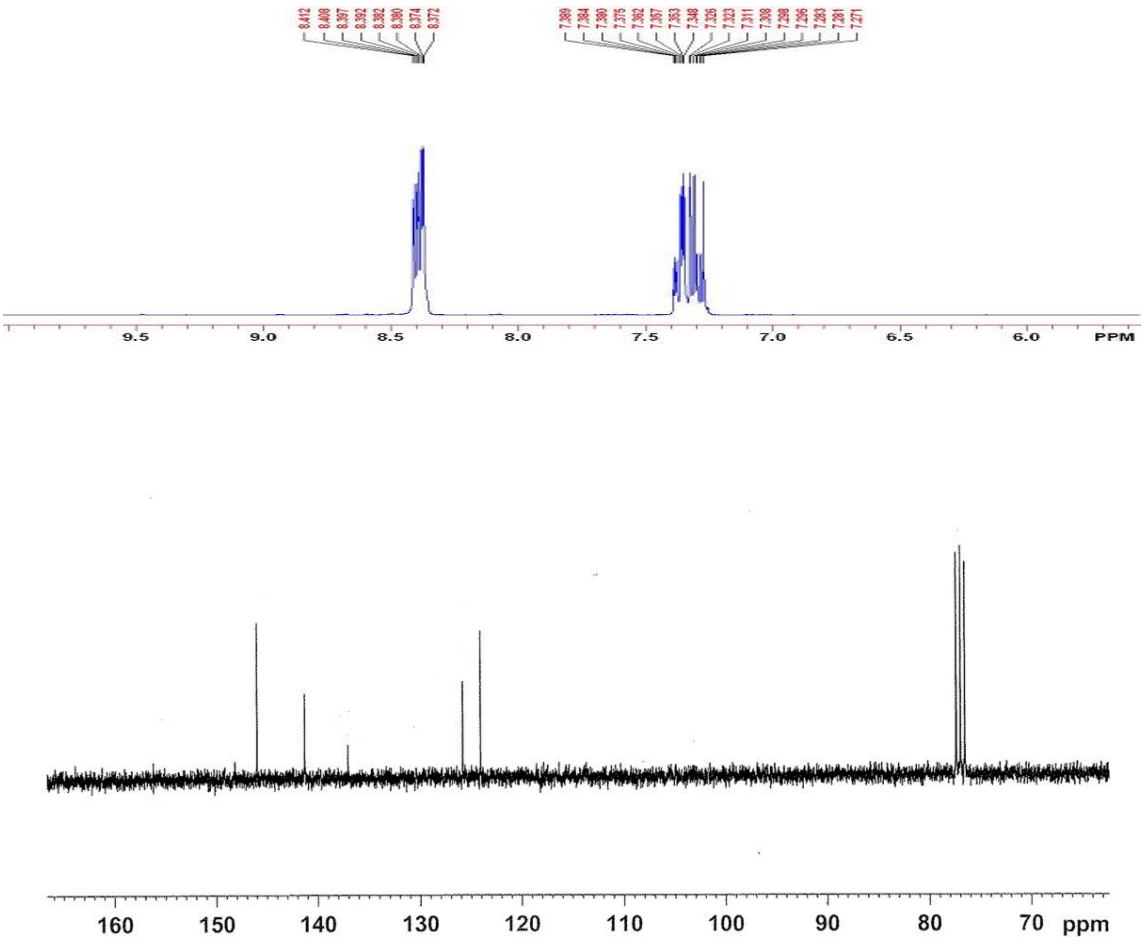

Figure 4 ^{1}H spectrum (top) and ^{13}C spectrum (bottom) of 3-azidopyridine.

IR spectroscopy: The spectrum is taken on a Bruker Tensor 27 equipped with a liquid nitrogen cooled detector. The spectra of 3-azidopyridine is taken with methelene chloride as the solvent. The sample cell used is made of CaF_2 window with a path length of 50 μm. Figure 5, shows the spectra of this compound with peaks at 2135 cm^{-1} and 2095 cm^{-1}. The molar absorbity is found to be 380 M^{-1} cm^{-1}, which is typical of organic azides.

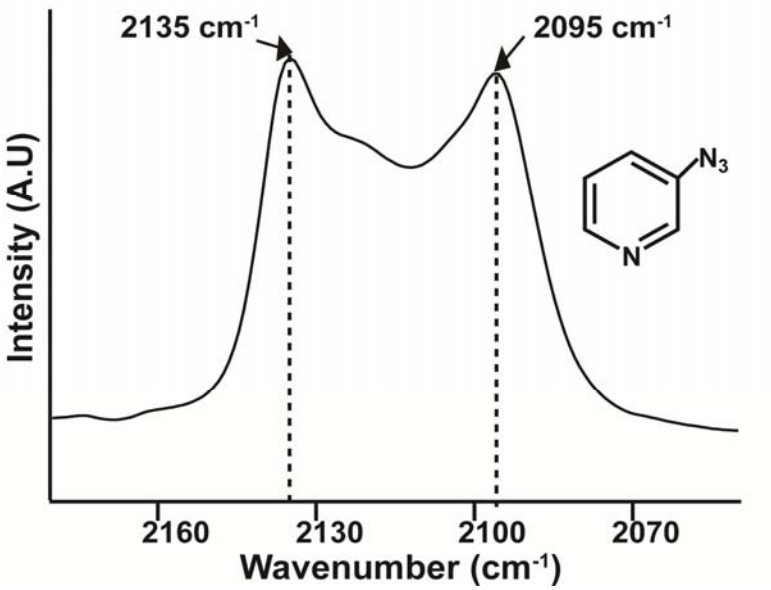

Figure 5 IR of 3-azidopyridine in methelene chloride.

2.2.2 Synthesis of 3-azidoNAD$^+$

We prepared the compound by modifying the synthesis protocols described elsewhere.[34]

1. **Preparation of Phosphate buffer**： 272 mgs of monopotassium phosphate (molar mass 136.08 g/mol) dissolvs in 100 mL water to give a 20 mM acidic solution. A solution of dilute sodium hydroxide added to this mixture to change the pH to 7.5, which is checked with accumet pH meter. All buffer

solutions in this research are prepared by this technique unless otherwise stated with varying concentration of salt.

2. **Assay of NADase:** To test the activity of NADase, 100 mgs of the commercially procured product is first treated with 1.5 ml water. The water is then discarded and the enzyme dissolved in 1.5 mL phosphate buffer. The solution is then stirred for 25 minutes. After 25 minutes, trypsin (0.25 % w/v) is added to digest the protein. The mixture is then incubated for 30 minutes, put in ice and centrifuged.

Solution a： 550 μL of phosphate buffer was added to 100 μL of enzyme solution above along with 100 μL of NAD^+ (15 mM). This reaction is allowed to react for 20 min at 37°C and quenched with 3M trichloroacetic acid.

Solution b： 200 μL of semi carbazide (75 mM) and 200 μL ethanol (12% v/v in phosphate buffer) is diluted with 2200 μL of sodium pyrophosphate buffer (pH 8.8). 0.4 mL of solution 'a' and 2.6 mL of solution 'b' is mixed and stirred for 2 minutes. 10 μL of freshly prepared solution of alcohol dehydrogenase (1mg/mL) is then added to this mixture and allowed to react for 5 minutes. The absorbance at 340 nm is recorded with Cary 300 UV-vis spectrometer. The absorbance recorded is 0.011 OD (optical density).

The blank test without the enzyme showed absorption of 0.048 OD.

$$\text{Unit/ml} = \frac{(A_{blank} - A_{actual}) \times 0.75 \times 3.01}{20 \times 6220 \times 0.1 \times 0.4} \qquad \text{Equation } \mathbf{1}$$

The result shows activity approximately 16 U/mL consistent with reported values elsewhere.[29]

3. **Preparation of NADase solution**： In a scintillation vial, 1g of NADase is suspended in 20 mM phosphate buffer (20 ml) at pH 7.5. The suspension is sonicated in dark maintaining a temperature at $\leq 5^{\circ}$C. After 45 minutes, 5

mg of trypsin is added to the suspension, which is then put in an oven at 37 ° C for further 45 minutes. A 0.1 M solution of serine protease inhibitor PMSF (360 μL) is added to the mixture. Once the addition is complete, the mixture is centrifuged at 20000g for 60 minutes at 5 ° C. The pale red solution obtained is carefully decanted to separate vial. The pH of this solution is found to be in the range from 7.2 to7.5.

4. **Preparation of 3-azidoNAD$^+$:** The reaction scheme is shown in Figure 6. In short, 18 ml of the above solution is taken in a vial and to this 3-azido pyridine (410 mg, 3.41 mols) dissolved in 5 mL of DMF is added in

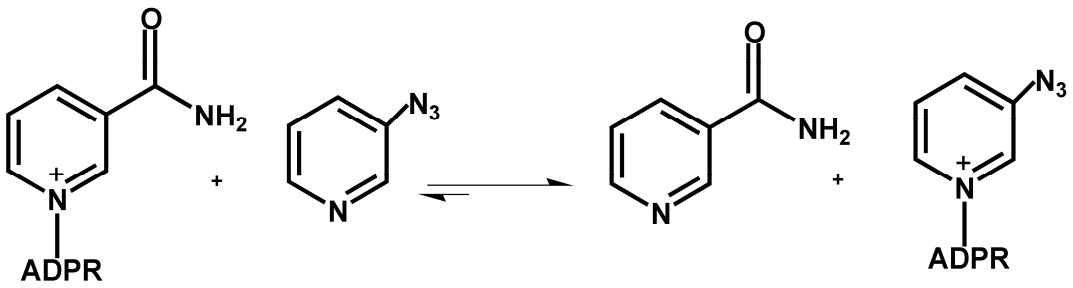

Figure 6 The reaction scheme of formation of azido-NAD$^+$.

dark. The pH is adjusted to pH 7.6. An aqueous solution of NAD$^+$ (150 mg, 0.23 mols) is then added to the mixture. It is important that the NAD$^+$ solution prepared be slightly alkaline or neutral. The addition of NAD$^+$ changed the pH to 7.2 but stabilize after a few minutes. The reaction is allowed to react for 12 hrs in dark at 37 °C. After 12 hours, chloroform (50 mL x 2) was added to the mixture . The turbid solution is centrifuged at 4 ° C , carefully decanted into filter tubes (Amicon, Millipore) and further centrifuged. The filtrate is checked for absorbance at 303 nm and lyophilized. A column packed with C-18 silica is prepared by suspending the gel in

methanol. The gradient is changed by adding water. The lyophilized powder dissolved in minimum water is allowed to be adsorbed in the column. The crude product is then chromatographed with methanol-water as solvent. Fractions with highest λ_{max} at 258 nm and 303 nm were combined, rotary evaporated and lyophilized to obtain the final product. An HPLC run in methanol-water gradient showed one major peak, which is assigned to azido-NAD^+. The product, a fluffy white powder was stored in -20°C in dark.

Yield = 100 mgs (66.8%, overall yield).

The characterization of azido-NAD^+ is given below

Stability and solubility : The azidoNAD^+ is soluble in phosphate buffer and methanol. The stability is determined by observing the change in UV absorption 303 nm. No significant change in optical density is observed for at least for 48 hours at ambient temperature.

Physical characteristic: The compound is usually fluffy white with in some occasions yellow tinge. The compound is highly deliquescent and is kept under dry conditions.

UV spectroscopy : Azido-NAD^+ showed a unique absorption at 303 nm apart from absorption at 260 nm. The spectrum taken on Cary 300 UV-Vis spectrometer is shown in Figure 7. The average ratio between λ_{260} nm to λ_{300} nm is found to be 4.2, after analyzing at least 20 samples. This ratio is later used as a guide to find both the concentration and purity of the compound. As mentioned elsewhere, the molar absorbity at 260 nm is taken to be 18000/M/cm and is used to correctly match the concentration of the solution as it is difficult to accurately weigh the delinquent powder

All spectrum are taken under ambient temperature at pH 7.5 with dilution to prevent the optical density(O.D) to exceed beyond 1 .

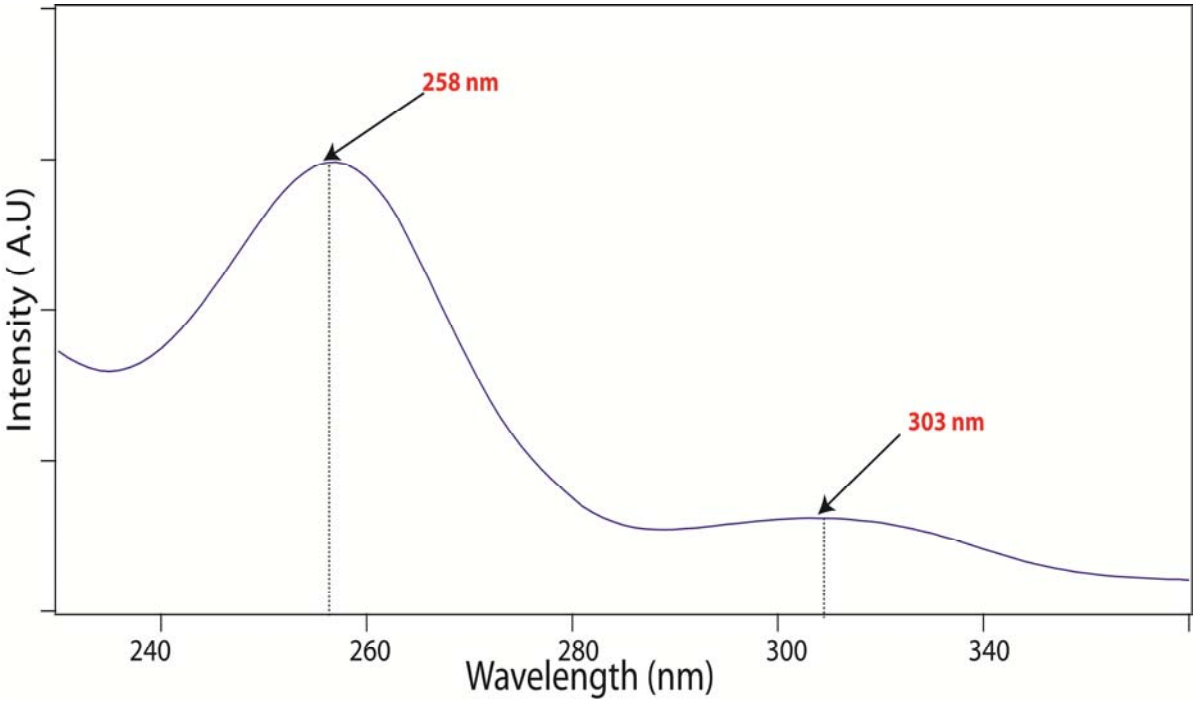

Figure 7 UV spectra of azido-NAD^+

^{1}H-NMR : The compound, azido-NAD^+(~ 1mg) is dissolved in D_2O (0.5 ml) in transferred to a clean NMR tube. The spectrum is taken on a Bruker Avance 300 as described elsewhere. Proper adjustment of shimming is done before acquiring the spectra as salts in the sample tends to make the sample harder to lock. In order to have a high resolution spectrum, an average of 1000 scans is taken for the final spectrum. Figure 8, shows the spectrum of this compound. The spectrum has the following peaks;

H-NMR (d, D_2O) : 4.4-3.9 (10H, m), 5.6 (1H, d), 5.8 (1H, d),7.6-7.7 (1H, m), 7.8 (1H, s), 7.9 (1H, s), 8.2 (1H, s), 8.3 (1H, d), 8.4 (1H, d).

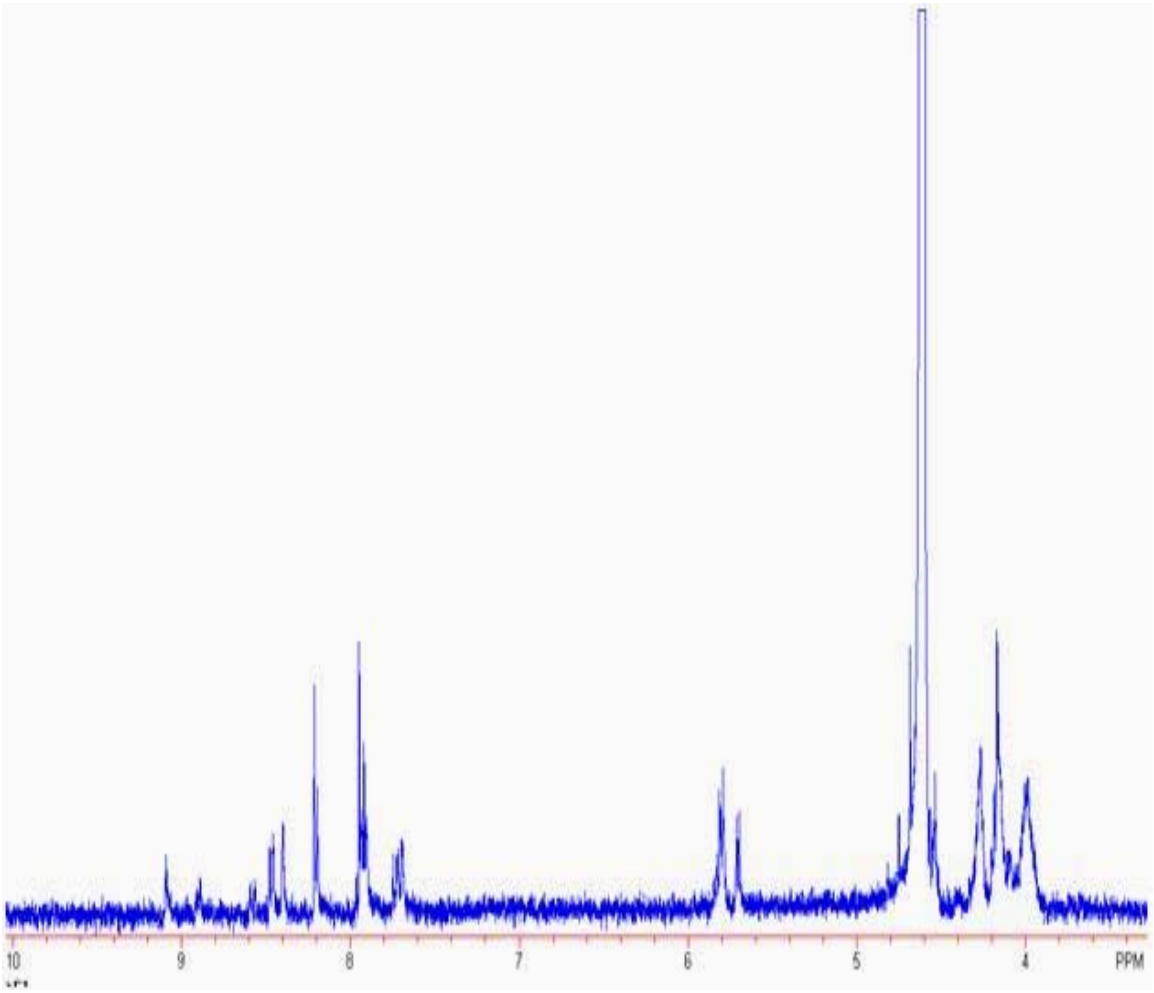

Figure 8 NMR of azido-NAD^+.

Infrared spectroscopy： A measure quantity of azido-NAD^+ is dissolved in phosphate buffer at pH 7.5 and injected to a press-on dismountable sample cell made of CaF_2 windows separated by 25 μm spacer. The spectrum was taken on Bruker Tensor 27 equipped with liquid nitrogen cooled mercury-cadmium-telluride (MCT) detector. The spectrum is background subtracted using phosphate buffer as reference. A peak is observed at 2140 cm^{-1} with full width half maximum (FWHM) of 33 cm^{-1}. The molar absorptivity is found to be between 220 to 250 cm^{-1} mol^{-1}.

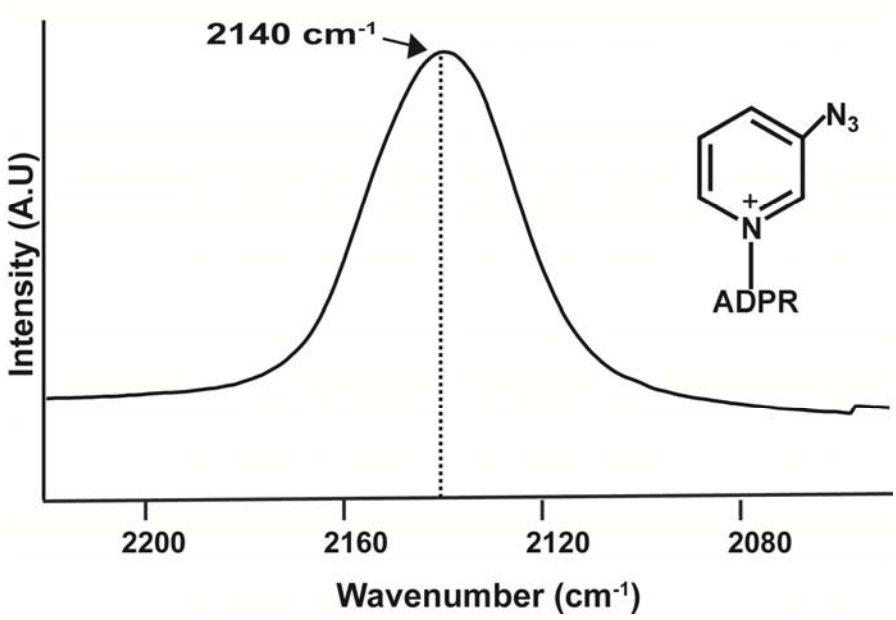

Figure 9 IR profile of azido-NAD^+

This spectrum is in contrast to starting material 3-azopyridine which shows two peaks at 2134 cm^{-1} and 2094 cm^{-1}. The concentration of this solution is checked by UV spectroscopy. Typically, 2-5 μL of the prepared solution is diluted to 1 mL and the absorption at 260 nm is recorded. The concentration is then calculated from Lambert-Beers law using ε_{260nm} = 18000/M/cm.[35] Usually, the recorded absorbance lies within 0-1 OD.

High Performance Liquid Chromatography (HPLC) : In a typical run, 10-30 μL of azido-NAD^+ (~ 1 mg/ml) is injected into an Agilent 1200 series system. The instrument is equipped with a diode array UV-Visible spectrometer for on-line detection. The solvents for the HPLC run are conventionally installed in channel **A** and **B**. In these experiments, solvent **A** is usually phosphate buffer and solvent **B** is a 40:60 mixture of methanol and water. A typical run usually takes 40-60 minutes which, includes equilibration time. The gradient

for the run is given in Table 1, followed by 3-D UV plot of the entire run .The prominent peak is assigned to azido-NAD^+.

Table 1 HPLC method for azido-NAD^+ separation

Time (min)	% A	% B	Flow Rate (ml/min)
0-4.9	100	0	0.8
5-11.9	85	15	0.8
12-19.9	75	25	0.8
20-30	0	100	0.8

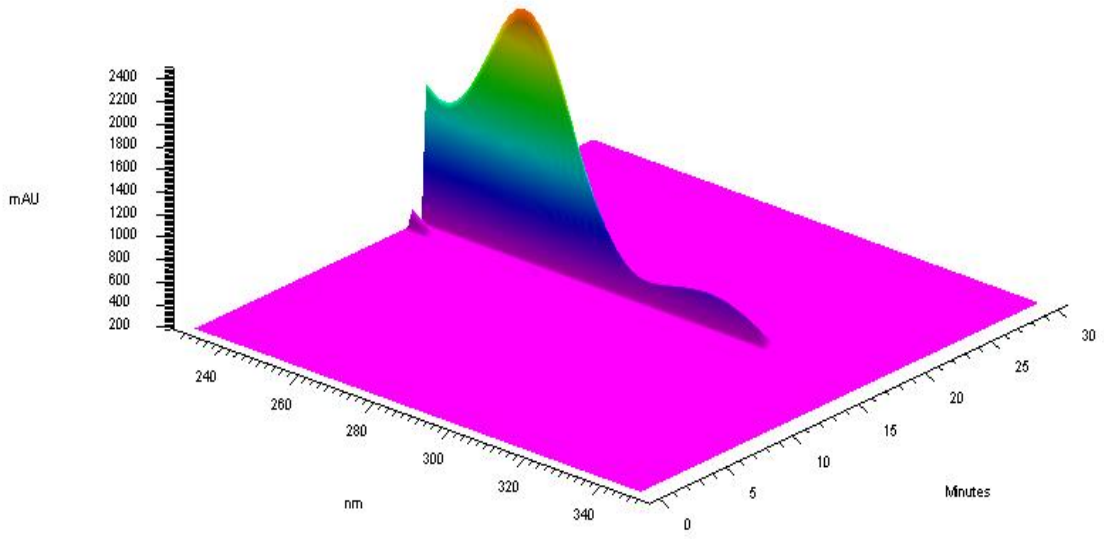

Figure 10 UV profile of azido-NAD^+ in the HPLC run

Mass spectroscopy : The spectrometry is perfomed on a double-focusing magnetic-sector mass spectrometer (Autospec, Micromass Inc). This

instrument is capable for electron ionization (EI), and electrospray ionization (ESI). Acetonitrile-water solvent is used as a carrier to detect azido-NAD^+. The experiment is run at low temperature to protect the molecule from fragmenting

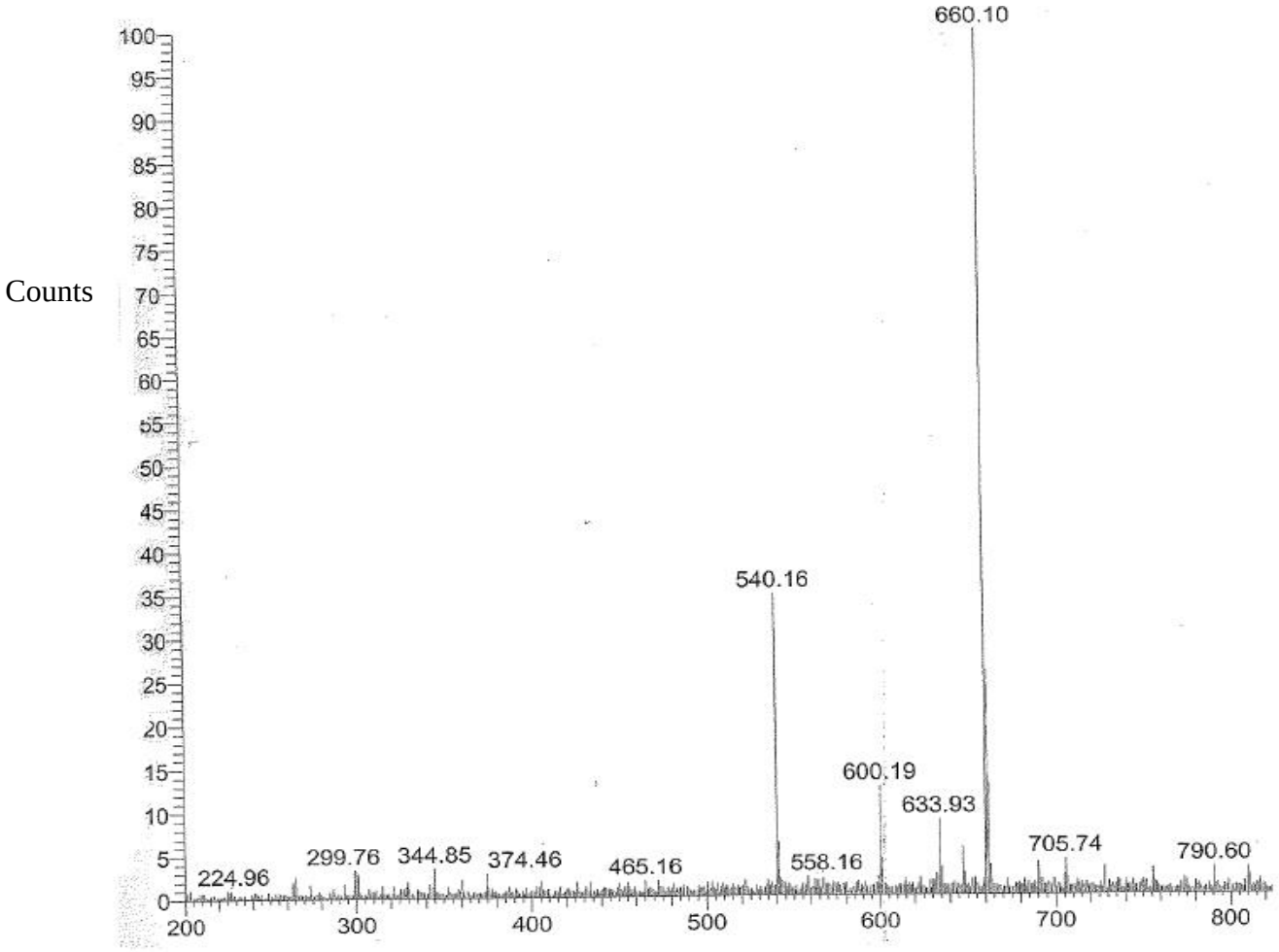

Figure 11 Mass spectrum of azido-NAD^+.

The peak at 660 .1 is assigned to M-1 of azido-NAD^+ and that of 540.16 is assigned to adenosine diphosphate M-1.

2.3 Survey of NAD^+ Dehydrogenase

More than 600 enzymes, are known to use NAD^+ as a cofactor. Several enzymes are isolated and are candidates for binding with azido-NAD^+ analog. A few commercially available NAD^+ dependent enzymes are listed below

1. Alcohol Dehydrogenase(ADH): This enzyme is an oxidoreductase that catalyses the reduction of alcohols, using NAD^+ or $NADP^+$. The reaction is reversible and the range of substrates, which this enzyme accommodates varies widely. Alcohol Dehydrogenase, isolated from baker's yeast (*Saccharomyces cerevisiae*) and horse liver, has been well characterized and studied extensively.[36, 37] It is a tetramer with each subunit containing a zinc atom.

2. Hydroxysteroid Dehydrogenase: It is a dehydrogenase, which chemically modifies steroids. This enzyme is commercially available mainly from *Pseudomonas testosteroni*, and is well characterized.[38, 39]

3. Lactate dehydrogenase (LDH). Mammalian lactate dehydrogenases exist as tetramers. They are quite stable and catalyses the conversion of lactate to pyruvate. This enzyme is a model enzyme for many computational studies.[40]

4. Malate dehydrogenase (MDH). It catalyzes the interconversion of L-malate and oxaloacetate using nicotinamide adenine dinucleotide as a coenzyme. This enzyme is found is eukaryotic cells and exists either in mitochondrial (m-MDH) or cytoplasmic (s-MDH) form, with a molecular weights approximately 70000 Da. This molecule exists as dimer.[41-43]

5. Aldehyde dehydrogenase: This enzyme catalyses the oxidation of aldehydes. There are two major isoenzymes; cytosolic and mitochondrial. The enzyme from yeast has a molecular weight of 200,000 and requires potassium and thiol ions for activity.

6. Lipoamide Dehydrogenase: Diaphorase catalyses conversion of lipoamide to dihydrolipoamide . It is found both in microbial and mammalian cells. Commercially available enzyme is extracted from porcine heart. It has two peptide chain bound by flavinadenine dinucleotide (FAD). The molecular weight of the porcine heart enzyme is between 100,000 and 114,000.[5, 44-51]

7. Glycerol-3-Phosphate Dehydrogenase: This enzyme is found both in plant and animal kingdom. It is commonly used in triglyceride kits to determine glycerol content. The enzyme acts a shuttle for electron in glycolysis cycle.

8. Glucose Dehydrogenase: Glucose Dehydrogenases (GDHs) occur in several organisms and commercially available from organism Bacillus *megaterium* and *Bacillus subtilis.* They accept both NAD^+ and $NADP^+$ as cofactor and can be used for the regeneration of NADH and NADPH. Glucose dehydrogenase from *B. subtilis* (EC 1.1.1.47) is a tetramer with a molecular weight of 126,000. The enzyme shows a pH optimum at 8.0 and a broad optimum temperature range between 45-50°C.

9. Leucine Dehydrogenase : Enzyme from *Bacillus cereus* is a hexamer with a molecular weight 245 kDa, which coverts leucine to α–Ketoisocaproate. Leucine dehydrogenase is a sulfhydryl containing enzyme which is strongly inhibited by p-chloromercuribenzoate and $HgCl_2$. Isoleucine, valine, norvaline, and norleucine may also be utilized as substrates. This enzyme is usually available as lyophilized powder.

10. L-Phenylalanine Dehydrogenase : L-phenylalanine-dehydrogenase having catalyzes oxidation of L-phenylalanine to phenyl pyruvic acid in the presence of ammonium ions and with NAD^+ as coenzyme. It commercially available from *Sporosarcina* sp as lyophilized powder.

11. Isocitrate Dehydrogenase (IDH) : This enzyme converts isocitrate to α-ketoglutarate, an important step in citric acid cycle. IDH consists of three

subunits which need Mn^{2+} or Mg^{2+}.The structure and mechanism of this enzyme from *E.coli* has widely been studied.

12. myo-Inositol Dehydrogenase: This enzyme converts myo-inositol and NAD to scyllo-inosose and NADH. Myo-inositol is a major nutritionally active component for the body. The enzyme from *Bacillus stubilis* has a molecular weight of 160 kDa and optimum pH 9 and can be obtained as lyophilized powder.

13. β –Galactose Dehydrogenase : These enzymes convert galactose to its lactone using NAD^+ as a cofactor. This enzymes is commercially isolated from *Pseudomonas fluorescens* and is available as suspension in ammonium sulfate solution. The enzyme from this organism has a molecular weight of 64 kDa and exists as a dimer. It is used to monitor galactose level for many hepatic diseases.

14. Formate Dehydrogenase : This class of enzymes converts formate to carbon dioxide. The enzyme obtained from *Candida boidinii* as a lyophilizate is a dimer with two identical units. It is specific for formate and is inhibited by Cu^{2+}, Hg^{2+}, 4-chloromercuribenzoate, azide, nitrate, cyanate, thiocyanate and nitrite.

The above enzymes are procured from various commercial sources.

For initial enzymatic studies, the criteria for selecting the enzymes includes a) availability and cost , b) physical condition ; either as a lyophilizate or crystals , c) stability , d) absence of metal centers and e) solubility to more than a concentration of 1 mM. Among the enzymes listed above, Formate Dehydrogenase, Malate dehydrogenase and Glucose Dehydrogenase obtained from commercial sources met all the criteria. Formate Dehydrogenase (FDH, *Candida boidinii*) is obtained from Roche Diagnostics, Germany. Malate Dehydrogenase (MDH, Porcine heart

mitochondria) is obtained from Calzyme Laboratories Inc. CA. Glucose dehydrogenase (GDH, *Bacillus megaterium*) is obtained from USB Corp, OH. These enzymes are used as received without any further purification. In all cases, the solubility is checked by dissolving a measure quantity of enzyme in phosphate buffer.

2.4 Enzyme Measurements

2.4.1 Formate Dehydrogenase(FDH)

1. Initial velocity study: This study is carried on Cary 300 UV-Vis spectrophotometer using of 340 nm as a guide to measure the kinetics. In a typical run, the components for the reactions are mixed and allowed to equilibrate for a few minutes. Addition of enzyme to this mixture initiates the reaction, which is followed by the change of absorption of 340 nm for at least two minutes. All measurements are done at 25^0 C in sodium phosphate buffer (100 mM) at pH 7.5. The concentration of azido-NAD^+ is varied in presence of saturating concentration of sodium formate. The plot of initial rate vs azido-NAD^+ was fitted to equation 2, using global analysis of several data sets.

$$V = V_{Max}[S]/K_M + [S] \qquad \text{Equation } \mathbf{2}$$

The Km and k_{cat} of azido-NAD^+ is 378.7 ± 42.2 μM and 7.2 s^{-1} respectively. The plot shown below is the plot of initial rate of corresponding concentration of the substrate. Each circles (o) are experimental data points for a single substrate concentration. The concentration of the enzyme is kept constant in all the measurements. This concentration is calculated by using the UV absorption at 280 nm. The molar absorbity calculated at 280 nm using the FDH protein sequence is 51340/M/cm. All the experiments, are conducted at 25^oC .

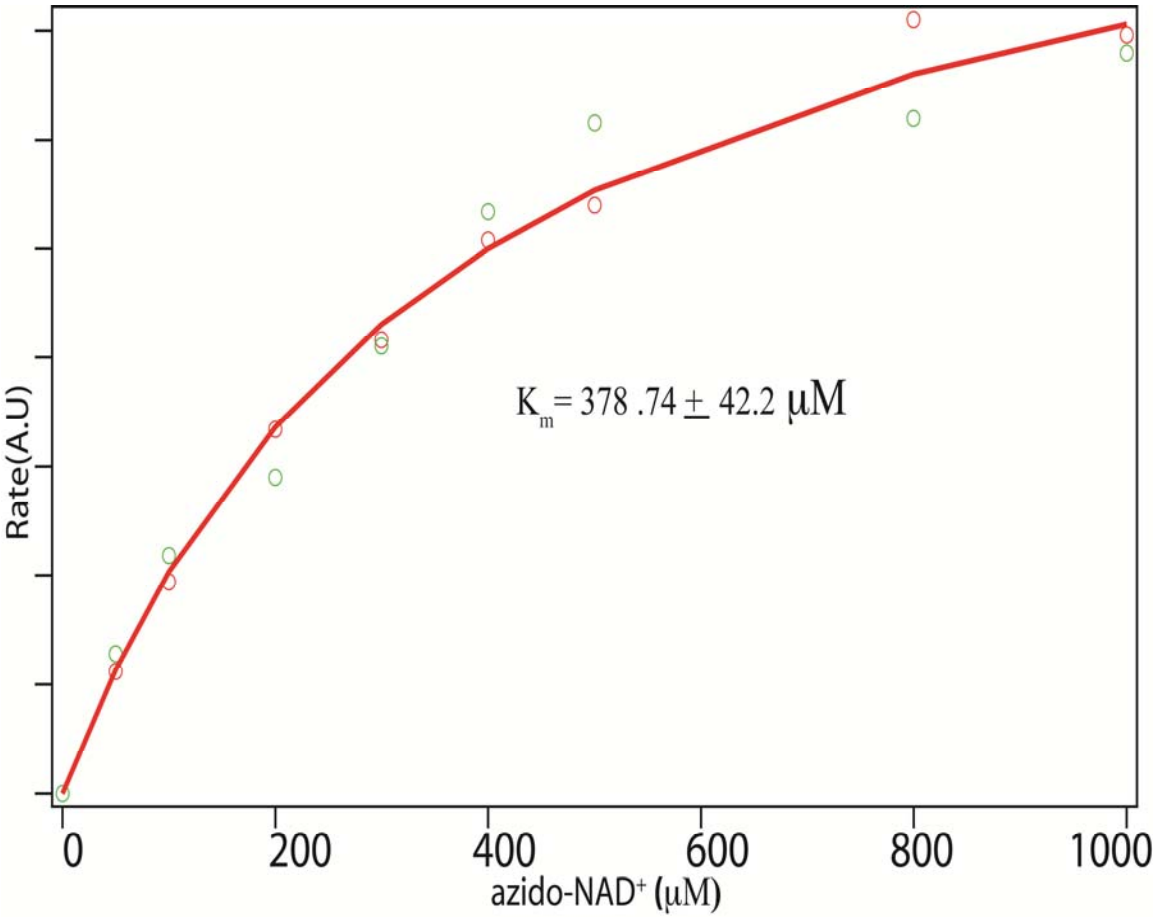

Figure 12 Kinetic plot of FDH with azido-NAD^+.

2 Isothermal Calorimetry (ITC) : Isothermal Titration Calorimetry (ITC) is the gold standard for measuring biomolecular interactions. ITC simultaneously determines all binding parameters (n, K, ΔH and ΔS) in a single experiment. This experiment is performed on a Microcal ITC. In a typical ITC experiment, a solution of a one biomolecule, in this case azido-NAD^+, is titrated into a solution of its binding partner. The heat released upon binding (ΔH) is monitored over time (Figure 13, top panel). Each spike in the figure represents heat evolution/release associated with the injection

of a small volume of sample into the ITC reaction cell. As successive amounts of the ligand are titrated into the ITC cell, the quantity of heat absorbed or released is in direct proportion to the amount of binding. As the system reaches saturation, the heat signal diminishes until only heats of dilution are observed. A binding curve is then obtained from a plot of the heats from each injection against the ratio of ligand and binding partner in the cell (Figure 13, bottom panel). The binding curve is analyzed with the appropriate binding model to determine the dissociation constant K_d. The design of the experiment depends on so called Wiesman c-parameter:

$$c = n[M]\ K_a$$

where K_a n[M] are the association constant and concentration of binding site respectively . The typical range that c should vary is between 0 to 1000 to obtain a proper titration curve.

In a typical experiment, FDH/FDH-azide is isothermally titrated with azido-NAD^+ to form binary/ternary complex. The concentration of the ligand (azido-NAD^+) is typically kept at least 10 times that of the enzyme to obtain a reasonable binding curve. In general, 14μL aliquots of the ligand is added to bind with enzyme in the solution. All solutions are degassed for 15 minutes prior to use, to avoid formation of bubble during the experiment. The experiments are carried out at 25 ^{0}C at pH 7.5, with constant stirring. All experiment are repeated thrice and the average dissociation constant for binary/ternary complex found out by fitting the data to a single binding model using Origin software, has a value of 63.3 ± 13.0 / 8.2 ± 2.6 μM. Figures 13 and 14 are representative Wiesman isotherms shown in the following pages.

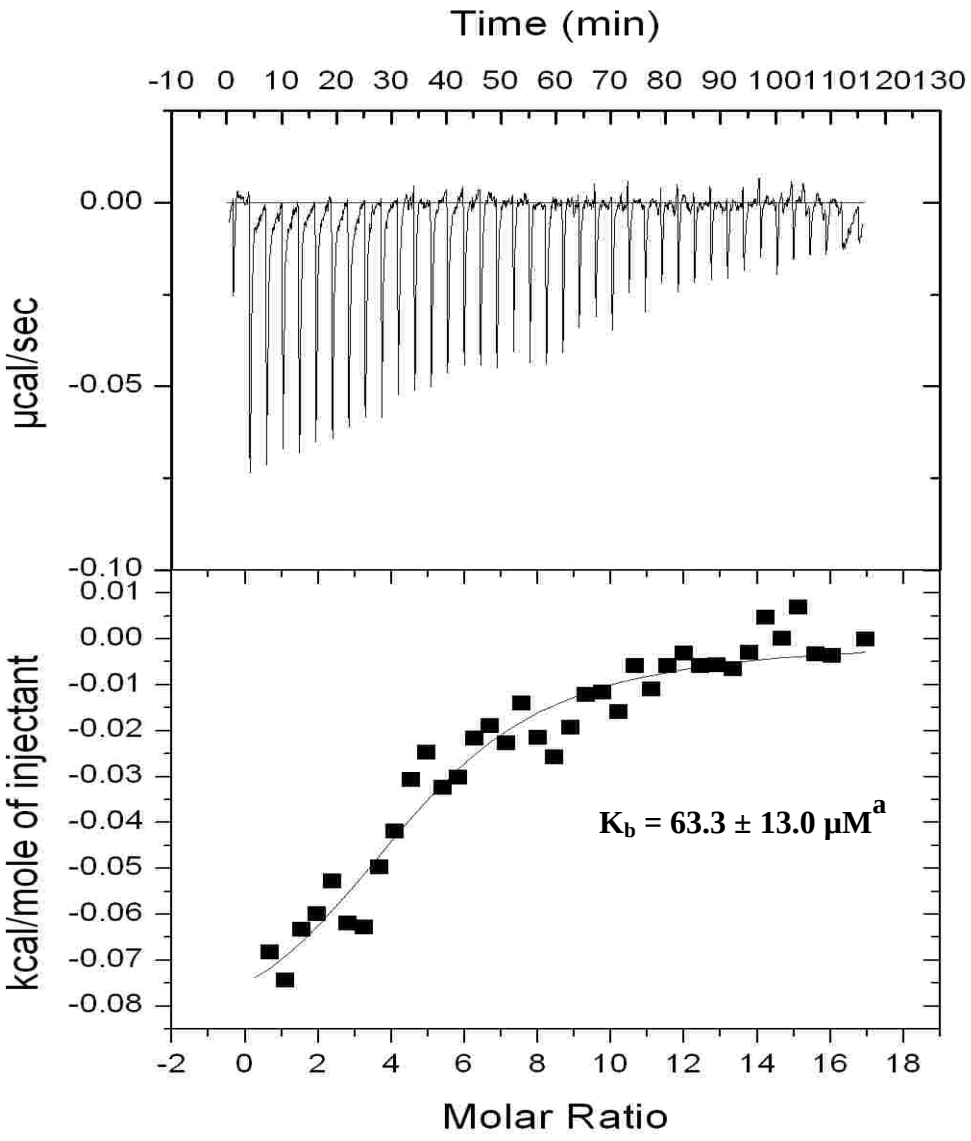

Figure 13 Representative ITC data taken on microcal on FDH-azido-NAD+. [a] Average of three measurements.

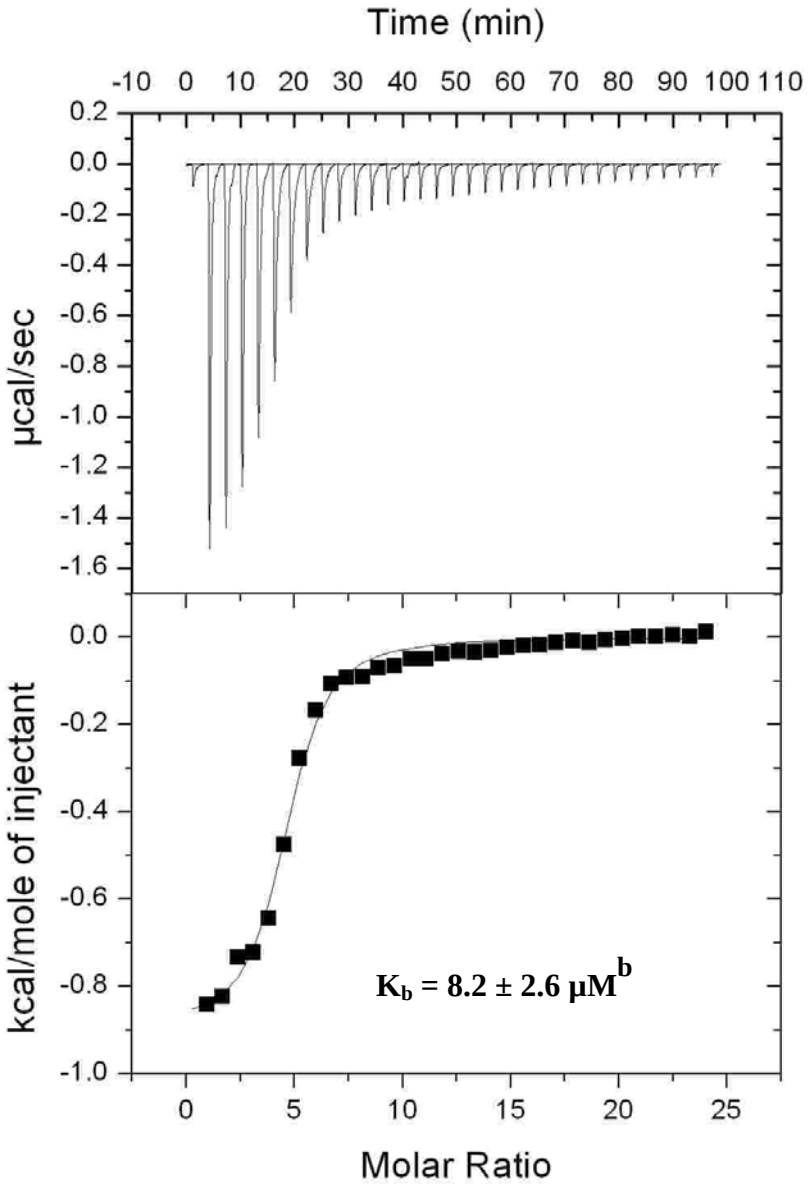

Figure 14 Representative ITC data taken on microcal on FDH-azido-NAD^+ - azide. [b] Average of three measurements.

3. Infrared Spectroscopy ： To prepare the binary complex , a solution of 25 mM FDH is prepared in 0.1 M phosphate buffer (pH 7.5) with 21 mM azido-NAD^+ as co-enzyme. The FTIR of this solution is recorded on a Bruker Tensor 27 using CaF_2 windows with a path length 50 μm. A peak at 2138 ± 2 cm^{-1} is observed with a full width half maximum (FWHM) of 26 ± 2 cm^{-1} after background subtraction with a blank solution of 25 mM FDH. Figure 15 shows the complete subtracted background with the region of interest in inset. Similar experiments are performed with ternary FDH-azide-azido-NAD^+ complex. In this complex, the azide peak is at 2046 ± 2 cm^{-1} with FWHM of 25 ± 2 cm^{-1} whereas the azido-NAD^+ peak is at 2142 ± 3 cm^{-1} with FWHM of 25 ± 2 cm^{-1}.

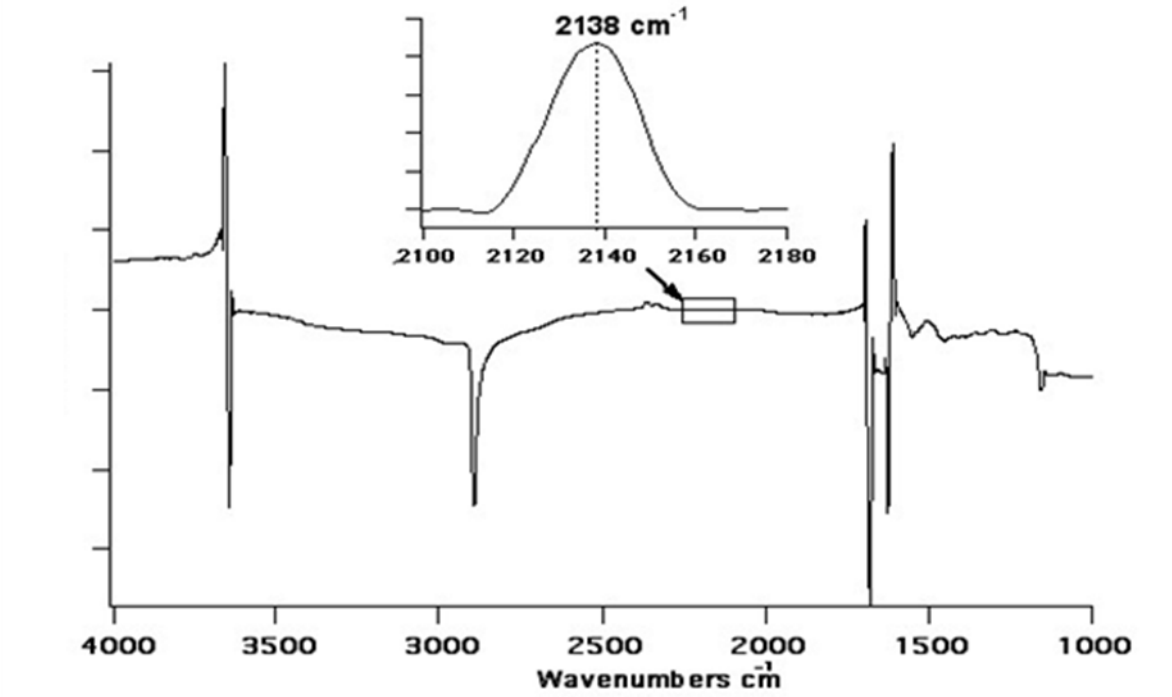

Figure 15 Full FTIR of FDH-azido NAD+ complex.(Inset) Magnified specturm in the relevant transition range

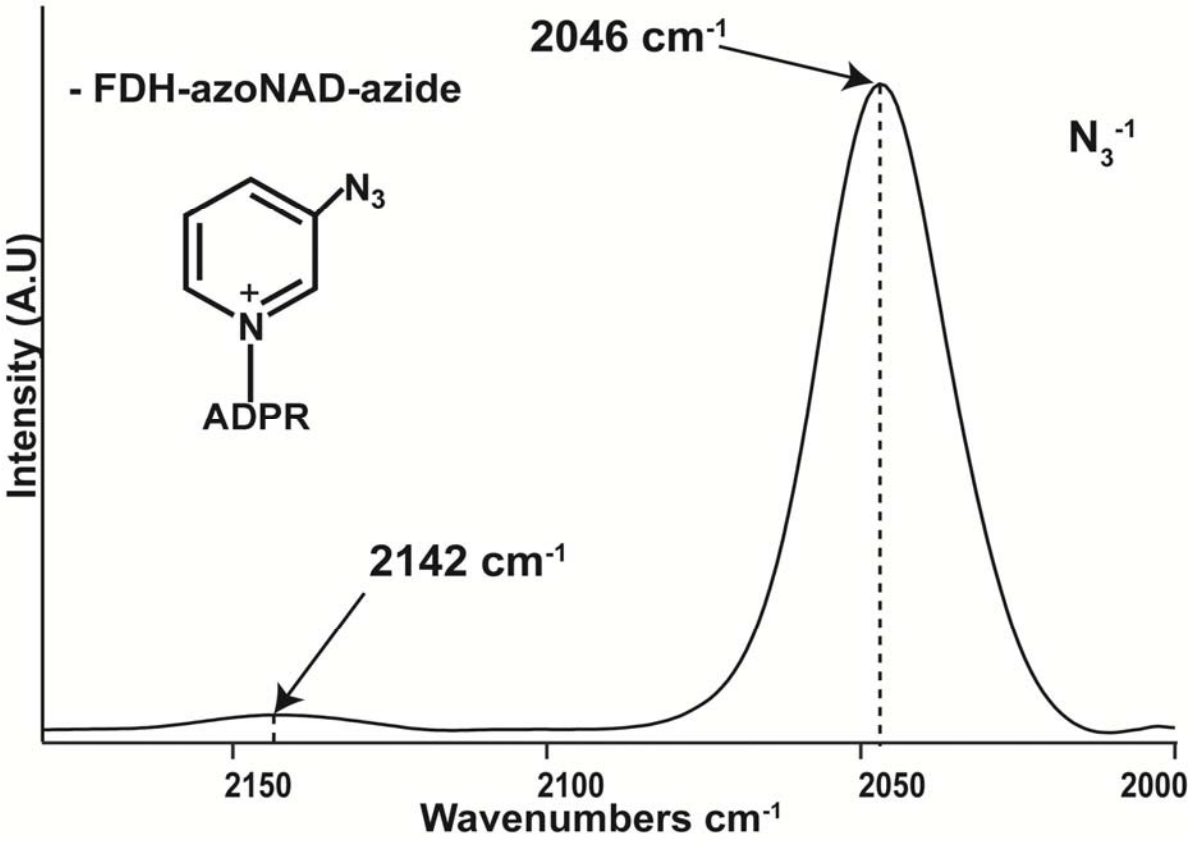

Figure 16 FTIR of FDH-azido-NAD^+ with background subtracted.

2.4.2 Malate Dehydrogenase (MDH)

1. Initial velocity study: This experiment is conducted in similar protocol as described for FDH. It is found to be an inhibitor and the competitive form of Michaelis–Menten kinetics (equation 3) given below is used to fit the data.

$$v = V_{max}*[S]/([S]+K_m*(1+[I]/K_i)) \quad \text{Equation 3}$$

where the symbols have their usual meanings. Figure 17 shows the plot of initial rate vs NAD^+ fitted to equation 3, using global analysis of several data sets. The fixed concentration of azido-NAD^+ is 0, 10 and 20 μM respectively indicated by red, blue and green. The K_I azido-NAD^+ is found to be 83 ± 12 μM.

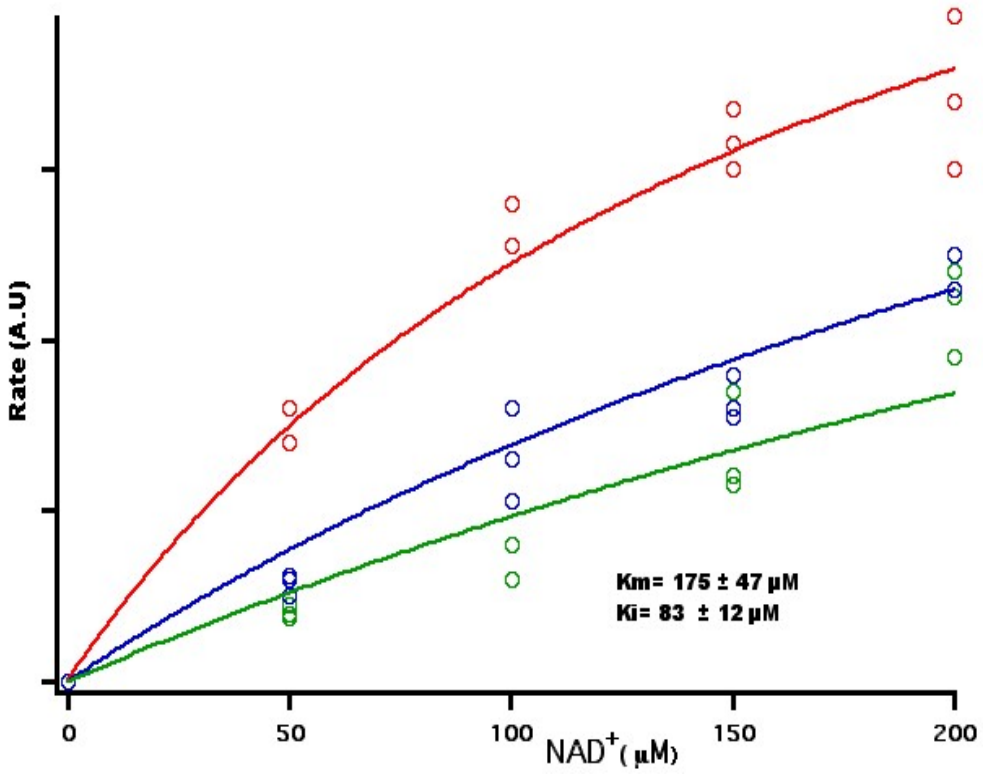

Figure 17 Kinetic plot of MDH with NAD^+ with different concentration of azido-NAD^+.

2 Isothermal Calorimetry (ITC) : This experiment is carried out with similar protocol as described for FDH. Malate is used instead of azide in the ternary complex. The concentration of malate was kept at 5 times its K_m value. The average dissociation constant for binary/ternary complex has a value of 152 ± 20 / 70 ± 14 μM. Figure 18 and 19 , represents the experimental data of the binary and the ternary complexes of MDH.

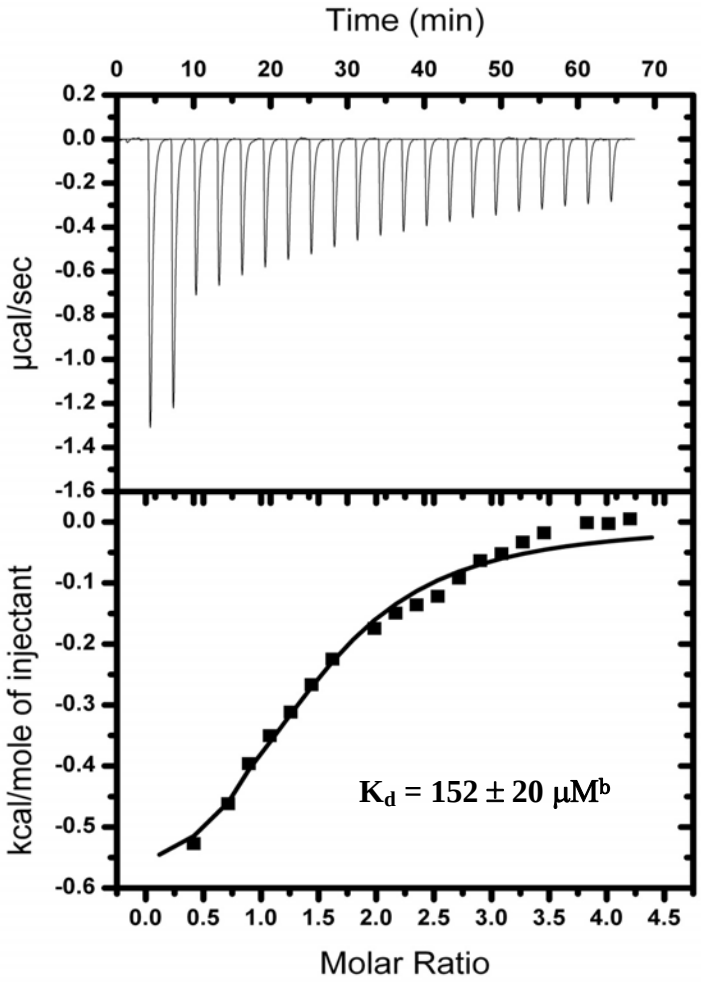

Figure 18 Representative ITC data on MDH-azido NAD^+ binary complex.

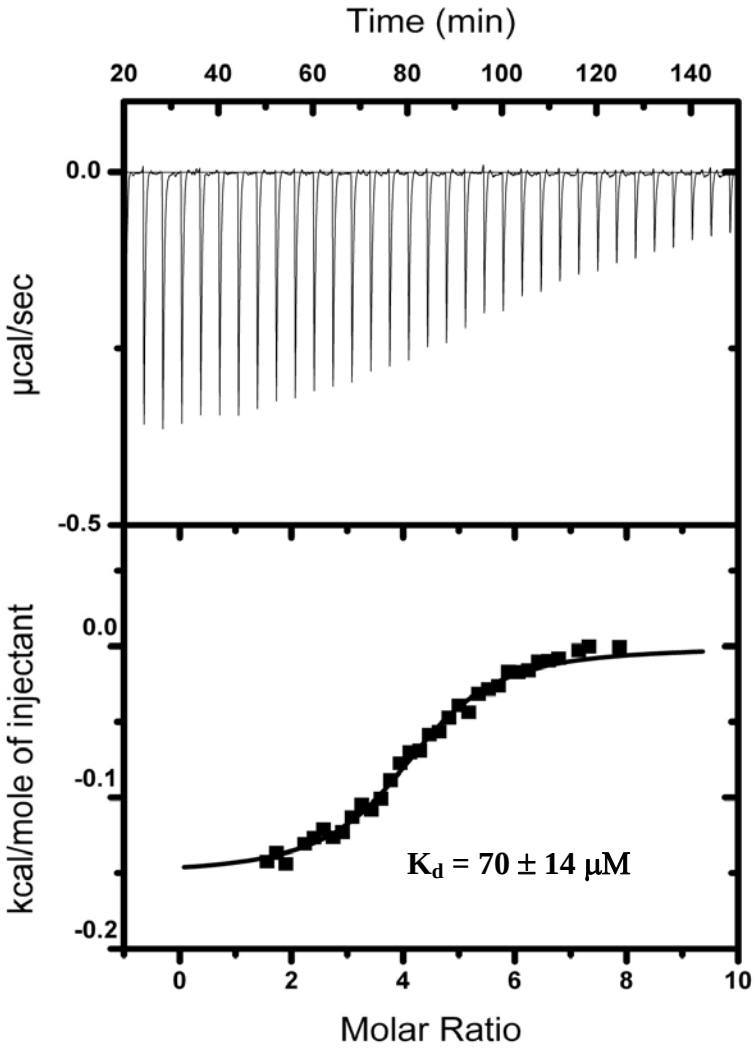

Figure 19 Representative ITC data on MDH-azido NAD^+ -malate ternary complex.

3. Infrared Spectroscopy ：The procedure is same as that of FDH. For binary experiments, approximately 15mM solution of MDH bound to 15 mM azido-NAD^+ is prepared for analysis. In case of ternary complex, a solution of malic acid neutralized by sodium hydroxide is mixed to the above solution, keeping

a fixed concentration of both MDH and azido-NAD^+. Figure 20, shows the binary complex (top panel) with a peak at 2138 ± 3 cm^{-1} with a FWHM of 28 $cm^{-1}$and the ternary complex MDH-azido-NAD^+-malate (bottom panel) which has a peak at 2138 ± 4 cm^{-1} with a FWHM of 26 cm.

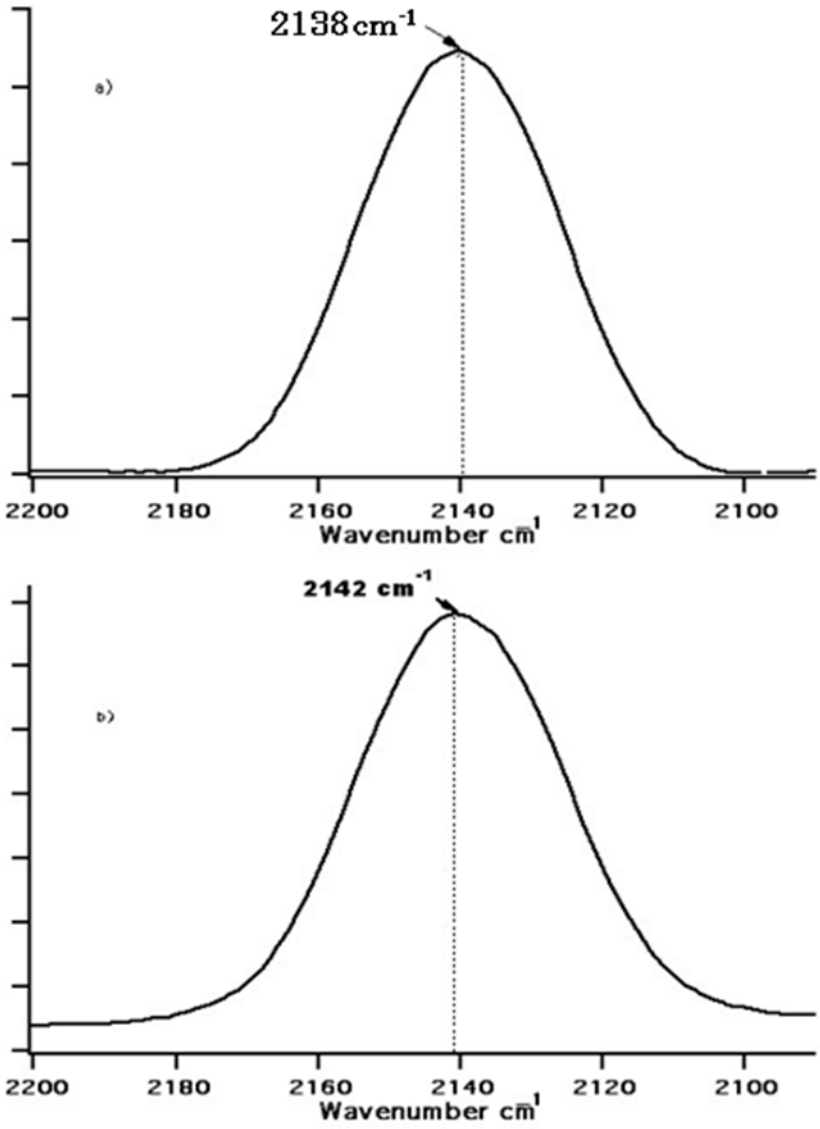

Figure 20 FTIR of binary MDH-azido-NAD^+ complex (top panel) and ternary MDH-azido-NAD^+-Malate complex

2.4.3 Glucose Dehydrogenase (GDH)

1. Initial velocity study: This experiment is conducted in similar procedure as described for FDH. Azido-NAD^+ is found to be a substrate. The concentration of azido-NAD^+ is varied while maintaining the concentration of glucose at 5 times its Km value. The initial rate of each concentration was obtained by observing increase in 340 nm absorbance with time. The plot of initial rate vs azido-NAD^+ is fitted to equation 2, using global analysis of several data sets. The K_m of azido-NAD^+ is found to be 72 ± 8 μM with a k_{cat} of 344/s.

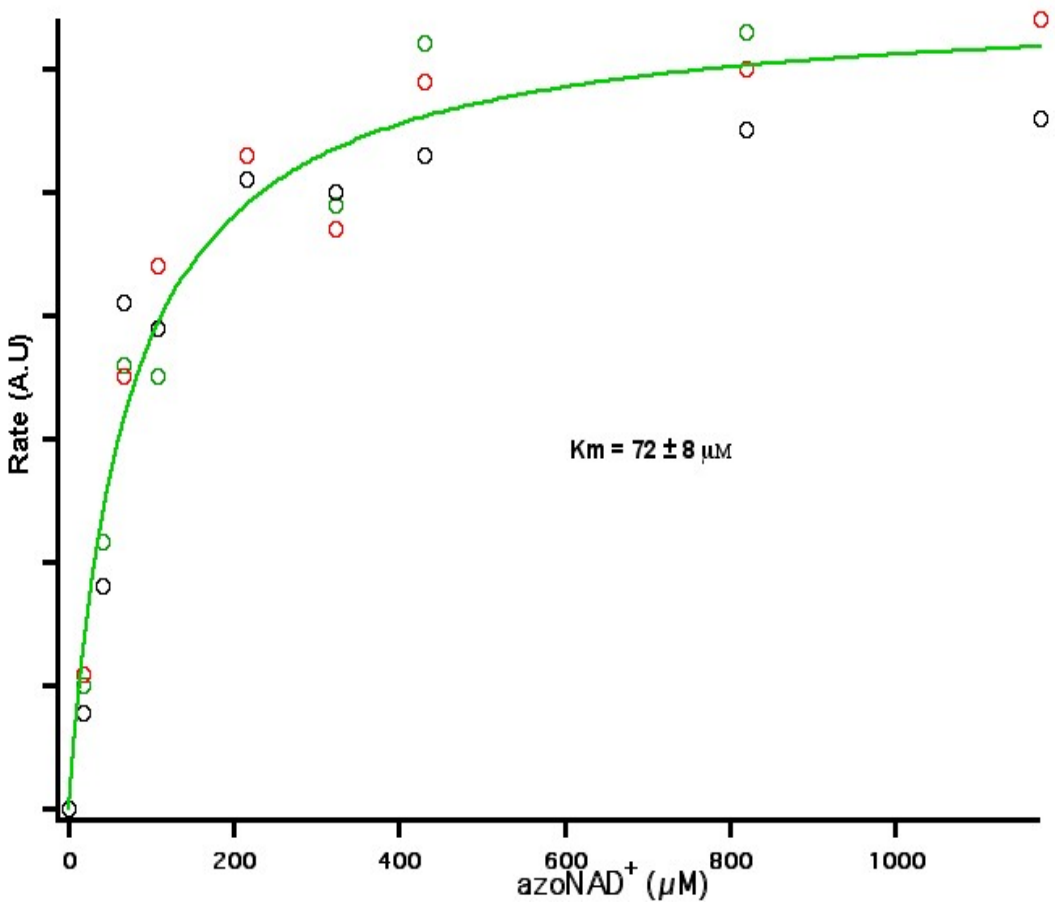

Figure 21 Kinetic plot of GDH with azido-NAD^+.

2 Fluorescence titration : This experiment is carried using a computer controlled Varian fluorescence spectrophotometer. GDH shows fluorescence maxima at 348 nm when excited at 310 nm in phosphate buffer at pH 7.5. The excitation and emission wavelength are kept fixed during the experiment. Typically, 10 nM solution of GDH is titrated with various concentration of azido-NAD^+ for the binary system. The fluorescence is quenched with the increase in concentration of the ligand. Similar trend is seen with the ternary complex, which has glucono-δ-lactone at the third binding partner. Peak fluorescence (Q_{max}) is defined as the fluorescence at 348 nm of GDH and observed fluorescence (Q_{obs}) is defined as the fluorescence at 348 nm of the liganded GDH with the binding partners, glucono-δ-lactone and azido-NAD^+. Percentage decrease of 348 nm from maximum ($(1-(Q_{obs}/Q_{max}))x100\%$) is calculated from the collected data. All titrations were performed in triplicate. Binding affinity was calculated by using the Langmuir binding equation, $Y = (B\max \cdot X)/(K_d+X)$, which will be described elsewhere. The data is analysed with Igor software (Figure 22). The results shows that the dissociation constant for binary/ternary complex are $300 \pm 41 / 142 \pm 25$ μM.

The concentration of GDH used in these studies is determined from molar absorvity, which has a value of 131800 M^{-1} cm^{-1} at 280 nm. These titrations are carried out in disposable methacrylate UV cuvette and equilibrated for at least 2 minutes before scanning the desired range. The binding partner glucono-δ-lactone for ternary complexes hydrolyses slowly in water. So, fresh solution is prepared before each titration. The decrease in 348nm absorbance is recorded by carefully adjusting the baseline with the relative peak position. All titrations are carried out at 25 °C.

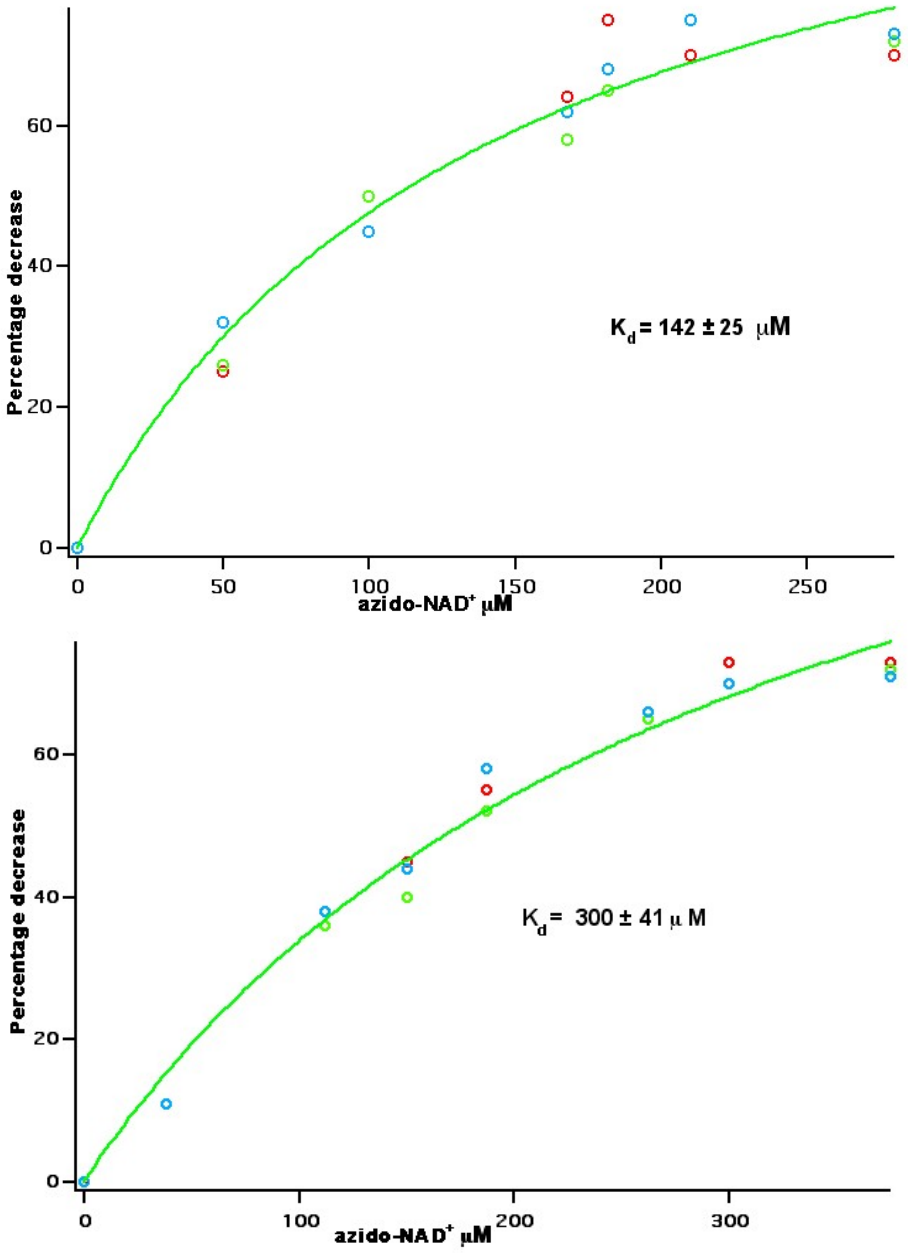

Figure 22 Fluorescence quenching kinetics of ternary (top panel) and binary (bottom panel) complexes of GDH

3. Infrared Spectroscopy : The procedure is same as that of FDH. For binary experiments, approximately 16mM solution of GDH bound to 15 mM azido-NAD^+ is prepared. In case of ternary complex, a solution of glucono-δ-lactone in phosphate buffer at pH 7.5 is added to the above solution keeping a fixed concentration of GDH and azido-NAD^+. The concentration of glucono-δ-lactone in the experiments with the ternary complex is kept at least 5 times K_m value of glucose. The FTIR spectrum of binary complex shows a peak at 2141 ± 2 cm^{-1} with a FWHM of 27 cm^{-1} whereas the ternary complex GDH-azido-NAD^+-glucose shows a peak at 2138 ± 4 cm^{-1} with a FWHM of 28 cm^{-1}.

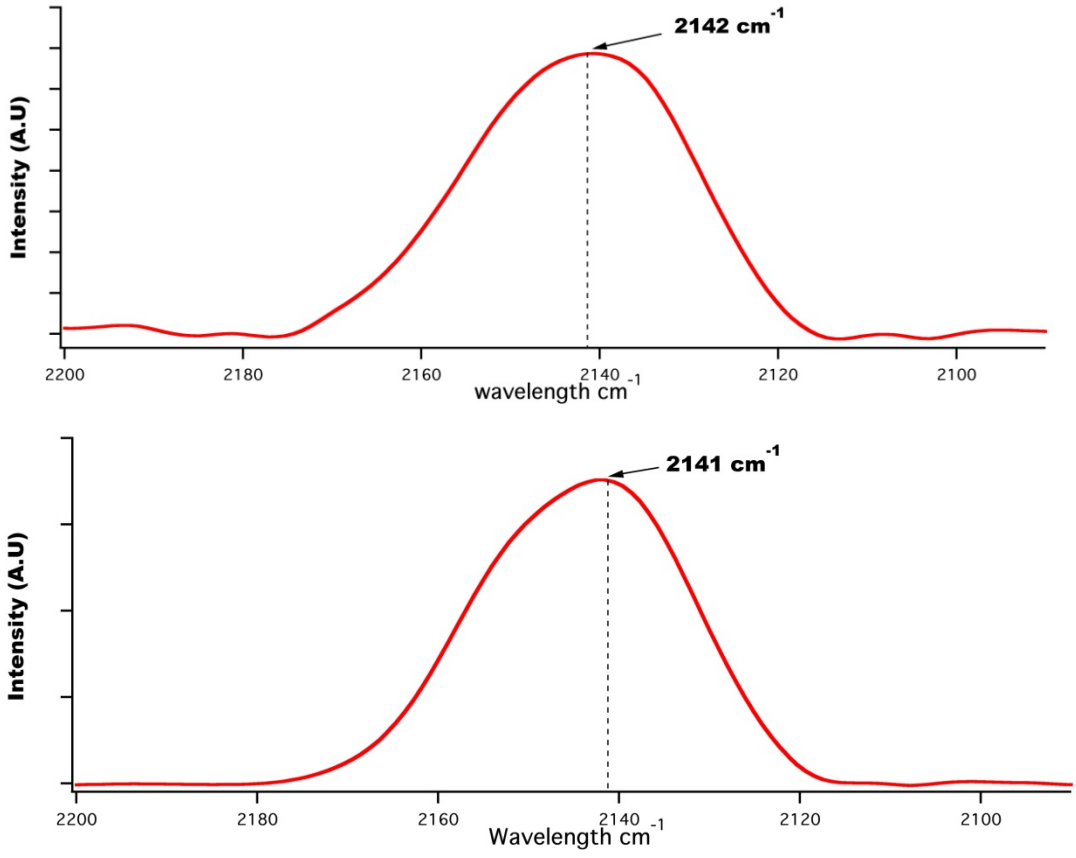

Figure 23 FTIR of binary (top panel) and ternary (bottom panel) complex of GDH

2.5 Preparative method of PAAD

2.5.1 Synthesis of 3-picolylazide

In a round bottle flask, we dissolve 3.4 g of 3-picolyl chloride hydrochloride in 50 mL of water and reacts it with 2.6 g of sodium azide. The mixture is then stirred at room temperature for 10 minutes, which yields a deep orange-red solution. A water cooled refluxing apparatus is attached to the flask and the reaction is allowed to react for 16 hours at 50 ^{o}C in a water bath. After 16 hours, sodium bicarbonate is added till the solution turns alkaline. The product is extracted with methelene chloride (2 x 200 mL) and finally washed with water. The extract is rotovaped to obtain a yellow oil.

Yeild = 1.6 g (47% overall product)

The characterization of 3-picolyl azide is given below

Density: 1.19 g/mL

UV spectroscopy: In a clean cuvette, 3-azido pyridine is dissolved in 1mL of phosphate buffer and analysed with a Cary 300 UV spectrophotometer. A weak peak at around 280 nm is seen, without any other features.

^{1}HNMR and ^{13} CNMR : The compound is dissolved in deuterated chloroform in a clean NMR tube. The spectrum is taken on Bruker Avance 300 NMR. The internal standards used in this analysis include both chloroform and trimethyl silane. For ^{1}H-NMR , 16 scans are taken, whereas for ^{13}C-NMR , 50 scans are averaged to obtain the final spectrum. Figure 24 shows the spectrum of this compound.

The ^{1}H-NMR spectrum shows peaks at 4.16 (2H,s), 7.3-7.38 (1H, m), 7.72-7.76 (1H, m), 8.6 (2H, s). ^{13} CNMR shows peak at 123.4, 135.5, 130.9,141.1, 141.9, 51.9.

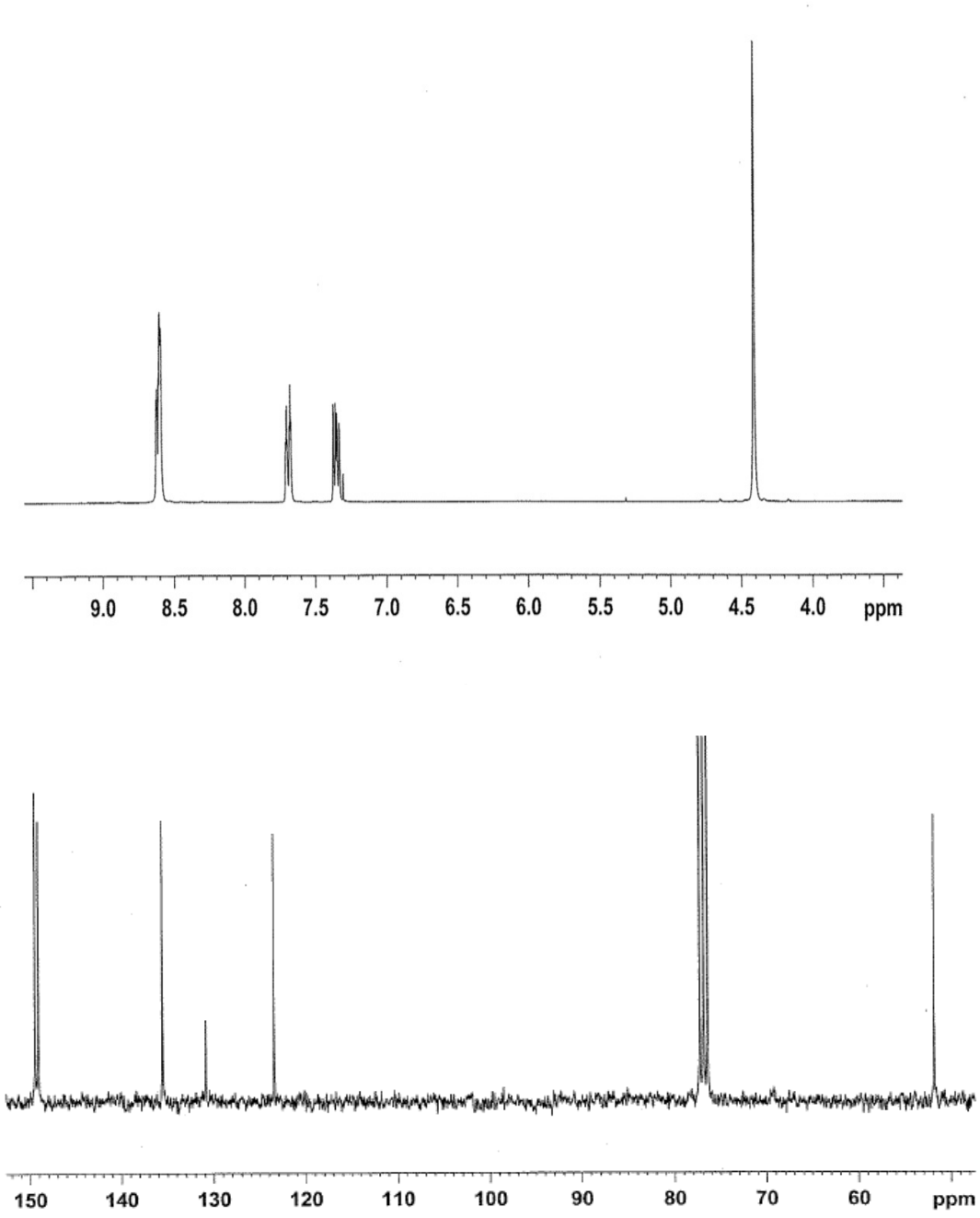

Figure 24 ^{1}H-NMR and ^{13}C-NMR of 3-Picolyl azide

Infrared Spectroscopy： A solution of 3-picolyl azide is prepared in 25 % dimethyl formaldehyde (DMF) in water. This solution is injected into a CaF_2 sample cell with a path length of 50 μ and the spectrum is taken as described elsewhere. The final spectrum as shown in Figure 25, is obtained by subtracting a blank sample of 25% DMF in water.

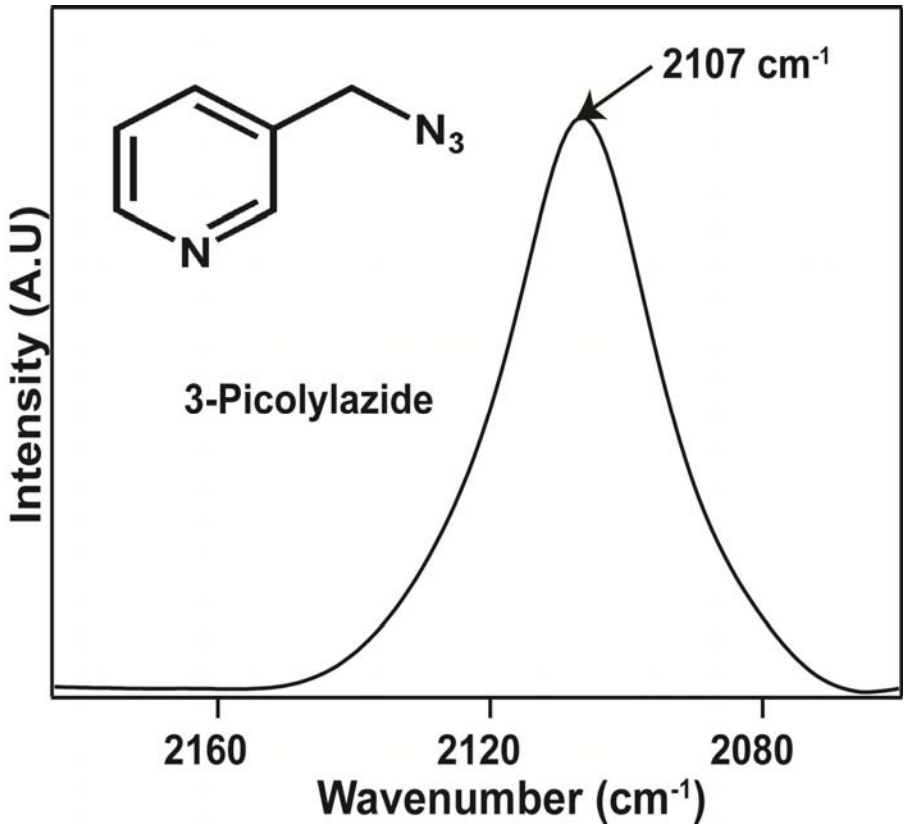

Figure 25 Infrared spectra of 3-Picolyl azide in 25% DMF in water

The peak position is at 2107 cm^{-1} with FWHM is 26 cm^{-1}. The compound is also soluble in methelene chloride with a peak in mid –IR at 2103 cm^{-1}

2.5.2 Synthesis of PAAD

The protocol for synthesis is similar as described for azido-NAD^+ with modification. A solution of NADase as described for synthesis of azido-NAD^+ is prepared in 100 mM phosphate buffer at pH 7.5. It is important to note that for azido-NAD^+ synthesis 20 mM phosphate buffer is used instead of 100 mM. In short, a solution of 3-picolyl azide (400 mgs, 2.9 mols) in DMF is added to 18 mL of 100 mM NADase solution and allowed to equilibrate for two minutes. This causes the pH of the solution to change from pH 7.5 to 7.7. An aqueous solution of NAD^+ (150 mg, 0.23 mols) is added to this alkaline mixture. The addition of NAD^+ changes the pH to 7.4 which stabilizes itself to pH 7.5, after a few minutes. The reaction was allowed to react for 12 hrs in dark at 37 ^oC. After 12 hours, chloroform (50 mL x 2) is added to the mixture . The turbid solution was centrifuged at 4 ^0C, carefully decanted into centrifuge tubes and further centrifuged with CH_2Cl_2. The aqueous layer is again decanted and poured into a round bottom flask. The solution is then lyophilized to obtain a white solid. An integrated liquid chromatogram-mass spectroscopy experiment is performed on this sample using water–acetonitrile mixure as carrier solvent, which shows a single peak (Figure 26) with a UV absorption at 258 nm. The eluent corresponding to the UV absorption peak has a molecular weight of 675.9, which is assigned to 3-Picolyl azide NAD^+(Figure 27). Other peaks at 697.9 and 719.8 is assigned to M+Na and M+2Na. The purity of the compound is $\geq$ 95 %. This product is used without further purification.

The compound is soluble in water and showed a mid-IR signature at 2119 cm^{-1} with a FWHM of 22 cm^{-1}. The molar absorbvity of this transition is 2000 /M/cm. It also has UV absorption at 258 nm. The compound is stable for at least 24 hours as it did not shown any change in either in IR or UV absorption within this stipulated period.

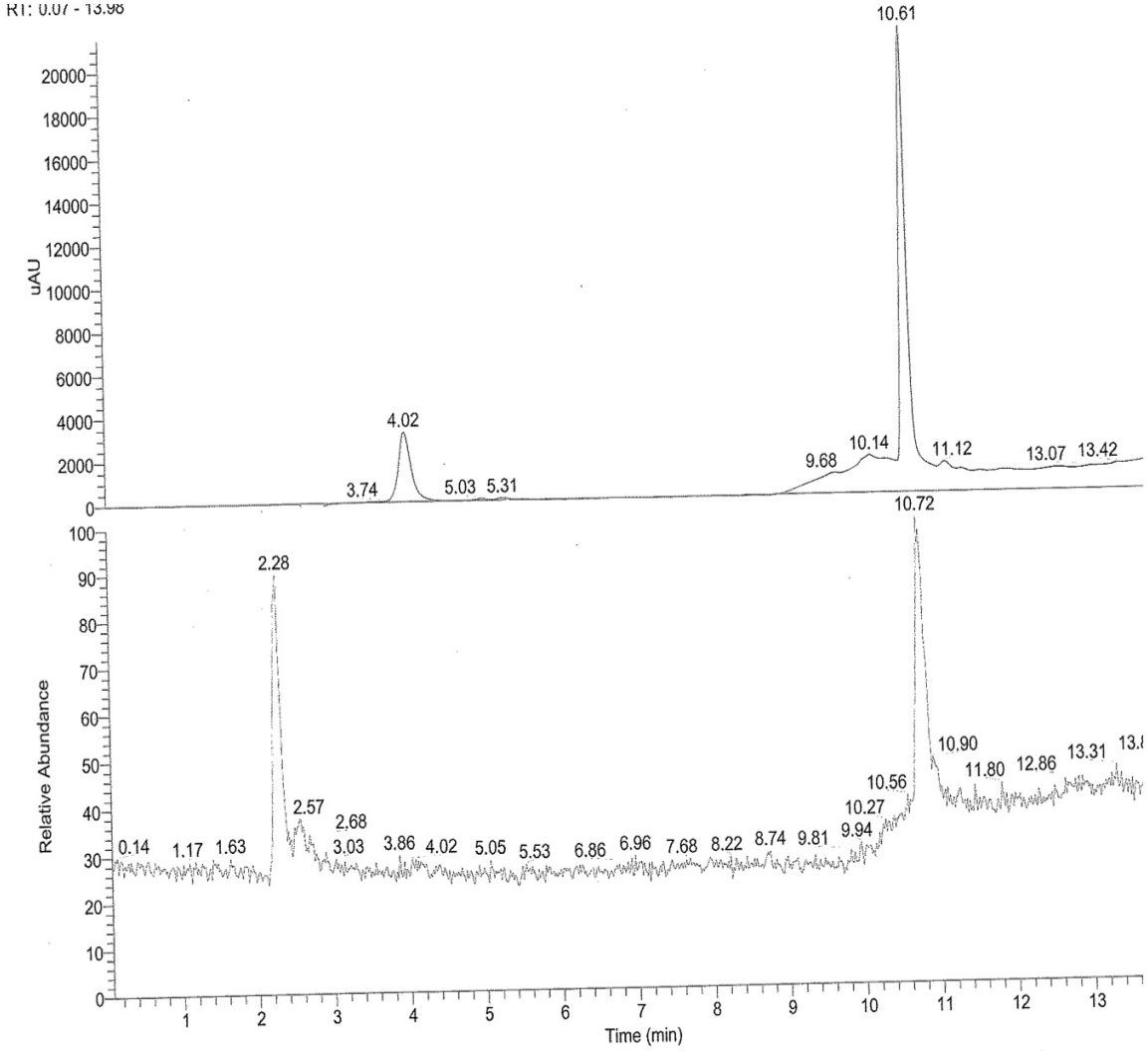

Figure 26 UV- LC spectrum of PAAD.

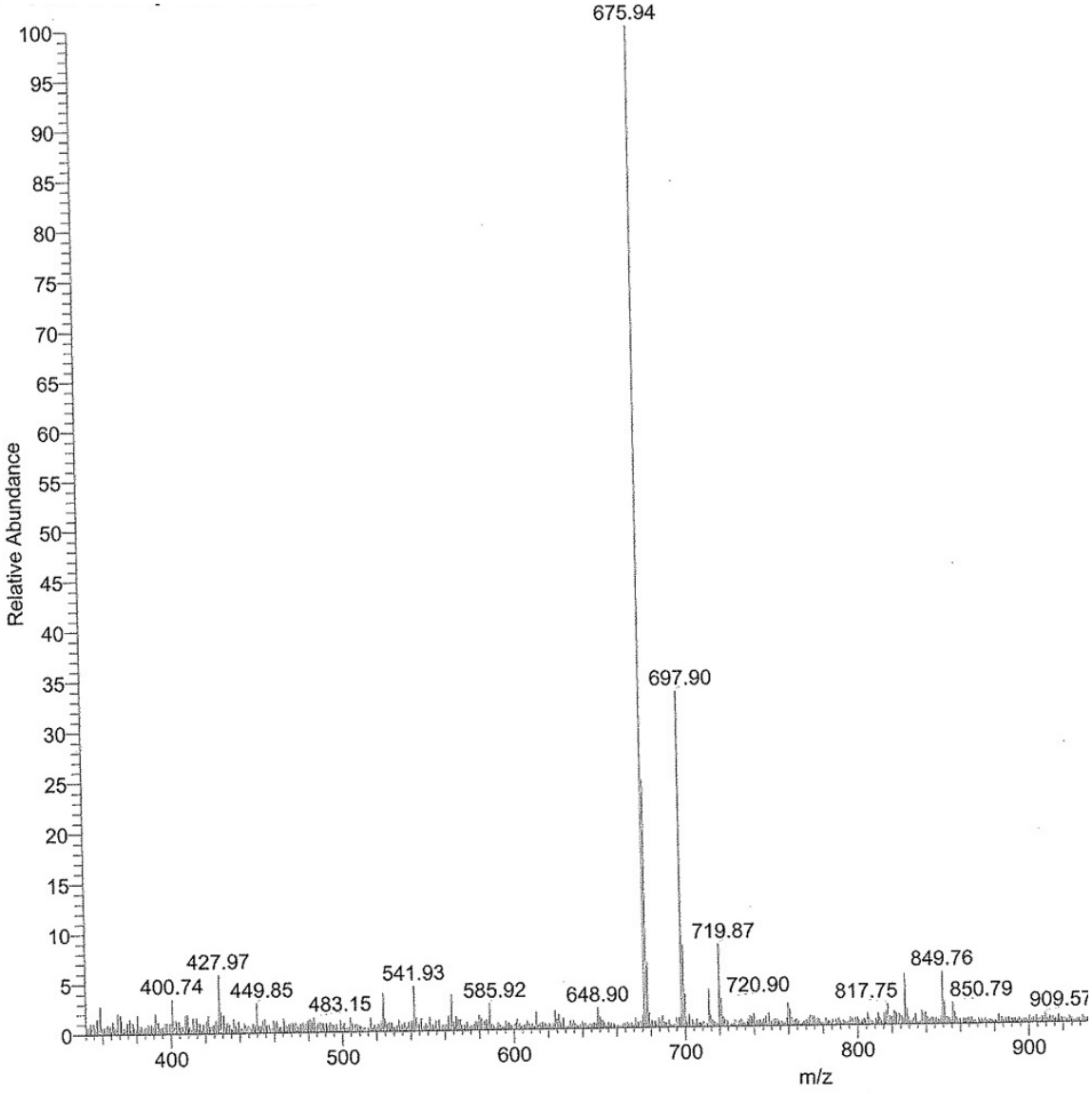

Figure 27 Mass spectrum of PAAD

.

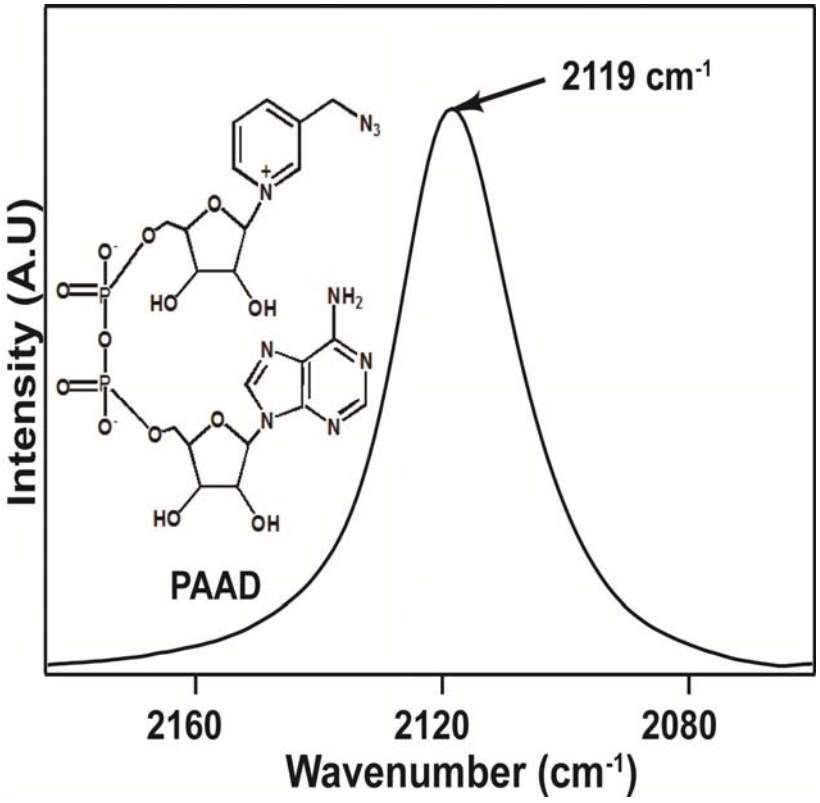

Figure 28 FTIR of PAAD in phosphate buffer.

2.6 Enzyme Measurements

2.6.1 Formate Dehydrogenase (FDH)

1. Initial velocity study: This experiment is conducted in similar procedure as described elsewhere. Briefly, PAAD reacts with formate to form reduced PAAD, which absorbs at 340 nm. The change of absorbance at 340 nm is followed for two minutes to calculate the initial rate. The initial velocity measurements for different concentration of PAAD is measured varied measured, while kepping fixed concentration of formate concentration at 5 times its K_m value. The plot of initial rate vs PAAD follows Michaelis – Menten hyperbolic equation as shown in Figure 29.

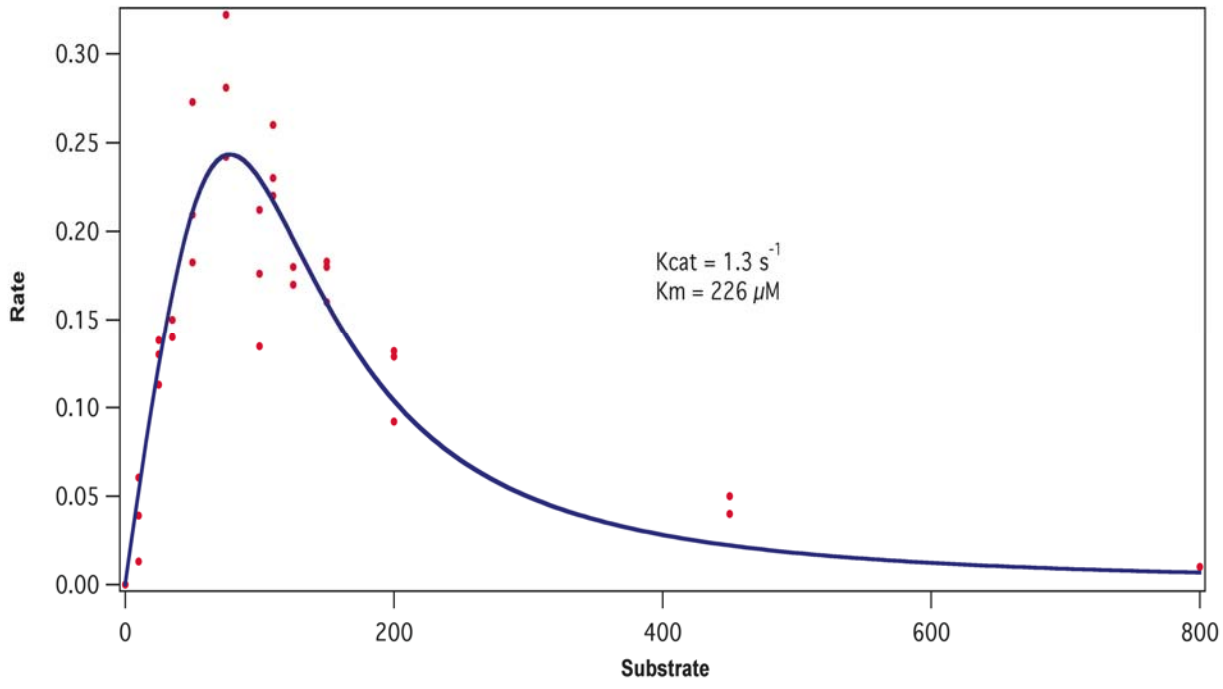

Figure 29 Kinetic plot of PAAD with FDH

The equation used for this plot is given below;

$$\text{Rate} = k_{cat}[S]/(K_m + [S](1+[S]^{2.3}/k_s) \qquad \text{Equation 4}$$

where the symbols have their usual meanings.

2 Isothermal Calorimetry (ITC)： These experiments are carried out as described elsewhere. Typically in binary experiments, PAAD is titrated with FDH where as in ternary complex it is titrated with FDH-azide. The concentration of FDH is within the range of 0.1-0.2 mM with the corresponding PAAD concentration is 10 times the given concentration of FDH. The average dissociation constant for binary/ternary complex reads as 7.2 ± 0.15 / 4.2 ± 0.20 μM.

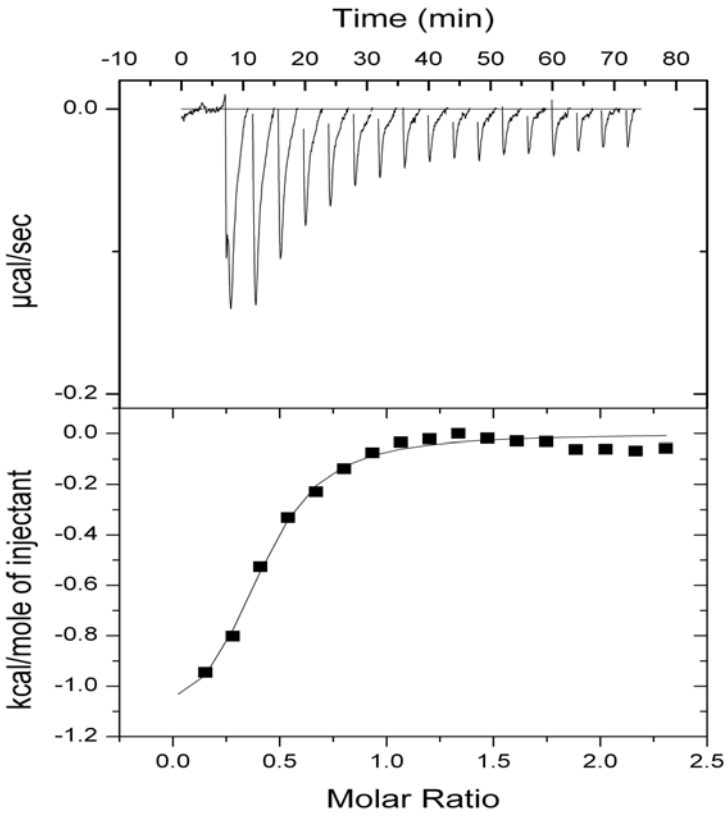

Figure 30 Representative ITC data on binary FDH-PAAD complex

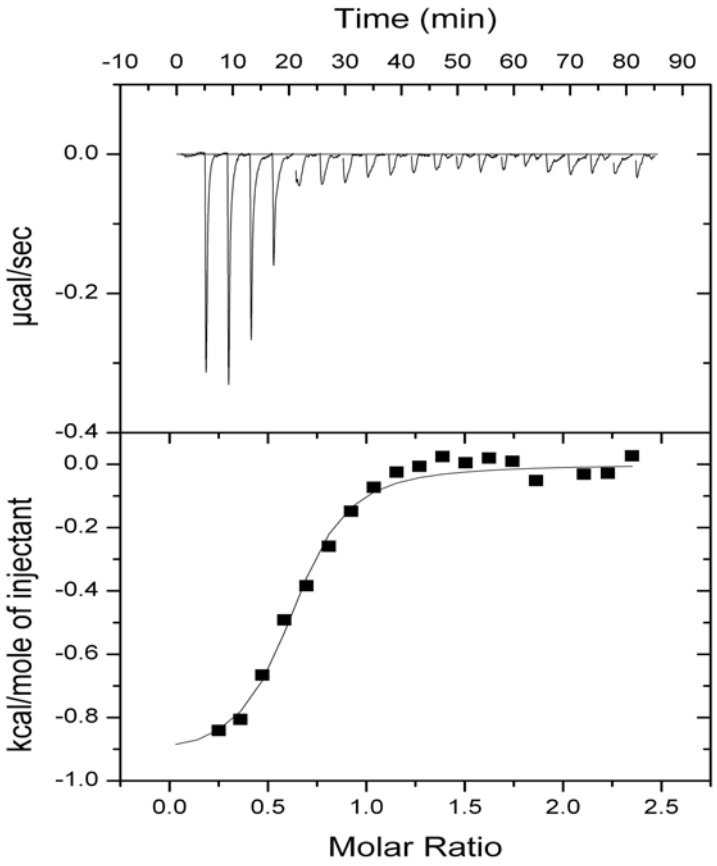

Figure 31 Representative ITC data of ternary FDH-azide-PAAD complex.

3. Infrared Spectroscopy : The procedure is same as described elsewhere. For binary experiments, approximately 26mM solution of FDH bound to 25 mM $PAAD^+$ is prepared in an eppendorf tube. In case of ternary complex, a solution of azide in phosphate buffer pH 7.5 is added to the above solution keeping the concentration of FDH and PANAD same as above. Typically, the azide concentration of the ternary complex is 25 mM. As seen in Figure 32, the binary complex has a peak at $2119 \pm 2\ cm^{-1}$ with a FWHM of $22\ cm^{-1}$ whereas the ternary complex FDH-PANAD-azide has two peaks; one peak is at $2119 \pm 2\ cm^{-1}$ with a FWHM of $23\ cm^{-1}$, and at the other peak is at $2048 \pm 2\ cm^{-1}$ with a FWHM of $24\ cm^{-1}$.

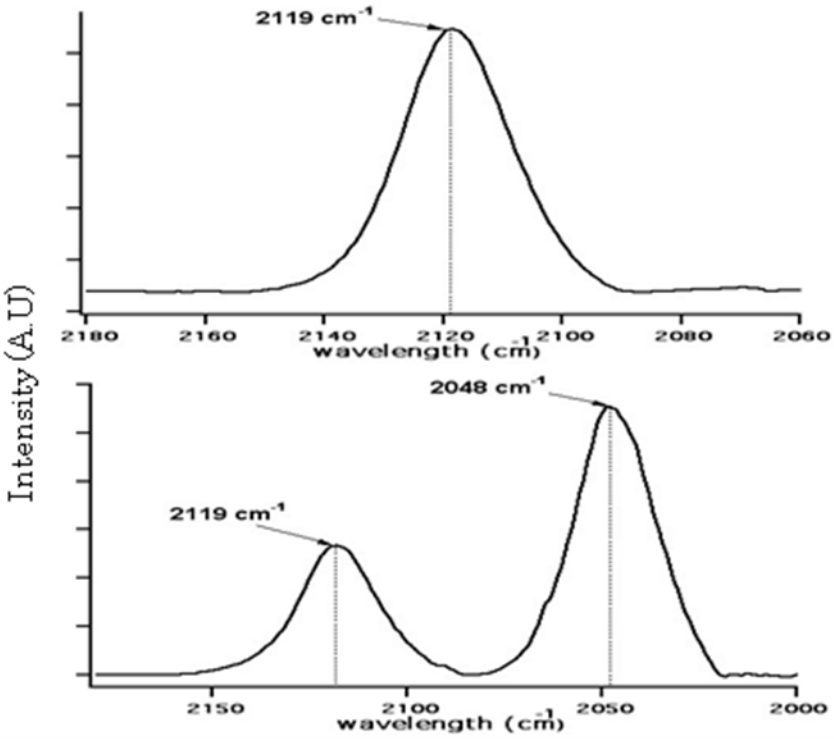

Figure 32 FTIR of binary (top panel) and ternary (bottom panel) complexes of FDH with PAAD

2.7 Two dimension infrared spectroscopy

Background: 2D-IR is a powerful tool to investigate solute-solvent interactions, vibrational relaxation, chemical exchange at equilibrium and non equilibrium systems. The main advantage of this spectroscopy is that its time resolution is many order of magnitude faster than other conventional spectroscopies. This resolution is possible because of short free induction decay and vibration lifetimes along with advance laser technologies which can generate femtosecond pulses. In this spectroscopy, the molecular response is spread over two frequency axis to produce a spectrum. The 1D-spectrum is present along the diagonal. The presence of off-diagonal peaks, tells us the coupling, chemical exchange and orientation between different modes. As the measurement is made with a picosecond or faster time resolution, it captures information on molecular structure in solution on a time scale fast compared to most dynamics. By progressively lengthening the "waiting time" one can follow time-dependent structural changes until the motion of molecules is no longer different from the next snapshot. Such molecular dynamics experiments not only records the motion of one state to another, but also mechanistically show the structure evolution along that path. Additionally, it characterizes distributions of molecular conformations or local solvent environments. This information is buried in the 2D IR lineshapes, which can be analyzed statistically to describe the variance in structural parameters.

A representative 2D-IR with global features is represented below; The data are usually expressed in the frequency domain as two-dimensional spectra of the coherence (ω_1) versus detection (ω_3) frequencies plotted in horizontal and vertical axis.

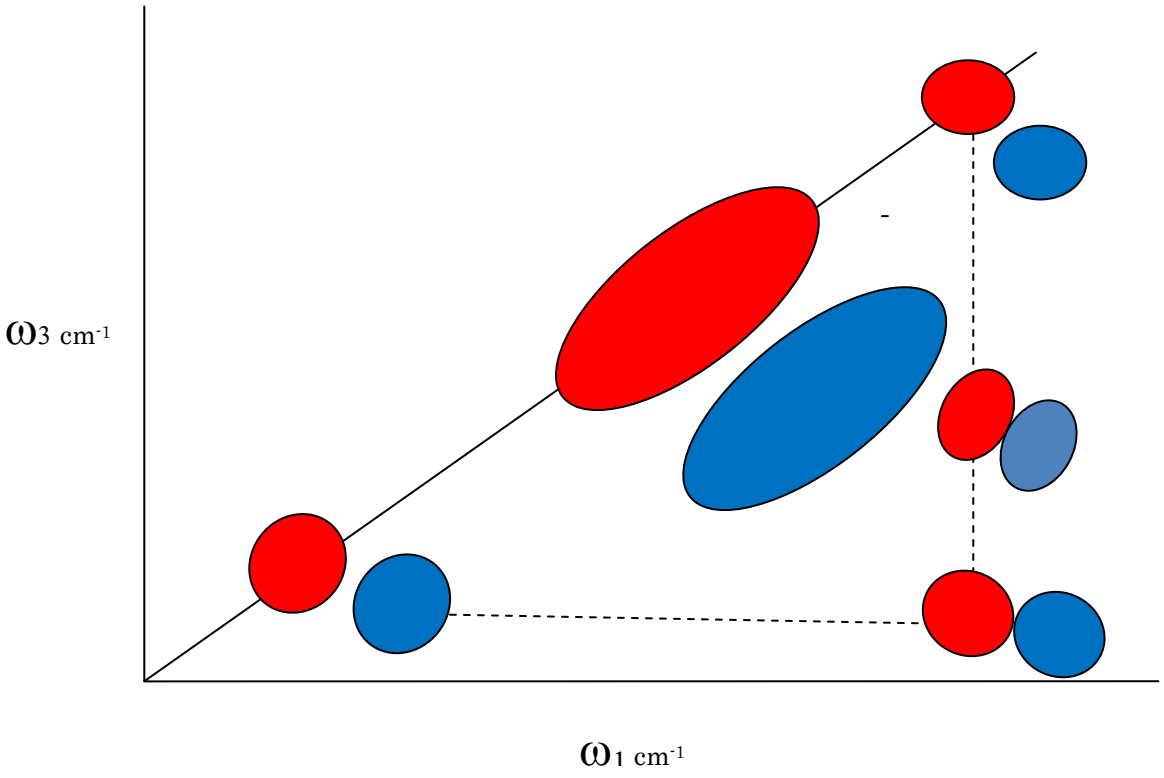

Figure 33 Representative 2D-IR features.

The contours along the diagonals are the infrared spectrum. The red contours represent 0-1 and 1-2 transition of the chromophore under investigation. The off diagonal contours can represent coupling, Fermi resonance, chemical exchange and energy transfer. Important dynamical features can be interpreted by observing time dependent changes of these features

There are two techniques to obtain the data, the quasi frequency domain double resonance and the time-domain vibration echo method. The later technique is pursued in this research to understand the time evolution of molecular structures.

2.6.1 The Experimental setup

The 2D IR experiment involves the three successive, well defined, ultrashort infrared pulses (see below) temporally spaced to an accuracy of a small fraction of a cycle. The 2D IR signal depends on the time, polarizations, and phases of the pulses which can be controlled by their directions (wave vectors) and/or by pulse shaping. The signal generated in phase-matched directions $k_s = k_1 + k_2 + k_3$ (echo) and $k_s = k_1 - k_2 + k_3$ (nonrephasing) can be detected by heterodyne mixing with a phase-locked fourth pulse.

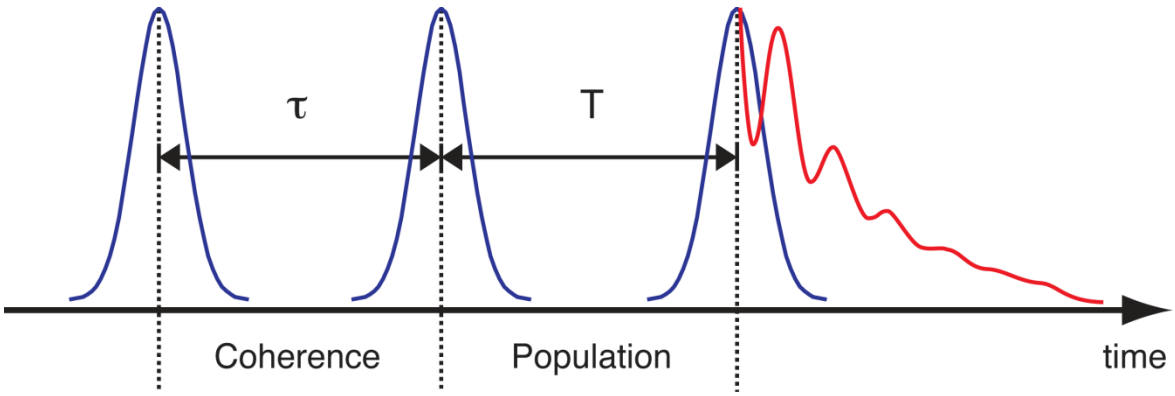

The figure 34 below shows the laser equipment. A solid state diode pumped laser is used to pump a Ti:Sapphire oscillator, which seeds a Ti:Sapphire regenerative amplifier. The seed light is centered around 800 nm with FWHM of 200 nm. The regenerative amplifier is pumped by a 1 kHz diode pumped Q-switched laser. The output of the regenerative amplifier at 800 nm is 3/4 W 35-100 fs pulses. The 800 nm pulses drive a multi-stage OPA, which produces pulses with 50-100 fs duration.

The OPA is tuned to the frequency of the vibrational mode under investigation. The IR pulses has enough bandwidth to span the spectral

region of interest. The time period between pulses 1 and 2 and between pulses 2 and 3 are called τ, and *T*, respectively. These three pulses are focused to the sample with off-axis parabolic gold reflectors to generate the vibrational echo signal. This signal emanates from the sample at a time 't' after the third pulse in a unique direction, which is collimated along with the other pulses by another off-axis parabolic refector. All other signals apart from the echo is blocked. The time zeros between excitation pulses are determined by iteratively scanning pulse 1 (or 2) with pulses 2 (or 1) and 3 with the homodyned signal keeping the local oscillator blocked. Once the time zeros between excitation pulses is determined within ± 5 fs, the temporal and spatial overlap of the LO with the vibrational echo signal is recorded by measuring a spectral interferogram. The spatial overlap is maximized by using steering mirror.

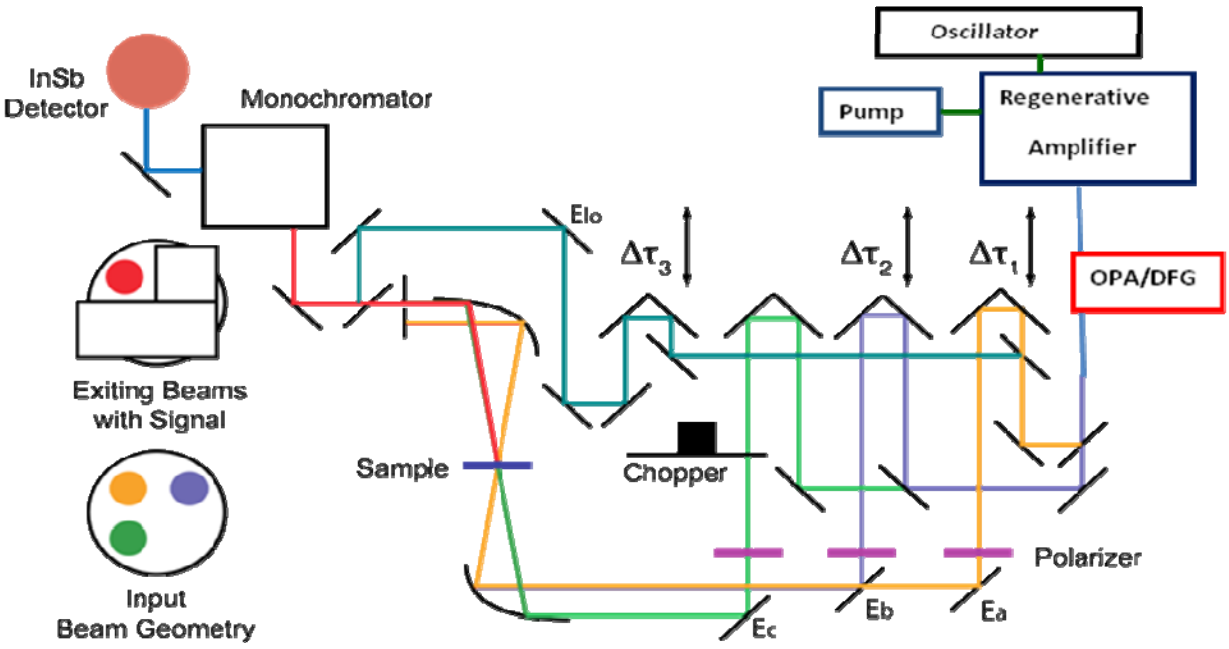

Figure 34 Laser arrangement to collect 2D-IR

This heterodyned signal is dispersed by a monochromator onto a detector. Such heterodyne detection provides both amplitude and phase information. If the vibrational echo is detected as it emerges from the sample, there is no phase information (Homodyned signal) and information about most dynamics in the system is lost. The heterodyned signal is chopped so that the signals detected is the cross term between the electrical field of homodyned electric field and local oscillator. The experiment set up above produces a 2D spectrum in the frequency domain. The vibrational echo signal is measured as a function of ω_3 with respect to two time variables τ and T. The monochrometer performs the Fourier transform to obtain ω_3. As τ is scanned keeping local oscillator fixed, it results in a interoferogram, which contain full information about amplitude, frequency and phase of the echo signal. These interoferogram are numerically fourier transformed to give ω_1.

2.6.2 Theoretical Background

2D-IR is a three wave four wave mixing. Three input electrical fields, $\mathbf{E_1}$,$\mathbf{E_2}$ and $\mathbf{E_3}$ each with a unique direction $\mathbf{k_1}$, $\mathbf{k_2}$ and $\mathbf{k_3}$ interact with the sample to produce a third-order nonlinear polarization $\mathbf{P^{(3)}}$. The unique single $\mathbf{E_{sig}}$ is radiated in an phase matched direction ($k_s = -\mathbf{k_1} + \mathbf{k_2} + \mathbf{k_3}$). The third order nonlinear polarization can be expressed in terms of a response function $\mathbf{R^{(3)}}(t_3 , t_2 , t_1)$. The radiated field can be expressed as

$$E_{sig}(K_{sig}, t) \propto iP^3(K_{sig}, t)$$
$$= \int_0^\infty dt_3 \int_0^\infty dt_2 \int_0^\infty dt_1 \, R^3 (t_1, t_2, t_3) \, E_3(k_3, t - t_3) \times E_2(k_2 t - t_3 - t_2) \times E_1(k_1, t - t_3 - t_2 - t_1) \qquad \text{Equation 5}$$

The response function above is a nested commutator of transition dipole moment $\mu(t)$.[52] Equation 6 describes the equation for this response function

where each symbols have their usual meanings.

$$R^{3}(t_1, t_2, t_3) = [\frac{i}{h}]^{3} \langle [[\mu(t_3 + t_2 + t_1), \mu(t_3 + t_2)], \mu(t_1)], \mu(0)] \rangle \quad \text{Equation 6}$$

The response function contains all information about the molecular evolution of the system.

The response function can be divided into nonrephasing $\mathbf{R}^{(3)}_{\mathbf{NR}}(t_3, t_2, t_1)$ and rephasing $\mathbf{R}^{(3)}_{\mathbf{R}}(t_3, t_2, t_1)$ quantum pathways depends on the oscillation frequencies during the evolution and detection time periods. $\mathbf{R}^{(3)}_{\mathbf{NR}}(t_3, t_2, t_1)$ pathways involve oscillations at the same frequency (same sign of the frequency) during both time periods, and thus they decay in time. $\mathbf{R}^{(3)}_{\mathbf{R}}(t_3, t_2, t_1)$ is called "rephrased" because the phase of the detected signal and the evolution time are conjugate to each other. In box car geometry, the rephrasing and nonrephasing diagram can be obtained by changing the sequence of the excitation beam. In heterodyne detection, the echo signal is written in terms of experimental time variables given by;

$$S(k_{sig;}\, \tau, T, t) \propto E_{LO}^{*}(k_{sig}).\, E_{sig}(k_{sig;}\, \tau, T, t) \quad \text{Equation 7}$$

where $E_{LO}^{*}(k_{sig})$ is the electric field of the local oscillator and $E_{sig}(k_{sig;}\, \tau, T, t)$ is the signal electric field which contains all the information. To obtain pure absorptive part, nonrephasing and rephrasing signals are collected separately. The signals are Fourier transformed and added.

$$S(k_{sig;}\, \omega_1, T, \omega_3) = S_{NR}(k_{sig;}\, \omega_1, T, \omega_3) + S_{R}(k_{sig;}\, \omega_1, T, \omega_3) \quad \text{Equation 8}$$

where $S_{NR}(k_{sig;}\,\omega_1, T, \omega_3)$ and $S_R(k_{sig;}\,\omega_1, T, \omega_3)$ are the nonrephasing and rephrasing 2D spectra defined as follows;

$$S_{NR}(k_{sig};\,\omega_1, T, \omega_3) = \mathrm{Re}[\int_0^\infty d\tau \int_0^\infty dt\, e^{(i\omega_m t + i\omega_\tau \tau)}\, S_{NR}(k_{sig};\,\omega_1, T, \omega_3)\,]$$

$$S_R(k_{sig};\,\omega_1, T, \omega_3) = \mathrm{Re}[\int_0^\infty d\tau \int_0^\infty dt\, e^{(i\omega_m t - i\omega_\tau \tau)}\, S_R(k_{sig};\,\omega_1, T, \omega_3)\,]$$

In these experiments, the t-axis $S(k_{sig;}\,\omega_1, T, \omega_3)$ is Fourier transformed by the monochrometer to give ω_3 and the τ axis is numerically Fourier transformed to give ω_1.

CHAPTER 3

CHARACTERIZING THE DYNAMICS OF FUNCTIONALLY REVELANT COMPLEXES OF FORMATE DEHYDROGENASE

3.1 Abstract

The potential for femtosecond to picosecond time scale motions to influence the rate of the intrinsic chemical step in enzyme-catalyzed reactions is a source of significant controversy. Among the central challenges in resolving this controversy is the difficulty of experimentally characterizing thermally activated motions at this time scale in functionally relevant enzyme complexes. We report a series of measurements to address this problem using two-dimensional infrared spectroscopy to characterize the time scales of active–site motions in complexes of formate dehydrogenase (FDH) with the transition-state-analog inhibitor azide (N^{3-}).We observe that the frequency-frequency time correlation functions (FFCF) for the ternary complexes with NAD^+ and NADH decay completely with slow time constants of 3.2 and 4.6 ps respectively. This result suggests that in the vicinity of the transition state, the active-site enzyme structure samples a narrow and relatively rigid conformational distribution indicating that the transition-state structure is well organized for the reaction. In contrast, for the binary complex, we observe a significant static contribution to the FFCF similar to what is seen in other enzymes, indicating the presence of the slow motions that occur on time scales longer than our measurement window.

3.2 Introduction

The functional role of protein motions at the femtosecond to picosecond time scale is a hotly debated topic in enzymology. While such a role could be of general nature, many experimental[4, 5, 46, 49-51] and theoretical studies[13, 18-20,

[53] of enzyme-catalyzed hydrogen transfers have invoked protein motions at this time scale to explain anomalous kinetic isotope effects and their temperature dependence. These studies result in the development of theoretical models, often referred to as Marcus-like models, in which the environmental reorganization that precedes the hydrogen-tunneling event has evolved to optimize the conformation of the transition state for tunneling.[3, 8, 46, 54] Figure 35 illustrates the physical picture underlying such models. Heavy atom motions along the reorganization coordinate carry the system to a point where the donor and acceptor wells in the double-well hydrogen atom potential are degenerate and tunneling can proceed. At this position, the donor-acceptor distance and its fluctuations determine the tunneling probability. Mathematically, the rate constant for hydrogen transfer in these models is given by expressions of the form,

$$k(T) = C \cdot e^{\frac{-(\Delta G^\circ + \lambda)^2}{4\lambda RT}} \int_{r_0}^{r_1} e^{f(DAD)} e^{\frac{-E(DAD)}{k_B T}} dDAD$$

where C is the fraction of reactive complexes, the first exponential, in analogy with the Marcus theory for electron transfer, reflects the reorganization of the heavy atoms that modulates the relative energies of the reactants and the products to minimize the energy defect between the zero-point levels of the donor and acceptor wells. ΔG° is the driving force for the reaction and λ is the reorganization energy. The second exponential gives overlap between the donor and acceptor wavefunctions as a function of the donor-acceptor distance that determines the tunneling probability, which is isotope dependent. The probability of having a particular donor-acceptor distance (DAD) is determined by the Boltzmann weight of the configurations having that DAD as given by the third exponential which is temperature

sensitive. These last two terms are integrated over the DAD coordinate to give the tunneling probability averaged over the distribution of DADs.

In the ideal case, near the tunneling ready configuration, the enzyme structure results in a DAD that strikes the optimum balance between wavefunction overlap and repulsive interactions between the donor and acceptor resulting in efficient tunneling that is insensitive to thermally induced fluctuations about the average DAD. Any perturbation of the reaction conditions, such as site-specific mutations, detunes the enzyme structure from the optimal DAD, so that local, femtosecond to picosecond time scale fluctuations of the active site are required to bring the donor and acceptor close enough for efficient tunneling to take place, thereby resulting in a temperature-dependent isotope effect.

Owing to the small transient population of the transition state, it is difficult to study the motions of reactive enzyme complexes in the vicinity of the transition state experimentally. A close experimental approximation to this ideal is to study the dynamics of an enzyme in a complex with a transition-state-analog inhibitor. There have been several infrared spectroscopic studies of enzyme-ligand interaction dynamics with substrate-analog complexes that mimic the ground state.[55-60] These studies use infrared echo and two-dimensional infrared (2D IR) spectroscopies to measure the frequency-frequency time correlation function (FFCF) that reveals the time scales for frequency fluctuations of the vibrational chromophore. These measurements use the stretching vibration of a small molecule bound at the active site of the protein to sample the conformational fluctuations and report them in the form of frequency fluctuations. Protein motions span time scales from femtoseconds to seconds. These IR studies are sensitive to motions from hundreds of femtoseconds up to 100 picoseconds, the lower limit being

dictated by the pulse-duration of the laser, and the upper time scale being determined by the vibrational lifetime of the reporter vibration. As a result, protein motions that occur on longer time scales appear as a static, heterogeneous conformational distribution in the FFCF. These studies of protein dynamics typically reveal fluctuations on three time scales: the first ranges from motionally narrowed to a few hundreds of femtoseconds, the second ranges from a few to 20 picoseconds, and the third involves motions at time scales longer than 20 ps that typically appear as a static contribution that typically represents 20-30% of the overall FFCF decay. These studies also show that solvent viscosity, point mutations of the protein, and substrate binding can modulate the time scales and relative amplitudes of protein dynamics.

We report a study of the enzyme formate dehydrogenase (FDH) that catalyzes the NAD^+-dependent oxidation of formate to carbon dioxide via hydride transfer to the C-4 carbon of the nicotinamide ring of NAD^+. FDH is an industrially important enzyme in the regeneration of NADH and NADPH for biocatalysis. Azide, which is an excellent vibrational chromophore, is a tight-binding inhibitor for FDH with an inhibition constant that we have measured as K_i = 40 nM. Because azide is isoelectronic with the carbon dioxide product and negatively charged like the formate anion reactant, it is a potent analog of the transition-state structure of the catalyzed reaction. Thus FDH serves as an ideal system to test the predictions of the Marcus-like model.

Figure 36 illustrates the active-site structure of the ternary complex of FDH with azide and NAD^+ based on a crystal structure of the ternary complex of FDH from *Pseudomonas* sp. 101, which has high sequence homology to the *Candida boidinii* enzyme used in our measurements. The

active-site structure is compact. It is located between two similar structural motifs each a sandwich of α-helix, parallel β-sheet, and α-helix. Several bulky, hydrophobic residues surround the azide and the nicotinamide ring bringing them close together. Azide forms H-bonds to a pair of residues on each end, Arg-284 (using *Pseudomonas* numbering) and His-332 on one end and Ile-122 and Asn-146 on the other. These highly conserved residues bind the substrate in the active site and orient it for reaction. These four residues also connect to both rigid structural motifs providing a link between these two structural domains of the enzyme that close together to isolate the active site. Arg-284 and Asn-146 lie at the ends of α-helices on either side of the β-sheet forming the α–β–α sandwich on one side of the active site. Ile-122 is in a loop connecting a β strand and an α–helix on the opposite side of the cavity. His-332 sits in a segment connecting a β strand on one side of the active site to one of the α-helices of the α–β–α sandwich on the other side of the active site. Ligand binding leads to conformational changes in the enzyme that close the active site drawing these two secondary structural domains together.

Our study of the temperature dependence of the KIE for FDH reveals a temperature independent isotope effect over the temperature range from 5 ºC to 45 ºC.[84] Under the framework of the Marcus-like model, this indicates that the active site of the enzyme provides an optimal DAD for tunneling, thus the fluctuations about this optimum DAD must be small amplitude motions suggesting that the active site structure samples a narrow conformational distribution and that the fluctuations occur on short time scales. This result is corroborated by our recent infrared echo study of the ternary complex of FDH with azide anion, a transition-state-analog inhibitor, and nicotinamide adenine dinucleotide (NAD^+) that reveals qualitatively distinct dynamics from those reported for other proteins. This ternary complex, whose

conformation closely resembles the transition state for the catalyzed reaction, exhibits no static, heterogeneous contribution to the FFCF decay. This result indicates that the structure of the enzyme as it approaches the transition state, is rigid and samples a narrow conformational distribution consistent with the emerging view of the catalyzed hydride transfer as described above.

The present work both extends and expands on these earlier studies by measuring 2D IR spectra that allow us to extend the upper limit on the waiting time to 5 ps, to confirm the absence of a static component, and probing the dynamics of two other complexes, the ternary complex of azide-NADH-FDH and the azide-FDH binary complex. These complexes allow us to test the hypothesis that the narrow conformational distribution and rigid dynamics observed for the ternary complex with NAD^+ reflect enzyme-ligand interactions that confer particular stability and rigidity consistent with the transition-state configuration.

3.3 Result and Discussion

Figure 37 shows 2D IR spectra for the ternary complexes with NAD^+(top), NADH (middle), and the binary complex (bottom). We show 2D spectra for T = 25fs (left), 500 fs (center), and 2.2 ps (right). The red lobe represents increased transmission as a result of ground state bleaching and stimulated emission whereas the blue lobes represent decreased transmission corresponding to the excited state absorption. At early waiting times, the lobes are elongated along the diagonal indicating a strong correlation between the frequency ω_1, measured before the waiting time, and the frequency ω_3, measured after the waiting time. At later waiting times, however, the lobes rotate toward horizontal indicating the loss of correlation between the frequency during ω_1 and that during ω_3. This loss of correlation and the corresponding change in peak shape reflect spectral diffusion

resulting from the equilibrium environmental fluctuations. The FFCF, which is given by $<\delta\omega(t)\delta\omega(0)>$, quantifies the time scales for the frequency fluctuations that report on the dynamics of the environment around the azide anion. To extract the FFCF from our 2D IR data, we use the center line slope (CLS) method introduced by the Fayer group.[61] In this method, we take slices through the 2D spectrum at each value of ω_1 and locate the position of the maximum in ω_3. The resulting sequence of points is the center line, shown as the blue circles in Figure 37, and the slope of this line is proportional to the FFCF for this value of T. The red lines in each spectrum show the linear fits to the CLS at each waiting time. By measuring the CLS as a function of T, we quantify the time scales for the structural fluctuations in the environment of the chromophore. Following the method described by Kwak et al., we fit the decay of the CLS to a sum of exponentials plus a constant offset. Then using the relative amplitudes and time scales of the decay as input we fit the infrared absorption line shape by varying the absolute amplitude of the FFCF.

Figure 38 shows the decay of the CLS vs. T for each of the three FDH complexes we have studied. In each case, we fit to as many as two exponentials and one static offset retaining the minimum number of terms necessary to accurately describe the decay. The CLS data are given by the points and the solid lines are the fits. The insets on each panel show the fits to the infrared absorption spectra using the fit decay parameters and adjusting the overall amplitude of the FFCF to fit the line shape in each case. It is important to note that the significant differences in the CLS decays, and thus the FFCF, are not apparent in the infrared absorptions spectra underscoring the fact that the infrared absorption spectra cannot be analyzed to yield detailed information about structural fluctuations. Table 2 shows the

values of the FFCF parameters resulting from the fits to the CLS decays and the infrared absorption spectra. These parameters correspond to the usual generalized Kubo line shape function of the form,

$$C(t) = \Delta_1^2 e^{-t/t_1} + \Delta_2^2 e^{-t/t_2} + \Delta_3^2$$

where the Δ's reflect to the amplitude of the frequency fluctuations and the τ's indicate the time scales of the motions responsible for those fluctuations. The ternary complex with NAD^+ has a fast time constant of 210 fs, and the values for the ternary complex with NADH and the binary complex are about 150 and 160 fs, respectively. These values are all the same within experimental error and consistent with our previous measurement of 250 fs for the ternary complex with NAD^+. The slow time constant for the ternary complexes with NAD^+ and NADH are 3.2 ps and 4.6 ps, respectively.There is a small amplitude slow time component for the binary complex with a decay time of 2.6 ps. The more significant feature of the binary complex, however, is the significant static term in the correlation function. This static offset corresponds to 50% of the overall decay. In contrast, for the ternary complexes, a static offset of more than 5% results in a qualitatively poor fitof the CLS decay. Figure 39 shows 2DIR spectra of each of the complexes at 5 ps. Comparing the CLS in each of these spectra at this relatively long delay time clearly illustrates the qualitative difference between the ternary complexes and the binary complex.

Proteins exhibit thermally activated motions on times scales ranging from hundreds of femtoseconds for very localized motions to milliseconds or longer for domain motions involving larger segments of the protein. 2D IR spectroscopy probes the FFCF, and thereby the protein motions that are

sensed by the transition state analogue (the IR-chromophore), only for a few tens of picoseconds at most. Although these experiments cannot identify the timescales for spectral diffusion for motions that occur beyond this time range, they do characterize the distribution of frequencies determined by the distribution of structures resulting from these slower motions. Motions at all timescales contribute to the initial value of the FFCF, but only those motions that occur on the femtosecond to picosecond timescale contribute to the FFCF decay probed in the 2D IR measurements. The remaining protein motions at longer time scales that still affect the chromophore give rise to an apparently static contribution to the FFCF. This static component does not mean that the protein does not move on longer timescales, rather there are slower motions that contribute to the frequency distribution that are not sampled within the experimental time window. The results of most previous studies of enzyme dynamics do exhibit a static contribution to the FFCF decay that is typically 20-40% of the initial value of the FFCF.

The ternary complexes of FDH with azide exhibit complete spectral diffusion within a few picoseconds. One possible explanation of the complete decay of the FFCF is that FDH actually does exhibit the expected slow structural dynamics but that azide is insensitive to those motions. Careful inspection of the structure of the ternary complex, however, casts doubt on this idea. The azide antisymmetric stretch transition frequency is sensitive to hydrogen bonding interactions. It is, therefore, reasonable to conclude that motions of the four hydrogen bonding partners, Asn-146, His-332, Ile-122, and Arg-284 make the dominant contributions to the observed FFCF. Each of these residues is located at the end of a major secondary structural component in the α-helix-β-sheet-α-helix motifs that flank either side of the active site. Given the locations of these residues at the ends of these

secondary structural elements, it is unlikely that these motifs could undergo large amplitude motions without modulating the hydrogen bond distances between these residues and the active-site-bound azide. Fluctuations of these hydrogen bond lengths as a result of large amplitude motions of the secondary structural domains would appear as a static contribution to the FFCF. Thus, it seems unlikely that these groups are undergoing such long timescale, large amplitude motion. That does not mean that no part of the protein may be exhibiting more typical slow fluctuations, but such motions must involve parts of the protein that do not directly influence the active site or else we would see evidence of those motions in our measurements.

The more likely explanation for the absence of a static contribution to the FFCF is that the ternary complex is rigid and samples a narrow conformational distribution. Thus, the fluctuations at the active site are high-frequency, small-amplitude motions that are fully sampled within a few picoseconds. This explanation is consistent with the idea that the enzyme evolved to minimize the energy of the transition state. In the degrees of freedom orthogonal to the reaction coordinate, a transition state corresponds to a deep energy minimum. A transition-state-analog complex, like the ternary complex with azide and NAD^+, takes advantage of those same interactions that stabilize the transition state, but does not have the unbound coordinate of a reactive complex. This structure is in a deep potential well with steep walls, the thermally accessible conformational space corresponds to a narrow structural distribution, and the fluctuations about the equilibrium structure are sampled on short timescales. That is not to suggest that the whole protein must be entirely rigid or that distal parts of the complex cannot undergo slow thermal motions. This rigidity perhaps exists only in the vicinity of the active site, the portion of the protein responsible for

the enzyme-ligand-cofactor interactions and contributes to the lowering of the free energy barrier for the reaction. In accordance with the temperature independent KIEs measured for this enzyme, and their interpretation by the Marcus-like model, this rigidity may also correspond to the precise organization of the residues at the tunneling ready configuration necessary to achieve efficient tunneling.

If this interpretation of the data for the ternary complexes is correct, then we would predict that the binary complex should behave qualitatively differently because the binary complex lacks the NAD^+ cofactor and, thus, is a poor mimic of the transition state structure. Although both the ternary complexes show complete spectral diffusion on the picosecond time scale, the FFCF for the binary complex has a significant static component indicating persistent conformational heterogeneity beyond the first several picoseconds. The enzyme undergoes significant structural rearrangements upon binding the coenzyme. Because the coenzyme is not bound in the binary complex, these rearrangements have not taken place, and the binary complex does not represent the transition-state configuration. Thus the result for the binary complex indicates that the lack of a static component is not a property of this enzyme in general, and supports our interpretation that complete spectral diffusion in the ternary complexes reflects the transition-state-analog nature of these complexes.

The fastest component of the FFCF in each complex, with decay times ranging from 150 to 210 fs, reflects the timescale of the local hydrogen bond fluctuations of the four conserved hydrogen-bond partners that bind and orient the substrate in the active site. These motions are present in both the ternary and the binary complexes with similar amplitudes and time scales. The corresponding motions may well involve collective compression of the

active site residues corresponding to the "gating motions" referred to in the Marcus-like model that modulate the donor acceptor distance. Simulations of different enzymatic systems have suggested that the gating motions or promoting vibrations have frequencies between 50 and 170 cm^{-1} corresponding to dynamics on a 200 to 700 fs time scale consistent with the dynamics we observe. The picosecond time scale component of the FCCF is somewhat faster for the ternary complex with NAD^+ than for NADH. This difference is reasonable since the ternary complex with the NAD^+ has a higher charge density with the anionic azide and the cationic nicotinamide ring located within 3 Å of one another. The consequence of this high charge density is that structural fluctuations cost more energy for the ternary complex with NAD^+ leading to faster dynamics.

3.4 Conclusion

We report the FFCF of azide, a transition state analogue inhibitor of FDH, in ternary complexes that mimic the transition state structure, and the binary FDH-N_3 complex that adopts a structure that is removed from the transition state. The FFCFs for the ternary complexes decay completely to zero with long time constants of a few picoseconds. In contrast, the FFCF for the binary complex exhibits a significant static contribution to the overall decay. These results are consistent with the interpretation that the active site structure of the enzyme is rigid in the proximity of the transition state exhibiting dynamics only at the ps to sub-ps time scale. Since the binary complex does exhibit a static component, it appears that the absence of the static component in the ternary complexes is a signature of the transition-state structure. This is consistent with the conclusion of our earlier KIE measurements that the active site environment is well organized for the reaction[62,84]. In addition, the subpicosecond contributions to the FFCF that

we observe in each complex are of similar time scales and may reflect the kind of compressive active-site motions that have been invoked in reactions where gating is necessary to modulate the donor-acceptor distance and that are believed to be present in the enzyme even if such motions do not influence the temperature dependence of the KIE, as is the case for FDH. In order to expand these observations to other enzymes, we need general probes which can bind to the active sites and report the dynamics in fs-ps timescales. However, there is a dearth of probes that can bind to the active sites, sensitive to local environmental changes and minimally perturb the native structure of the protein. Currently, we are developing general probes with simple transition, largely decoupled vibrational mode at mid-IR with a relatively intense band separated from rest of the molecule.

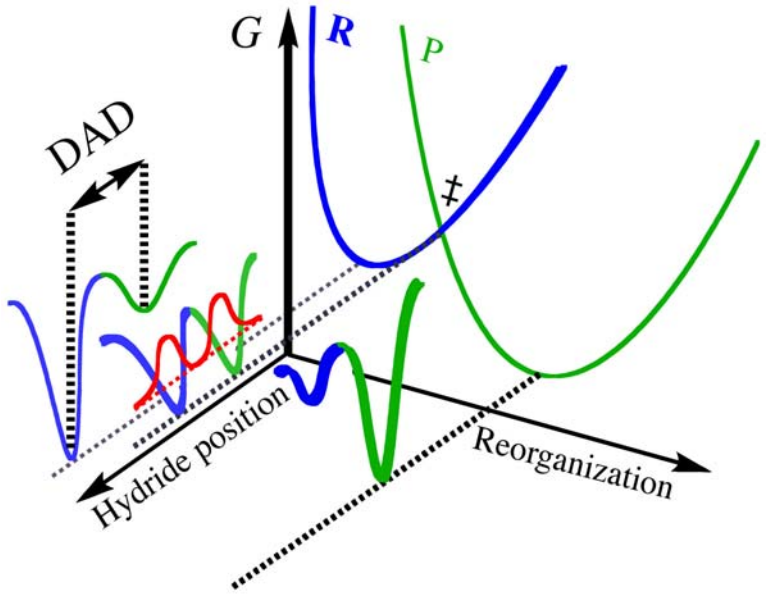

Figure 35 An illustration of Marcus-like model

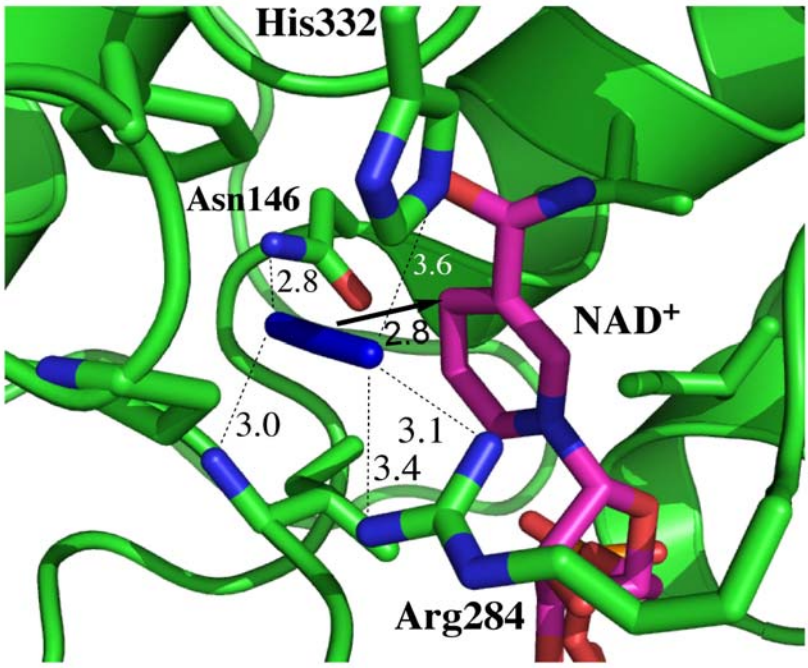

Figure 36 Active site structure of FDH-azide- NAD^+

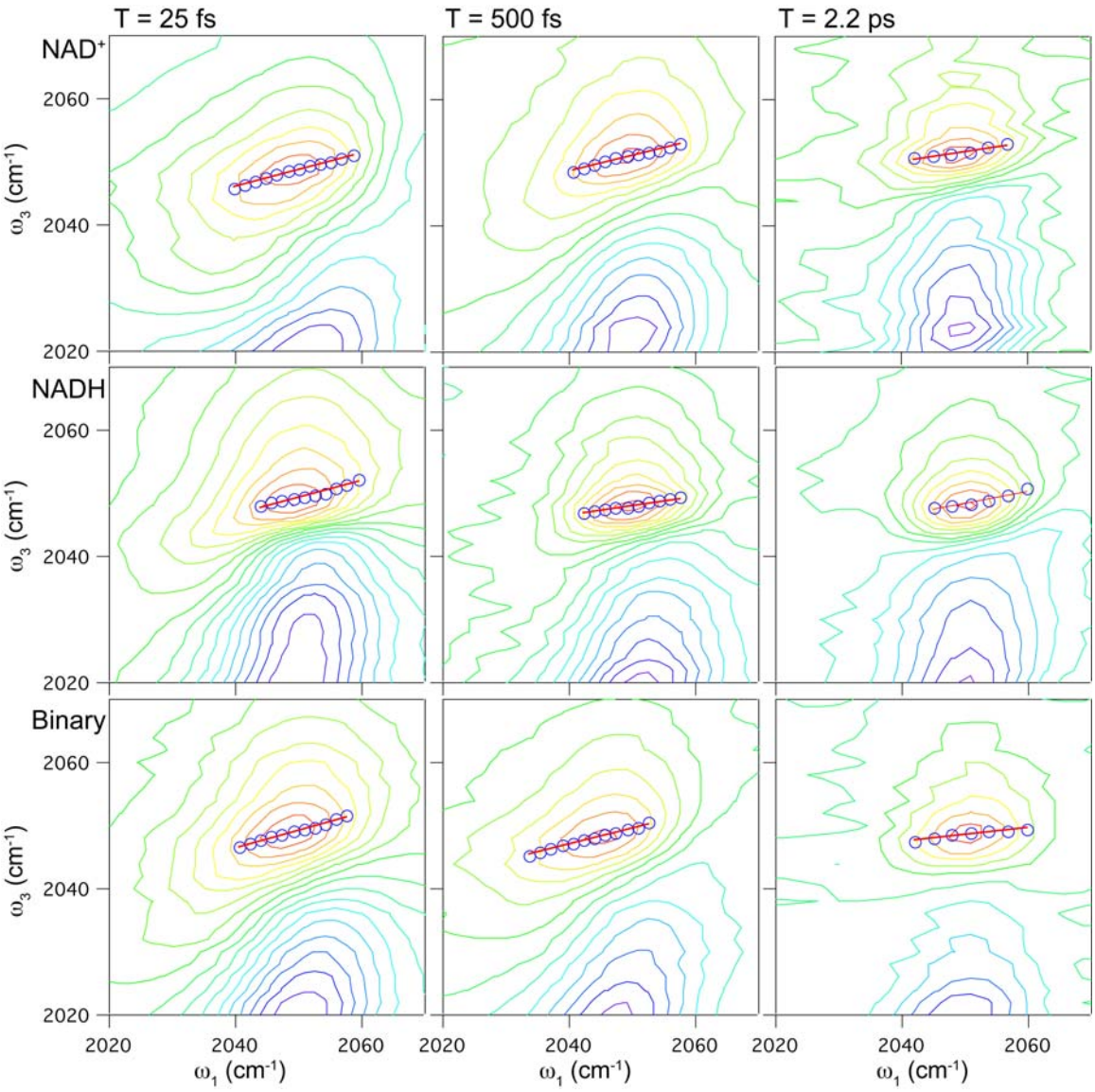

Figure 37 2D-IR spectra of azide in different complexes for waiting time of T = 25 fs, 500fs and 2200 fs

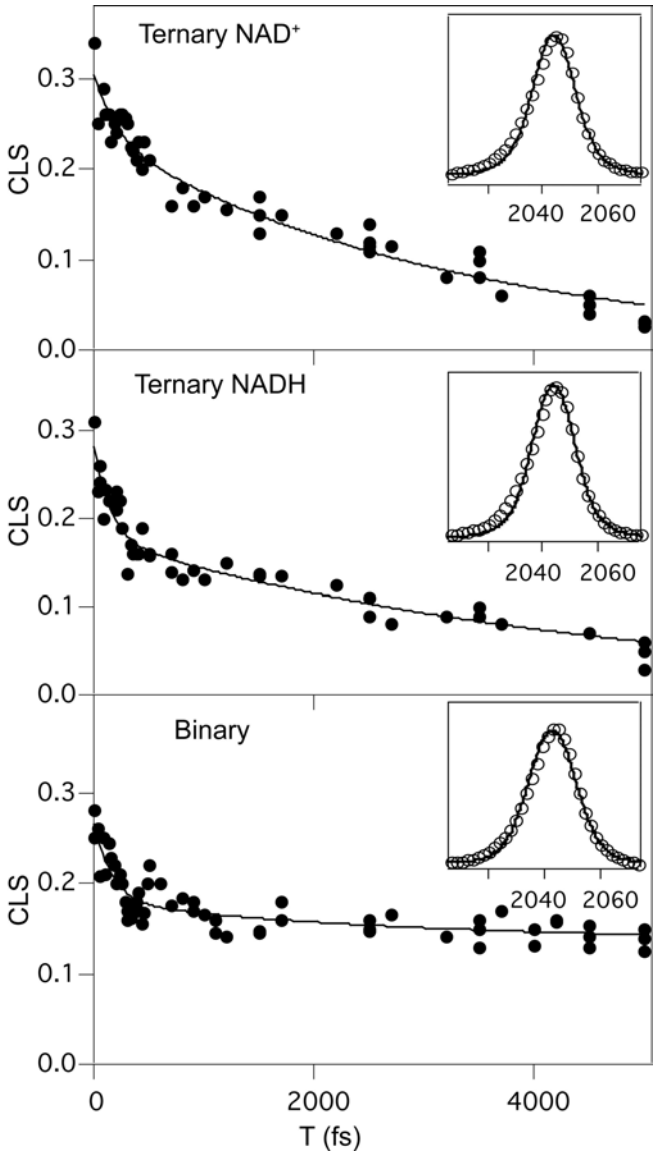

Figure 38 CLS decays for FDH complexes. The markers are experimental values and the solid lines are fit to decays. The inset shows experimental spectra fitted to an FFCF with fit parameters obtained from CLS decays.

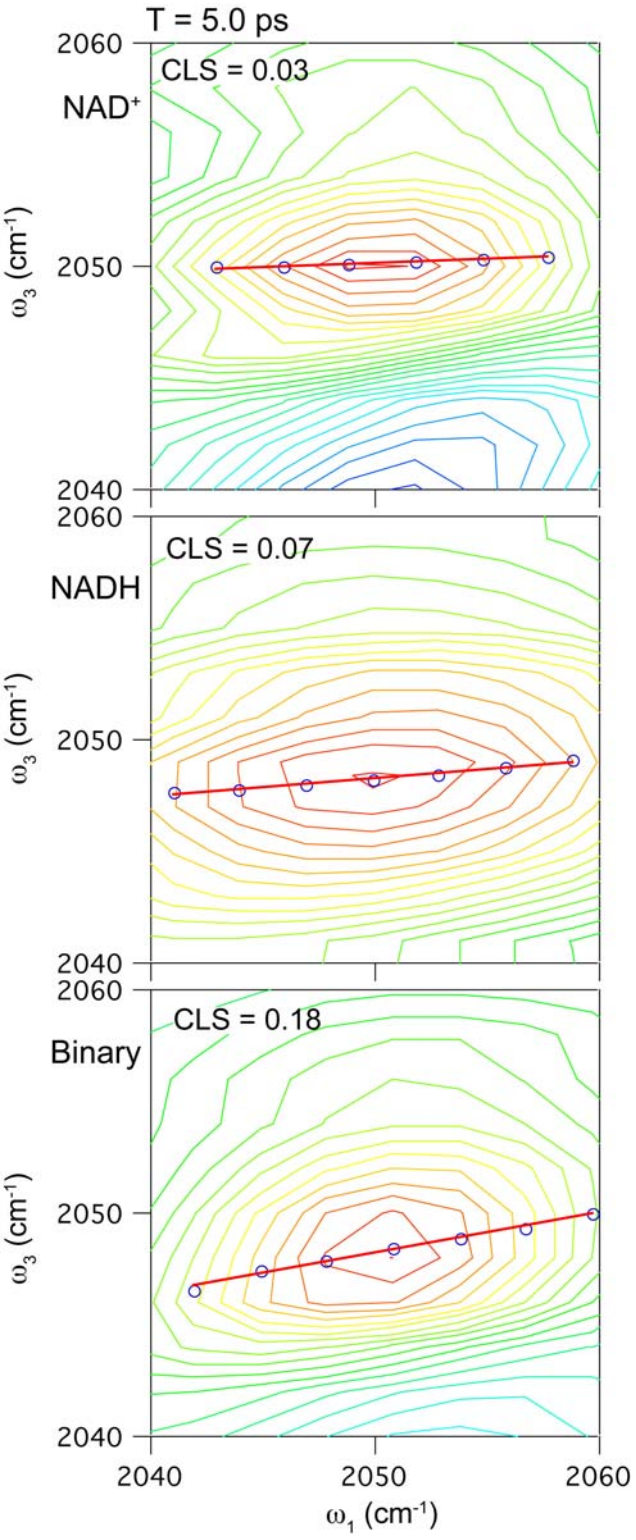

Figure 39 2D-IR at T = 5 ps for FDH with NAD^+ (top) and NADH (middle) and the binary complex (bottom)

Table 2 Frequency-frequency time correlation function (FFCT) parameters from the fits to the CLS decays and the linear absorption spectra

	Δ_1 (ps^{-1})	τ_1 (ps)	Δ_2 (ps^{-1})	τ_2 (ps)	Δ_3 (ps^{-1})
NAD	0.9 ± 0.2	0.21 ± 0.1	1.4 ± 0.2	3.2 ± 0.5	-
NADH	1.0 ± 0.2	0.15 ± 0.1	1.3 ± 0.2	4.6 ± 0.5	-
Binary	1.1 ± 0.2	0.16 ± 0.1	0.8 ± 0.2	2.6 ± 0.5	1.4 ± 0.2

CHAPTER 4

CHARACTERIZATION OF AZIDO-NAD$^+$ TO ASSESS ITS POTENTIAL AS A 2D IR PROBE OF ENZYME DYNAMICS

4.1 Abstract

Enzyme active site dynamics at femtosecond to picosecond time scales are of great biochemical importance, but remain relatively unexplored due to the lack of appropriate analytical methods. 2D IR spectroscopy is one of the only methods that can examine chemical and biological motions at this time scale, but all the IR-probes used so far were specific to a few unique enzymes. The lack of IR-probes of broader specificity is a major limitation to further 2D IR studies of enzyme dynamics. Here we describe the synthesis of a general IR-probe for nicotinamide dependent enzymes. This azo analog of the ubiquitous cofactor nicotinamide adenine dinucleotide is found to be stable and bind to several dehydrogenases with dissociation constants similar to the native cofactor. The infrared absorption spectra of this probe bound to several enzymes indicate that it has significant potential as a 2D IR probe to investigate femtosecond dynamics of nicotinamide dependent enzymes.

4.2 Introduction

Protein motions are necessary for an enzyme's biological function,[2, 4, 5, 63, 64] but the role of enzyme dynamics at various timescales and their contribution toward catalytic activity is not clear. Enzymes undergo slow conformational sampling that involves large regions of the protein moving on time scales of nanoseconds to seconds. In addition, there are local motions that occur on the picosecond to femtosecond time scale. Theoretical studies by Schwartz and others[18, 20, 21, 65] have suggested that, in some enzymes, protein promoting vibrations and internal motions at femtosecond (fs) to picosecond (ps) timescales are necessary for catalysis as they modulate the width and

height of the activation barrier. Indirect experimental evidence of such motions comes from the anomalous kinetic isotope effects (KIEs) seen in many enzymes.[66-69] This behavior is a hallmark of quantum tunneling, which requires that the nuclear wave functions of donor and acceptor potential wells should be close to each other and have degenerate energies. It has been suggested that protein dynamics[70, 71] at the active site can cause fluctuations in the donor and the acceptor distance that result in coupling of these environmental dynamics to the C-H bond activation. Although theoretical studies have suggested that enzyme motions at the fs-ps time scale are more likely to be involved in covalent bond activation than slower motions, they are relatively unexplored. The main reason is the lack of a suitable analytical tool that will afford exploration of these dynamics in a large and significant group of enzymes and other biological systems.

Recently developed nonlinear vibrational spectroscopies can directly investigate the fast motions in proteins.[55, 58, 72] Infrared photon echo and 2D IR spectroscopies can record equilibrium fluctuations with sub-picosecond time resolution.Previous studies of globular proteins,[56, 59] membrane proteins,[73] amyloid fibers,[74, 75] HIV-1 reverse transcriptase,[57] carbonic anhydrases,[62]and formate dehydrogenase[76] have provided insights into protein structural dynamics at fs to ps time scales. The mid-IR chromophores used for these studies, however, are not generally applicable to most enzymatic systems. For example, we have recently reported the dynamics of formate dehydrogenase complexes using the azide anion as a probe of the active site motions. This anion is a transition–state-analog inhibitor, has a nanomolar binding constant, and forms stable complexes with FDH that exhibit a vibrational transition in the mid-IR in a region that is devoid of localized transitions from the enzyme. Unfortunately, azide ion does not bind

to a broad range of enzymes. Furthermore, when it does bind it is not generally a good transition state analog. A general probe in mid-IR for 2D IR studies of protein dynamics is thus lacking. A suitable IR probe for 2D IR studies should (a) bind with the enzyme at the active site, (b) have a broad specificity, to afford examination of a significant number of enzymes and biological systems, and (c) have a suitable transition in the mid-IR region.

Nicotinamide-dependent cofactors are necessary for the function of many enzymes and other biological systems. Analogs of nicotinamide adenine dinucleotide (NAD^+) have been widely studied to assess their binding affinities, optical properties, and enzymatic reactivity.[29] Here, we report the synthesis of a mid-IR active analog of NAD^+ in which the amide group in the nicotinamide ring has been replaced with an azide. We also characterize its infrared absorption spectra to assess its potential as a 2D IR probe to investigate enzyme active-site dynamics. On the basis of these studies we conclude that azido-NAD^+ is a suitable chromophore for 2D IR spectroscopy that can readily be incorporated into the active sites of NAD-dependent enzymes. Because NAD^+ is a cofactor for numerous enzymes, such an analog should have widespread applicability for 2D IR studies of enzyme dynamics.

4.3 Result and Discussion

Although azido-NAD^+ has been synthesized previously, it was never purified and neither its kinetic nor spectroscopic properties were characterized quantitatively. The synthesis of azido-NAD^+ requires control of both the pH and the mole ratio between 3-azopyridine and NAD^+. Once prepared, the analog is a white solid that is soluble in phosphate buffer and methanol at room temperature and has a unique UV absorption at 303 nm that is distinct from both 3-azidopyridine, and NAD^+ as shown in Figure 40. The ratio of the UV absorbance at 260 nm to that at 303 nm is 4:1. This ratio

remains unchanged in phosphate buffer pH 7.5 for 24 hrs at 25 ^{o}C indicating that the analog is stable under normal physiological conditions. As seen in Figure 41, azido-NAD$^+$ also exhibits a single peak in the mid-IR at 2140 cm^{-1}, in contrast to 3-azopyridine, which has two peaks.

The analog can behave as either an inhibitor or a substrate depending on the enzyme. With both FDH and GDH, it is an active substrate that reacts to form azido-NADH and CO_2 or gluconolactone, respectively. The formation of azido-NADH is apparent from the UV absorption at 340 nm as seen in Figure 42. Azo-NADH also fluoresces at 430 nm, when excited at 340 nm in contrast to native NADH, which fluoresces at 460 nm.

Table 3 shows the kinetic parameters for azido-NAD$^+$ interacting with three different NAD-dependent enzymes: formate dehydrogenase (FDH), malate dehydrogenase (MDH), and glucose dehydrogenase (GDH). The dissociation constants (K_d) for the binary complexes of the enzymes with azo-NAD$^+$ are typically within the range of 5-300 μM. Measurements of the dissociation constant for ternary complexes employ either the substrate, if azido-NAD$^+$ is an inhibitor, or an inhibitor for enzymes where azido-NAD$^+$ is an active substrate. In the case of FDH we use the transition-state-analog inhibitor azide, for MDH we use the substrate, malate, and for GDH, we use the product of the catalyzed reaction, gluconolactone. As expected, the K_d of azido-NAD$^+$ for each ternary complex is lower than for the corresponding binary complex. Note that, in contrast to the other enzymes, for which we measure K_d by ITC, the binary and ternary dissociation constants of GDH were obtained by measuring the quenching of tryptophan florescence upon binding with the analog.

The kinetic results indicate that the binding affinity of the azido-NAD$^+$ is comparable to that of native NAD$^+$ for each of these enzymes.[29, 77] The

azido-NAD^+ analog behaves as a substrate for with FDH and GDH and as a competitive inhibitor with MDH. It seems likely that the analog binds in the enzyme active site in a geometry that is similar to that for the native cofactor. The turnover number for *Candida Boidinii* FDH with NAD^+ is reported to be 3.7 s^{-1}, which compares favorably to our observation of 7.5 s^{-1} with azido-NAD^+.[78] The dissociation constant for NAD^+ with GDH from *Bacillus magenterium* was reported to be 600 μM,[79, 80] which is similar to the 300 μM dissociation constant we report for the azo-NAD-GDH complex. With MDH from *sus scrofa*, azido-NAD^+ behaves as an inhibitor (K_I = 83 μM) which is similar to K_m of NAD^+ (140 μM) with the same enzyme.[41, 81]These binding behaviors suggest that azido-NAD^+ forms stable complexes with these three enzymes that are structurally and functionally similar to the enzyme with the native cofactor. Consequently, it seems likely that azido-NAD^+ will be a general tool to probe the dynamics of NAD-dependent enzymes by 2D IR spectroscopy.

The azide antisymmetric stretching transition of azido-NAD^+ is centered at 2140 cm^{-1} with a full width at half maximum (FWHM) of 33 ± 2 cm^{-1}. The molar absorptivity at the maximum of this transition is 250 $M^{-1}cm^{-1}$, which is a little more than a factor of 10 smaller than that for the antisymmetric stretch of the azide anion. Thus, azido-NAD^+ is a weaker chromophore than azide, but it still has a substantial transition moment suggesting that it could still be of significant potential value as a probe of protein dynamics using 2D IR spectroscopy. Figure 43 shows the FTIR spectra of azido-NAD^+ free in solution and bound in the binary complex with FDH. Although the transition frequency does not shift much, the band narrows considerably, from 33 cm^{-1} to 26 cm^{-1}. Similar band narrowing of the absorption spectrum upon binding to the protein has been seen frequently for

chromophores that have been used to study protein dynamics via 2D IR spectroscopy, and it reflect that there is considerably less conformational heterogeneity in the enzyme than there is free in solution as is apparent too from the results of the 2D IR measurements. Table 4 summarizes the peak positions and line widths of the azo-transition in the binary and ternary complexes with each of the enzymes we have studied. In general there is very little change in the peak position or the line width among these enzymes even in comparing the binary and ternary complexes. Although the absorption spectra are not quantitatively different, it is well known that systems with quantitatively similar absorption profiles can exhibit qualitatively different dynamics when probed by 2D IR spectra. That is because the infrared absorption line shape cannot be used to uniquely determine the character of the underlying spectral dynamics.

Azides are very sensitive probes of environmental dynamics and organic azides hold great potential for exploring protein dynamics using 2D IR spectroscopy. Azido-NAD^+ provides a unique opportunity to investigate the active sites of numerous NAD-dependent enzymes that would otherwise be inaccessible by 2D IR. Based on our results, we can conclude that azido-NAD^+ binds to several NAD-dependent enzymes with an affinity that is similar to that for native NAD^+ and that the substitution of the azide at the amide position of the nicotinamide ring is a minor perturbation that, in at least two cases, does not inactivate the complex. Thus, we are able to use this analog to incorporate a vibrational reporter at the active site of the enzyme in a position where it is most likely to report dynamics that are functionally relevant. Furthermore, this chromophore should have widespread applicability to enzymes that utilize both NAD^+ and $NADP^+$. The development of an infrared chromophore that can be bound in the active site

of a wide range of enzymes and is suitable for 2D IR spectroscopy is a significant result.

A particularly interesting case for further study is that of the ternary complex in FDH where we can probe both the azo-stretching vibration of azido-NAD^+ as well as the azide anion antisymmetric stretch using 2D IR spectroscopy. Figure 44 shows the infrared absorption spectrum of this complex with both the azide anion and azido-NAD^+ absorption bands. Because we have previously characterized the dynamics of the ternary complex of FDH with azide and NAD^+, the complex with the azido-NAD^+ coenzyme is an especially interesting one in which we can determine the extent to which the two probes measure the same dynamics, and assess the magnitude of the perturbation to the dynamics of the active site caused by azido-NAD^+. Even more significant is the potential of azido-NAD^+ has to be a general probe of enzyme dynamics in NAD-dependent biological systems (e.g., dehydrogenases, reductases, oxidases, membranal proteins involved in cellular respiration, and more). Because the vibrational reporter is located on the coenzyme, it is possible to prepare a wide range of complexes with different substrates and inhibitors and to study both the binary and ternary complexes in these enzymes using 2D IR. In addition, because azido-NAD^+ is also an active substrate for some of these enzymes, it is straightforward to reduce it to azido-NADH, and to study complexes with the reduced form of the cofactor, with a complementary set of substrates and inhibitors. Furthermore, the same synthetic approach can also be extended to the preparation of azido-$NADP^+$, which is an even better substrate of NADase. Azido-$NADP^+$ and azido-NADPH would further extend the potential applications of vibrational spectroscopy as a probe for $NADP^+$ and NADPH dependent enzymes.

4.4 Conclusion

We have synthesized, purified, and characterized the interaction of azido-NAD^+, an azide derivatized analog of the NAD^+ coenzyme. We have also measured the infrared absorption spectra of this analogue of the ubiquitous nicotinamide cofactor both free in solution and bound to several enzymes. For both FDH and GDH, azido-NAD^+ is an active substrate and binds with an affinity that is comparable to the natural coenzyme. For MDH, it is a competitive inhibitor. Azido-NAD^+ exhibits a distinct vibrational transition associated with the antisymmetric stretching vibration of the azo group at 2140 cm^{-1}, which is located in an ideal spectral region that is clear of other transitions associated with either the solvent or the protein. Although the transition moment is not as strong as for the azide anion, at 250 $M^{-1}cm^{-1}$, the molar absorptivity is certainly high enough to make it accessible 2D IR spectroscopy.[82]2D-IR studies of azido-NAD^+ in water have demonstrated that it is an excellent probe of the dynamics of the water molecules that are solvating the azo moiety. In addition, the line shape of the transition shows a distinct narrowing upon binding indicative of the sensitivity of this vibrational mode to its environment. Taken together, the interactions of this probe with several NAD-dependent enzymes and its ability to probe dynamics at the fs-ps time scale in 2D-IR experiments, suggest that azido-NAD^+ is a promising new broad specificity probe of the active-site dynamics of NAD-dependent dehydrogenases and potentially other systems. Studies of the 2D IR spectroscopy of azido-NAD^+, azido-$NADP^+$ and a variety of enzymatic systems are underway to further demonstrate the applicability of this probe.

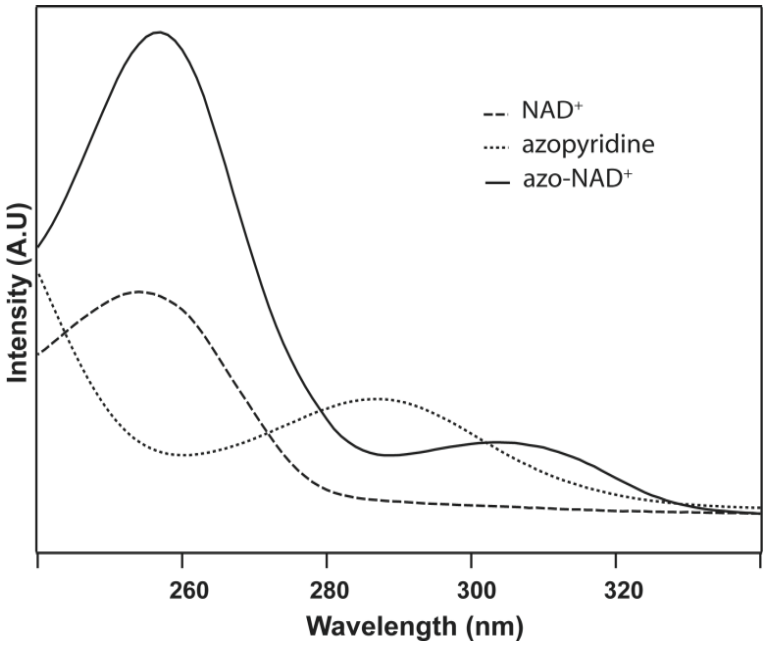

Figure 40 Normalized UV absorption spectra of azido-NAD^+ (-), azidopyridine (…), and NAD^+ (- -).

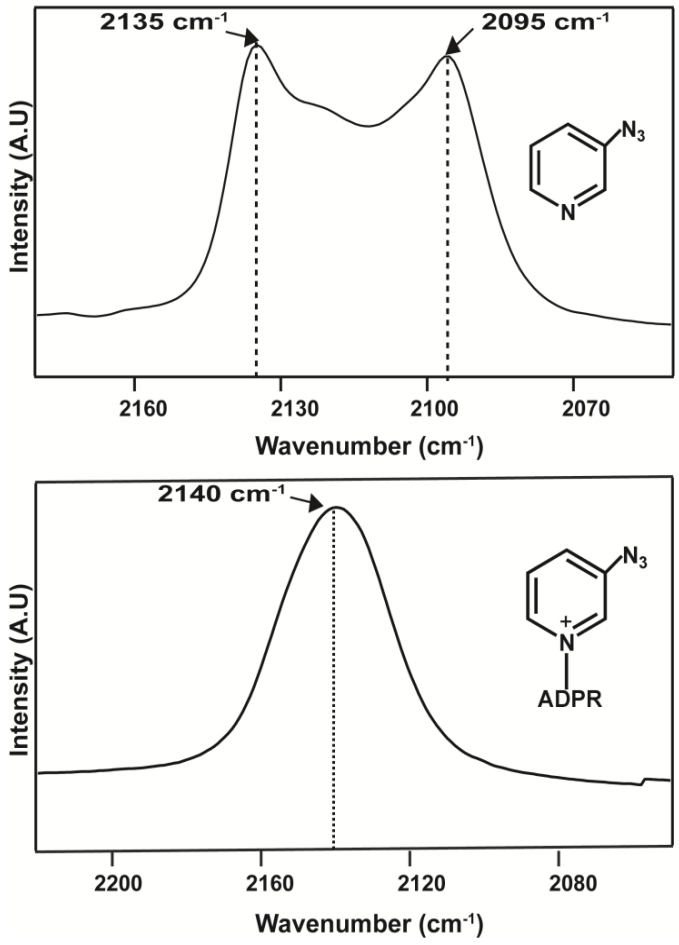

Figure 41 IR absorption spectra of azopyridine (upper panel) and azido-NAD+ (lower panel).

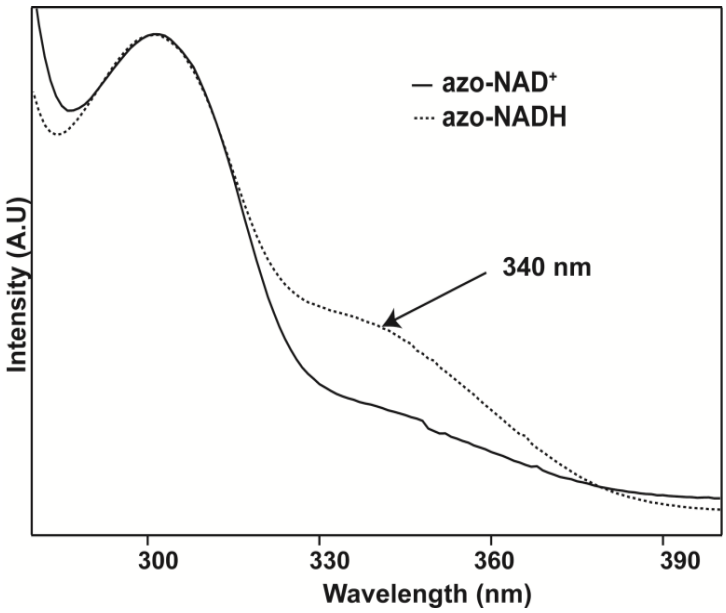

Figure 42 UV absorption spectra showing the conversion of azido-NAD+ to azido-NADH.

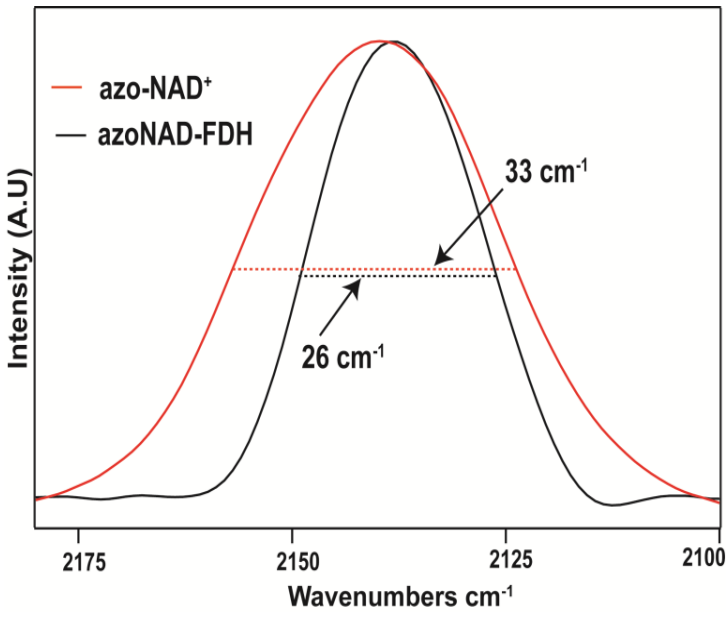

Figure 43 IR absorption spectra of azido NAD+ in solution (-) and bound to FDH (-).

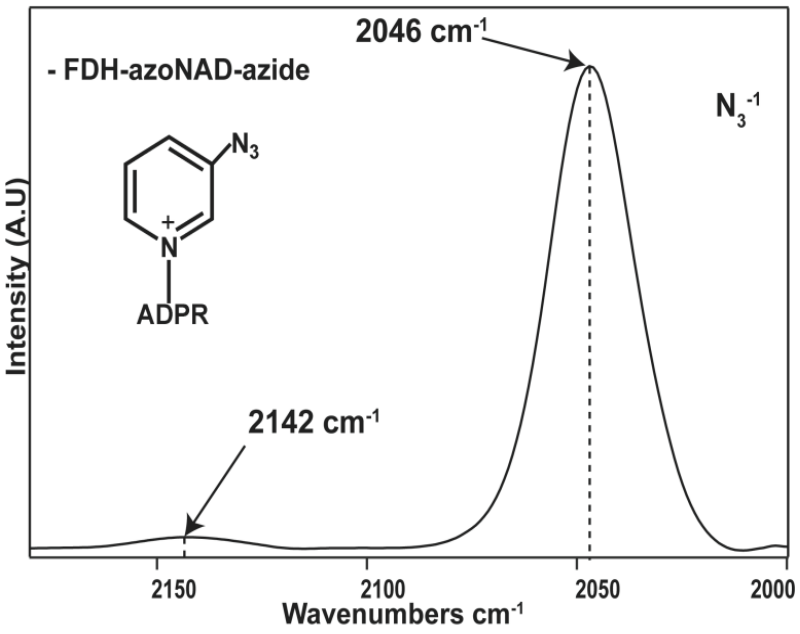

Figure 44 FTIR of ternary complex of FDH-azide-azido NAD^+

Table 3 Kinetic and binding parameters of enzymes with the azido-NAD^+ analog.

	K_d µM (Binary)	K_d µM (Ternary)	K_i µM	K_m µM		k_{cat} s^{-1}	
				Azido-NAD^+	NAD^+	Azido-NAD^+	NAD^+
FDH	63	8.2	-	378	90[b]	7.5	3.7[c]
MDH	152	70	83	-	140	-	45
GDH	300[a]	142[a]	-	72	370[d]	344	390[d]

[a] Fluorescence experiments; [b]Ref [78], [c]Ref [77], [d]Ref[83]

Table 4 IR parameters

	Peak Position (cm^{-1})	FWHM (cm^{-1})
Azido-NAD^+	2140	33
FDH-Azido-NAD^+	2138	26
FDH-Azido-NAD^+-azide	2142 [a]	27
MDH-Azido-NAD^+	2142	28
MDH-Azido-NAD^+-malate	2138	26
GDH-Azido-NAD^+	2141	27
GDH-Azo-NAD^+-Glucono-δ-lactone	2142	28

[a] Azide anion shows a peak at 2046 cm^{-1} compared to 2042 cm^{-1} for FDH-NAD^+- azide

CHAPTER 5

2D IR SPECTROSCOPY OF AZIDO-NAD$^+$

5.1 Abstract

Mid-IR active analogs of enzyme cofactors have the potential to be important spectroscopic reporters of enzyme active site dynamics. Azo-NAD$^+$, which has been recently synthesized in our laboratory, is a mid-IR active analog of nicotinamide adenine dinucleotide (NAD$^+$), a ubiquitous redox cofactor in many biological processes. In this study, we measure the frequency-frequency time correlation function (FFCF) for the antisymmetric stretching vibration of the azo group of azido-NAD$^+$ in water and show that it is sensitive to local environmental fluctuations, which, in water, are dominated by hydrogen-bond dynamics of the water molecules around the probe. Our results demonstrate the potential of azido-NAD$^+$ as a vibrational probe.

5.2 Introduction

There is growing evidence that femtosecond to picosecond time scale protein dynamics can affect the rate of enzyme-catalyzed hydrogen transfers[18, 20, 50, 84-88]. With the advent of non-linear vibrational spectroscopies like 2D IR, it is possible to explore the structure-dynamics-function relationships of proteins at the time scales most relevant to the catalyzed chemical conversion. Mid-infrared probes, such as pseudohalide anions, nitriles, and carbon monoxide are ideal as environmental reporters to monitor conformational fluctuations of proteins on the picosecond to femtosecond time scale because their absorptions fall within the "transparent" window of the protein and water absorption spectra from 1800 cm^{-1} to 2300 cm^{-1}.[56, 58, 59, 89, 90] There have been several reports of protein

dynamics measured using these mid-IR active chromophores as chelating agents, substrates, or inhibitors. For example, carbon monoxide has been used to study several heme proteins including myoglobin, hemoglobin, neuroglobin, and horseradish peroxidase. Azide anion has been used to study bovine carbonic anhydrase II,[62] and both wild-type and several mutants of human carbonic anhydrase II, and a transition-state analog complex of formate dehydrogenase. In addition, the nitrile chromophores of the nonucleoside inhibitor TMC278 have been used to study the dynamics HIV-1 reverse transcriptase.[57] The number of proteins for which femtosecond to picosecond dynamics have been studied is small because only a few proteins have a natural propensity to bind a mid-IR active chromophore. Thus, at present, the approach of using established probes to study protein dynamics is limited because such probes cannot be used with a wide variety of proteins. One strategy that has been pursued to address this problem is to attach a chromophore to the protein by chemical modification at a desired position within the protein. For example, nitrile or azido substituted amino acids such as p-cyano-phenylalanine, 5-cyano-tryptophan, or azido-alanine can be incorporated in the protein,[91-93] and their infrared spectroscopy has been shown to be sensitive to electrostatic interactions in their local environments. Another approach is to convert cysteine residues in the protein to an IR-active chromophore by chemically modifying the cysteine thiol in the protein to a thiocyanate. Yet another approach involves incorporating deuterated amino acids such as Met-d_3 and Leu-d_{10} into the protein site selectively and probing the C-D stretching vibrations of these deuterated amino acids.[94-97] A major challenge in all of the approaches, however, is that they all involve significant protein modifications that require site-specific mutations of the protein, and, sometimes, even involve expression the protein in fragments

and linking the fragments together to be able to make the whole protein with the label located in the desired position. Because of the significant protein chemistry involved, these approaches provide only limited opportunities for nonlinear spectroscopy since significant amounts of protein can be required, sometimes in excess of 100 mg for a single experiment. Thus, there is a great need for spectroscopic probes that can be incorporated into a wide range of proteins and offer a simpler path to obtaining the sample in adequate quantities than those currently employed.

Nicotinamide adenine dinucleotide (NAD^+), the related coenzyme 2′-phosphate-NAD^+ ($NADP^+$), and the reduced forms of these cofactors are ubiquitous redox agents for many biological processes.[98, 99] In fact, NAD^+ is a coenzyme for more than 600 enzymes that are involved in metabolism and protein posttranslational modifications. Analogs of NAD^+ are widely used as mechanistic probes to understand enzymatic pathways.[29, 38, 100-106] We have recently synthesized a mid-IR active analog of NAD^+, azido-NAD^+, that has the potential to be a general probe to investigate active-site dynamics in nicotinamide-dependent enzymes. In azido-NAD^+, the amide group on the nicotinamide ring is replaced with an azo group to serve as an infrared reporter that is expected to minimally perturb the interactions with enzymes to which it binds. Kinetic studies of this analog with a few enzymes suggest that it behaves similarly to native NAD^+ and behaves favorably. Azido-NAD^+ has a single transition at 2140 cm^{-1}, which has potential as a reporter of the active site dynamics as there are no major absorbances of proteins or water in this region. In aqueous solution, the line shape of this transition is considerably broader, 33 cm^{-1} than the typical line width for the enzyme-bound analog, 26-28 cm^{-1}. In addition, the azido antisymmetric stretching vibration is known for having a large transition dipole moment. It seems

likely that this chromophore can be a viable probe to study enzyme dynamics, but it is necessary to further spectroscopically characterize it to determine its population lifetime and to assess its sensitivity to solvent dynamics. In this letter, we report 2D-IR spectroscopy of this probe in phosphate buffer to characterize the aqueous solvation dynamics experienced by the azo group in azido-NAD^+. Our results demonstrate that hydrogen bonding fluctuations of the hydrogen-bonded waters in the first solvation shell make the dominant contribution to the observed dynamics. Furthermore, our results demonstrate the feasibility of using azido-NAD^+ as a probe of environmental fluctuations and suggest that it should be an excellent probe of protein dynamics in NAD-dependent enzymes.

5.3 Result and Discussion

Figure 45 shows 2D IR spectra of the azido stretching transition of azido-NAD^+ at three different waiting times. The red lobe represents increased transmission as a result of ground state bleaching and stimulated emission whereas the blue lobes represents decreased transmission corresponding to the excited state absorption. At early waiting times, the lobes are elongated along the diagonal indicating a strong correlation between the frequency ω_1 and the frequency ω_3 measured after the waiting time. At later waiting times, however, the lobes rotate toward horizontal indicating the loss of correlation between the frequency during ω_1 and that during ω_3. This loss of correlation and the corresponding change in peak shape reflect spectral diffusion resulting from the equilibrium environmental fluctuations. The two-point FFCF, which is given by $<\delta\omega(t)\delta\omega(0)>$, quantifies the underlying dynamics. To extract the FFCF from our 2D IR data, we use the center-line slope (CLS) method first introduced by the Fayer group.[107] In this method, we take slices through the 2D spectrum at each value of ω_1 and

locate the position of the maximum in ω_3. The resulting sequence of points is the center line, and the slope of this line is proportional to the FFCF for this value of T. By measuring the CLS as a function of T, we can quantify the time scales for the structural fluctuations in the environment of the chromophore. Following the method described by Kwak et al.,[61] we can then use the relative amplitude for the exponential decay and the time scales of that decay to fit the infrared absorption line shape to determine the FFCF. In Figure 45, the open blue circles show the center line for each spectrum along with the fit (red line). The CLS can have a maximum value of 1 in the absence of motional narrowing. The initial value of the CLS for azido-NAD^+ in water, however is just over 0.40 indicating that there is significant motional narrowing of the line shape.

Figure 46 shows the CLS as a function of T. We fit the decay of the CLS to a single exponential, which corresponds to a simple Kubo line shape. As is clear from the plot, however, the first 150 fs of the decay are nonexponential. Most likely, this nonexponential component corresponds to a fast oscillatory contribution to the FFCF that we cannot completely resolve because our pulse duration is too long, ~120 fs. Such oscillatory behavior has been predicted for azide in water,[108, 109] and it seems likely that the nonexpoential behavior that we observe is consistent with that theoretical prediction. Because we cannot fully characterize the fast nonexponential component of the dynamics, we fit the CLS decay after the initial 150 fs where the decay becomes a single exponential. Even though there is an additional faster component of the FFCF, because we cannot characterize it quantitatively, we will treat it as a motionally narrowed contribution to the line shape, which is reasonable as the absorption line shape is insensitive to the form of such a short time contribution as has been seen for azide in water.

We then fit the infrared absorption line shape to determine the FFCF. To do the fitting, we assume a Kubo line shape model for the FFCF, $C(t) = \Delta^2 e^{-t/\tau}$, and we include a homogeneous contribution to the line shape, Γ, associated with the fast structural fluctuations that result in a motionally narrowed contribution to the FFCF. The parameters that result from the fitting are $\Gamma = 12\ cm^{-1}$, $\Delta = 2.0\ ps^{-1}$, and $\tau = 655$ fs. The inset in Figure 46 compares the calculated and the experimental absorption spectra of azido-NAD^+. The calculated spectrum is in excellent agreement the measured spectrum. The FFCF for azido-NAD^+ reflects similar dynamics to those seen previously for aqueous solutions. The timescale of the exponential decay of the FFCF, $\tau = 655$ fs, is very similar to the FFCF decay seen for cyanide anion in water where the correlation function decays with a 464 fs time constant. For cyanide this time scale was suggested to involve the weakening and strengthening of hydrogen bonds between water and the anion. This interpretation is consistent with the interpretation of the FFCF decay for azide in D_2O as well.[44,45] By analogy with these previous studies, we conclude that the dynamics represented by the 655 fs decay in the FFCF of azido-NAD^+ correspond to local fluctuations of the hydrogen bonds between water and the azo group.

Azido-NAD^+ is prepared by substituting the amide group in the 3-position of the pyridine ring of native NAD^+ with an azide functional group (Figure 46).[41] In aqueous, solution, we expect the adenine and pyridine rings to lie parallel to one another to take advantage of favorable π-stacking interactions between the rings. It is known from NMR studies that this motif is the favored conformation for the natural coenzyme in water, and that this conformer exists in equilibrium with an unfolded conformation that is present as a minor component.[110] The time scale for these equilibrium

fluctuations should be quite long compared to the time scale of our measurements. We see no apparent contribution to the FFCF that would correspond to this slow equilibrium between the open and closed conformer of azido-NAD^+. As a result, we conclude that only local hydrogen bond dynamics significantly influence the FFCF decay dynamics that we observe. This conclusion is significant as it provides the general framework within which the dynamics of this compound can be interpreted when it is enzyme-bound.

The amplitudes of the peaks in the 2D IR spectra decay with increasing waiting time as a result of population relaxation. As is apparent from the spectra in Figure 45, this decay is quite fast for the azo stretching vibration of azo-NAD^+ in water. Although the 2D IR spectra do not allow us to definitively quantify the population relaxation because of the time it takes to complete the individual scans, we can estimate that the population lifetime of the azo-stretching vibration of azido-NAD^+ in water is less than 1 ps. Such rapid population decay is not surprising in water. For the azide anion, for example, the relaxation in H_2O is approximately two times faster than in D_2O.Thus, although the population lifetime of azido-NAD^+ is rather short, it is likely that it will be longer when bound to an enzyme.

Azides are very sensitive probes of environmental dynamics and organic azides hold great potential for exploring protein dynamics. Azo-NAD^+ provides a unique opportunity to investigate the active sites of numerous NAD-dependent enzymes. The greatest shortcoming of azo-NAD^+ as a chromophore for 2D IR spectroscopy is its molar absorbtivity, $\varepsilon = 250\ M^{-1}\ cm^{-1}$, which is smaller than that for the azide anion by about a factor of 10. As the signal scales unfavorably, ε^2, the decreased transition moment potentially limits the use of this probe to enzymes that are stable at very high

protein concentrations, ≥10 mM. Another potential shortcoming of this probe is that it exhibits a short population lifetime that may only be adequate to sample the dynamics of enzymes up to 1 ps or so. In spite of these potential shortcomings, however, the analog has distinct advantages as a viable mid-IR probe to investigate enzyme dynamics. The mid-IR transition of this analog is at 2140 cm^{-1}, which is located in the "transparent" window of the aqueous protein absorption spectrum that can be accessed by nonlinear vibrational techniques. We have studied the binding characteristics of this analog and it forms stable complexes with several enzymes that catalyze a variety of redox reactions in biological systems. In addition, kinetic studies show that it not only binds but also that, in some cases, it even retains activity as a substrate for the enzyme. These observations indicate that azido-NAD^+ is a promising probe to study fast dynamics of numerous NAD^+-dependent dehydrogenases.

5.4 Conclusion

Using cofactors as mid-IR probes has great potential, as they open exciting new areas of study. The results presented here suggest that azo-NAD^+ will be sensitive to local environmental fluctuations particularly those of its hydrogen bonding partners. In this study of azido-NAD^+ in water, we observe dynamics that are consistent with the time scale for fluctuations of the hydrogen bond that water makes with the azo group. In fact, the FFCF is very similar to that for other small chromophores previously studied to understand the dynamics of water. Thus, our work shows that azido-NAD^+ should be a powerful new probe of the environmental dynamics of NAD-dependent enzymes.

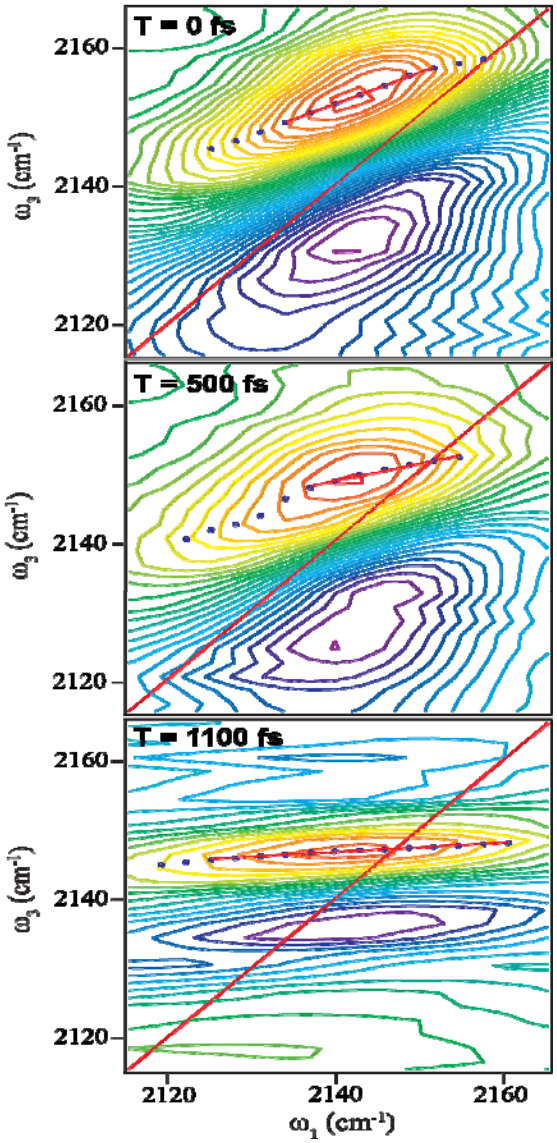

Figure 45 2D-IR spectra of azido-NAD$^+$ at different waiting time.

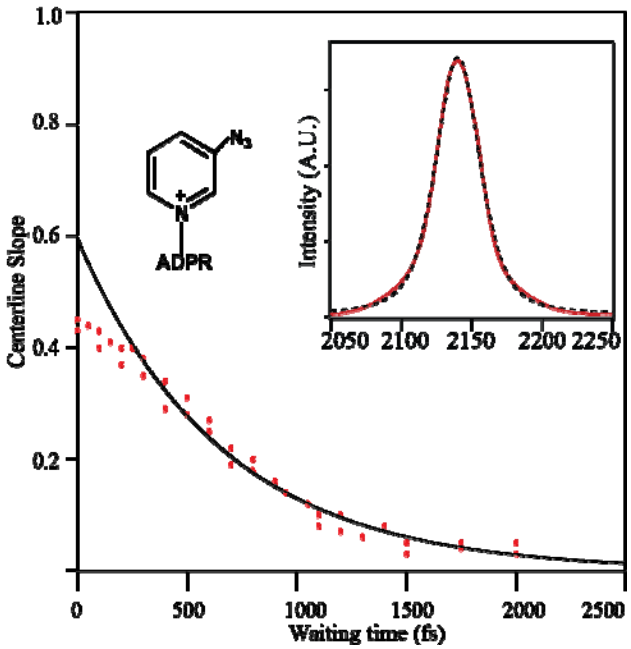

Figure 46 CLS decay of azido-NAD in water. The inset shows experimental spectra fitted to an FFCF with fit parameters obtained from CLS decays

CHAPTER 6

3-PICOLYL AZIDO ADENINE DINUCLEOTIDE AS PROBE OF ENZYME DYNAMICS

6.1 Abstract

Functionally relevant femtosecond to picoseconds dynamics in the active site is relatively unknown due to the lack of proper spectrosopical probe. We have developed a new NAD^+ analog, which has the potential to be a general spectroscopic probe. This analog is stable and binds in the active site with similar way as native NAD^+. It high molar absorptivity makes its suitable for observing enzyme dynamics. 2D-IR studies with this analog shows that this probe is sensitive to the local environment. In bound complex with our model enzyme, it shows a large static offset , which is expected for enzymes as their active site is modulated by slow fluctuations.

6.2 Introduction

Enzyme motions can span from femtosecond to milliseconds timescales both on the exterior as well as in the active site.[6, 111] Understanding these protein motions is essential to establish the structure-function relationship of proteins. In the recent past, there is a growing interest to understand the motions at femtosecond to picoseconds time scales as it has been suggested that proteins promoted vibration modes and internal motions modulate the activation barrier and influence the complex energy landscape of the catalyzed reaction. The importance of fast dynamics at active site is also invoked in many enzymes which show anomalous kinetic isotope effects. These results have led to the development of theoretical Marcus-likemodels that predict environmental reorganization of the active site of enzymes involved in H-transfer reactions.[2, 13, 68, 70, 112, 113] This model predicts that prior to hydrogen-tunneling event, the active site reorganizes to have an optimal

geometry between the donor and acceptor, insensitive to thermal fluctuations at donor acceptor distance. Any perturbation of this complex, such as a mutation, then results in a disturbance of the optical geometry and necessitates thermally activated motions at the femtosecond to picosecond time scale to effect the reaction resulting in a temperature dependent isotope effect. Such dynamics were until recently experimentally inaccessibale at this time scale but with the advent of nonlinear vibration techniques like 2D-IR spectroscopy, it is now possible to access these events.[114-116] The fast dynamics of proteins previously studied by non-linear techniques, which include globular proteins, native and folded cytochrome c, Horseperoxide, HIV- reverse transcriptase, carbonic anhydrase and formate dehydrogenase, shows interesting features in the complex dynamic landscape of the active site of proteins.[56, 58, 59, 117, 118] Unfortunately, the probes in these studies cannot be extended to a broad range of enzymes as all the chromophores used in those studies are system specific and thus lacks generality. Another approach that is commonly used to study enzyme dynamics is by site-specific labeling. However, segmental labeling has its own limitations. Such process are time consuming, needs refolding procedures , needs protocols to remove unliganded pecusors and can compromise with the integrity of the native protein structure. As such, it limits the scope of utilizing techniques 2D-IR spectroscopy to understand the dynamics of a broad range of enzymes at the active site. There is a dearth of general spectroscopic reporters, which can bind to the active sites of many enzymes with minimal perturbation to the native structure of the protein and can report the dynamics at fast time scales.

Mid–IR active analogs of NAD^+ can be useful as general probes as NAD^+ is ubiquitous biological molecule and a cofactor for more than 600

enzymes. As a cofactor, it binds close to the actives site and thus can be a good reporter of femtoseconds-picoseconds dynamics in the binding pocket of enzymes. Chromophores substituted at 3-position of nicotinamide ring of NAD^+ are suitable candidates for mid-IR probes as they preserve their biological functionality and bind to the active site in similar way as native NAD^+.[29-31, 99, 101, 119-124] Probes, which have strong transition and relatively narrow band that is well separated from other absorption bands are ideal for spectrocopical studies. We have recently shown that an azido analog of NAD^+ have the potential to become a general probe to investigate the active site dynamics of NAD dependent enzymes.[125] We have extensively studied this analog and found that its binding and kinetic properties are similar to native NAD^+ in a number of enzymes. This means that the analog binds with the enzyme with minimal perturbation. We have also studied its dynamics in water and found that the azide in the moiety is sensitive to hydrogen bond fluctuations as would be expected. Its binding properties for NAD-dependent enzymes, transition at suitable region, clear difference in linear infrared spectroscopy bound and unbound and its water dynamics makes this analog a good general probe. However, this probe has weak transition moment compared to free azide, which limits its application to study enzyme dynamics. In general, enzymes have poor solubility, which makes it difficult to probe even with strong chromophores. As signal scales ε^2, having a probe with higher signal can make it easier to probe. A strategy can be to synthesize derivatized NAD^+ analogs retaining all the other characteristics except that the analogs will have high molar extinction coefficient in mid-IR and can access the active site dynamics of proteins which have limited solubility. Such probes are ideal for four waves mixing techniques, like 2D-

IR, as molecular response of the probes is critically depend on the molar extinction coefficient of the chromophore.

Here, we report picolyl azide adenine dinuceotide (PAAD), a derivative of NAD^+ with high molar absorvity at mid-IR, its binding and kinetic studies along with 2D-IR spectroscopic analysis of this compound in solution and bound to an NAD^+ dependent enzyme, Formate Dehydrogenase. The observed dynamics of this analog in water is governed by global hydrogen bond dynamics, and the FFCF is similar to azido-NAD^+ and other small chromophores in water. Binary complex of PAAD bound with the enzyme shows completely different dynamics compared to water that are consistent with what we would expect for a binary enzyme complex. These results reveal the potential of this analog to report dynamics based on the environment. Our results demonstrates, the ability of this analog to bind with FDH, sense fast fluctuations in water and report dynamics at the active site of FDH. All these observations, points out to the capability of this analog as an excellent probe of active sites of NAD dependent enzymes.

6.3 Result and discussion

The preparation of the analog PAAD is straight forward and analogous to synthesis of azido-NAD^+. PAAD is stable, soluble in water and can be obtained in high purity. This molecule is structurally analogous to native NAD^+ except that the amide in the nicotinamide ring is replaced by an azido group with a methelene linker. As with native NAD^+, PAAD too have a characteristic UV (Ultraviolet) absorption at 260 nm with similar extinction coefficient. This common peak corresponds to adenine moiety present in both molecules. However, unlike native NAD, this analog is mid-IR active. Figure 47 shows the linear infrared spectrum of picolyl azide and PAAD. As seen in the figure, the center frequency of the starting material (picolyl azide) is

shifted from 2107 cm $^{-1}$ to 2119 cm^{-1} in the product (PAAD). This shift can be attributed to the formation of glycosidic bond in the final product. The molar absorvity of PAAD is ~ 2000/M/cm at 2119 cm^{-1}, which is similar to analogous compounds reported elsewhere. This enhancement in molar absorvity is circumvents the limitation of most azido derivatives to investigate biological systems with low solubility.

As a coenzyme, PAAD acts as a substrate in presence of formate with FDH. It reacts with formate to form reduced PAAD, which like reduced NAD^+, has a characteristic UV absorbance at 340 nm in addition to the peak at 260 nm. Figure 48. shows the change in initial velocity of 340 nm absorbance with concentration of PAAD. It clearly shows substrate inhibition resulting in lower reaction rates at high concentration of PAAD. The data fits best to competitive substrate inhibition (Eq.1). The fitting parameters shows k_{cat} of 1.3/s , K_m = 226 μM and K_s = 2 mM . The binding studies of PAAD with FDH by ITC show K_d = 7 μM. These values are comparable to native NAD^+, so it is likely that this analog bind to the active site similar to NAD^+ in FDH. The turnover number for *Candida Boidinii* FDH with NAD^+ is reported to be 3.7 s^{-1}, which compares favorably to our observation of 1.3 s^{-1} with PAAD. All these observations suggest that PAAD forms a stable complex with the enzyme and structurally binds in similar way as native NAD^+.

Figure 49. shows 2D-IR of free PAAD in water at different waiting times. The fundamental transition (0-1 vibrational transition) represented by red lobes, is a noticeable feature which change with waiting time T_W. The red lobes are elongated at early waiting time and become symmetrical at longer time. There is a strong correlation at early waiting time between frequency ω_1 and the frequency ω_3, which is lost at long time. This change is a hallmark

of spectral diffusion, where all the environmental conformations are sampled and, therefore all frequencies are sampled. The FFCF (frequency frequency correlation function) given by $<\delta\omega(t)\delta\omega(0)>$, connects the experimental observations to underlying dynamics. This statistical correlation shows the probability of an oscillator at a given frequency oscillating at the same frequency at later time. We follow the simple method of CLS (center line slope) to determine the FFCF as described by Fayer.[61] The centerline slope is a new experimental observable to quantify the spectral diffusion dynamics. In this technique, vertical frequency slices are taken in 2D-IR spectrum. The open blue circles in Figure 49, shows the peak position of these vertical frequency slices obtained by fitting the frequency slices to an appropriate routine. The line that joins these blue circles, represented by the red line, is "the center line". The important characteristic of this center line is that as T_w increase, slope decreases. If the spectral diffusion is complete, the spectrum becomes symmetrical, the center line becomes horizontal and the slope goes to zero. As FFCF is related to center line slope, the decrease in slope at longer waiting time represents loss of correlation between ω_1 and ω_3 axis and represents the dynamical feature of the system. In general, the amplitudes and timescales of CLS decay of 2D-IR are used to determine FFCF. For PAAD in water, the CLS decay fits to a single exponential (Figure 50), with vibrational dephasing lifetime of 778 fs. We assume a simple Kubo line shape model for the FFCF, $C(t) = \Delta^2 e^{-t/\tau}$, and fit it with linear absorption spectrum keeping the CLS decay and initial amplitude constant. The parameters that result from the fitting are $\Delta = 0.002$ fs^{-1} , and $\tau = 778$ fs. As seen in the inset of Figure 49, the calculated (dashed line) and experimental spectra (solid line) agree well.

The FFCF of PAAD in water is similar to that for azido-NAD^+ and other small chromophores. The timescale of spectral diffusion represented by the 778 fs decay is consistent with the global fluctuations of hydrogen bonds around the azido moiety of PAAD. Similar timescales is observed for cyanide ions in water. It is well known that NAD^+ in solution is a mixture of folded and unfolded forms with the aromatic rings stacked parallel in close proximity for the folded moiety. The equilibrium between the folded and the unfolded structure is long compared to the time window for our measurement. In our experiments, we do not observe contribution from this slow equilibrium and as a result we conclude that local hydrogen bond dynamics have the greatest influence in the decay dynamics in FFCF. Unlike azido-NAD^+, PAAD has a methelene linker between the azide and the pyridine moiety but the resulting increase in flexibility does not significantly influence the FFCF. A noticeable observation from the 2D-IR plots at different time scales is that the decay of the amplitude of the peaks is quite fast suggesting rapid population relaxation. We cannot use the amplitude intensity to quantify the population relaxation, however, as the each individual scan takes at long time to complete. A reasonable estimate of lifetime of 1 ps is assumed for the azido stretch of PAAD in water in analyzing our data. Such fast population decays are common for chromophores in water. We expect the lifetime of the enzyme-bound PAAD to be longer than in water.

Figure 51 shows 2D-IR spectra of different time slices of binary FDH-PAAD complex. We perform similar CLS analysis as described above with this bound complex. Figure 52 shows the CLS decay vs T_W. The CLS data are presented as dots and the fit is represented as solid lines. The inset on Fig 52 shows the fit to the infrared absorption spectrum using the fit decay

parameters and adjusting the overall amplitude of the FFCF to fit the line shape. To represent the FFCF in this complex, we use generalized Kubo line shape function of the form,

$$C(t) = \Delta_1^2 e^{-t/\tau_1} + \Delta_2^2 e^{-t/\tau_2} + \Delta_3^2$$

where the Δ's reflect to the amplitude of the frequency fluctuations and the τ's indicate the time scales of the motions responsible for those fluctuations. We fit the correlation function, with minimum number of terms, such that this correlation function adequately represents the linear absorption spectrum. The fit parameters from the fitting are $\Delta_1 = 1.03$ ps^{-1}, $\tau_1 = 522$ and $\Delta_2 = 1.1$ ps^{-1}. The simulated spectra with these fit parameters in good agreement with the linear absorption spectra.

The infrared transition of PAAD is at 2119 cm^{-1} with FWHM 22 ± 2 cm^{-1}. This peak is at a suitable range to study enzyme dynamics as most proteins are devoid of localized transitions within the so called "transparent window" from 1800-2000 cm^{-1}. The molar absorvity (~ 2000M^{-1} cm^{-1}) of azido transition of PAAD is comparable to free azide, which makes it an excellent probe to study enzyme dynamics by 2D-IR spectroscopy. As the signal scales as ε^2 in 2D-IR spectroscopy, it is advantageous to work with chromophore with high transition dipole moments. PAAD favorable absorptivity makes it a suitable candidate to accesses the dynamics of enzymes, which are often limited by their solubility and functional integrity at higher concentrations. Analysis of infrared spectrum of free PAAD in solution with that bound to FDH shows no quantitative difference. Though there is no quantitative difference, it does not mean that they do not have a qualitative difference. These qualitative differences can be probed by 2D-IR, which can be used to determine the sensitivity of this azido-probe to environmental dynamics and

reveal the dynamical features of the active site of FDH. An important feature of 2D-IR is to remove the ambiguity in defining the correlation function that can generate the linear absorption spectra. Our experimental analysis clearly show that both bound and unbound complex have distinct correlation functions even though they have exact same infrared lineshapes. The distinct correlation functions signify that there is difference in dynamical character of the probe depending on the environment where it is placed.

The FFCF of PAAD in water and that bound to FDH by 2D-IR are different and shows the versatility of the probe to sense to different environments. PAAD is sensitive to hydrogen bond dynamics, which decays with a vibrational dephasing lifetime of 778 fs. However, PAAD bound to FDH shows completely different spectral diffusion, which agrees well with previously studied dynamics in enzymes. Unlike in free state, where the CLS decays completely, PAAD in FDH shows decay with a large static offset. Comparing the CLS decay at relatively long delay time clearly illustrates the qualitative difference between the free PAAD and the binary complex. In FDH-PAAD bound complex, we can take 2D-IR data up to 3.5 ps confirming that in bound state the lifetime of the chromophore is longer than in free state. The environment of the active site is very hydrophobic and less heterogeneous compared to the aqueous phase, which influences the relaxation of the excited state. As such, PAAD can be a good general probe of fast dynamics as the azido frequency in the moiety is dephase differently depending on fluctuations of its surrounding environment. The fastest component of FFCF in the binary complex has a fit parameter of 522 fs with a small amplitude (Δ_1 =1.03 ps^{-1}) and a significant static term which is 60% of the overall decay. This result is typical feature of fast dynamics of several reported enzymes, where there is 20-30% static contribution to FFCF decay.

The FFCF of PAAD-FDH complex had resemblance to FDH-Azide complex, which was earlier investigated in our laboratory. Both of the complexes have a significant static term which contributes more than 30% in the FFCF decay. This similar dynamical trait of PAAD and azide is unexpected as each of them are bound differently within the catalytic domain. In enzymes, NAD^+ adopts a extended conformation and is bound to a pair of mononucleotide-binding domain (Rossmann fold).[126] The crystal structure of binding site FDH from *Pseudomonas* sp. 101, which has high sequence homology to the *Candida boidinii* enzyme shows that each half of the coenzyme binds to a pair of α–β–α motifs with the nicotinamide ring close to the catalytic domain. We assume that PAAD will bind in similar way as native NAD^+ as the kinetic and binding parameters are comparable with experimental errors. Our probe PAAD can sample motions up to a couple of picoseconds but any motions beyond 10 ps appear as static in our measurements. In our experiments, we observer a significant static component in PAAD-FDH complex, which means that spectra diffusion in not complete and that there are thermal motions which are evolving the structure around the active site in a timescale longer than 10 ps. This observation is consistent with the fact that motion at all time scales effect the FFCF and only the fast structural motions are completely sampled by our experimental window and all other motions at longer timescales appear as static. As with FDH-azide complex, we assume that PAAD-FDH complex also represents a configuration far away from transitional state. However, there is a sub-200 fs decay in FDH-azide complex, which is not seen in counterpart with FDH-PAAD complex. This feature is because of local hydrogen bond fluctuation of azide bound to four highly conserved residues in FDH-azide

complex. PAAD binds in different portion on active site motif, so this local feature is missing but the global dynamics in both the complexes are similar.

NAD^+ plays an indispensible role as a coenzyme in numerous enzymatic reactions. Apart from intercellular processes, it is now known that NAD^+ is involved in extracellular signaling. The use of analogs of NAD^+ has been extensively been explored to understand enzyme-coenzyme interactions, label the active site and to investigate the mechanistic pathways. However, the use of analogs as mid-IR probes to understand the dynamics at the active site is relatively unknown. As with other studies, the basic requirement to use such analogs is their ability to function as a coenzyme. The binding and kinetic studies of PAAD with FDH indicate that this analog is not different from the native NAD^+. Its strong mid-IR transition at a spectrally transparent window makes it suitable candidate to study enzyme dynamics. This property is unique for this probe as most organic chromophores in mid-IR are known to have low molar absorvity, which limits their application to study enzymes. The clear difference in dynamics in bound and free state shows the environmental sensitivity of the probe and its potential as a general probe. As an analog of NAD^+, we expect it to bind with more than 600 known NAD^+ enzymes. Apart from reporting the dynamics at active site, it can also be an important mid-IR maker in biological systems, where NAD^+ plays a role. In addition, similar synthetic methods can be applied to prepare $NADP^+$ analogs, which can be used to probe $NADP^+$ enzymes.

6.4 Conclusion

Enzymes are biocatalyst, which have motion under thermal fluctuations, encompassing a broad range of timescales. The functional significance of such random motion, specifically for femtosecond and picoseconds timescales, is a challenge to both experimentalists and theorists.

With the advent of 2D-IR, it is now possible to map the dynamical landscape of enzyme active site. PAAD provides the window to examine the active site dynamics of a broad range of NAD^+ dependent enzymes

We report the synthesis, characterization and kinetics of an azido analog of NAD^+. It binds with FDH with an affinity comparable to native NAD^+. PAAD shows a strong transition at 2119 cm^{-1}, a region suitable for enzymatic studies. It has a high molar extinction coefficient comparable to that of free azide ion, which makes it an ideal candidate to probe enzyme dynamics by 2D-IR technique. This property can be helpful to study those proteins which are limited by their solubility or lose their functionality at higher concentrations. The azido antisymmetric stretch of this PAAD is very sensitive to environmental conditions. In aqueous medium, the spectral diffusion is complete within hundreds of femtosecond whereas when bound to FDH, PAAD shows a static component which extends beyond our spectral window of couple of picoseconds. This observation is consistent with other enzymes where slow motions influence the FFCF.

PAAD ability to bind, form stable complex and report the dynamics depending on the environment, signifies that PAAD can be a general spectroscopic tool to understand femtosecond-picosecond dynamics of numerous NAD^+ dependent and other systems, where NAD^+ plays a role. Studies of this probe bound to different enzymes both wild type and mutants are currently underway.

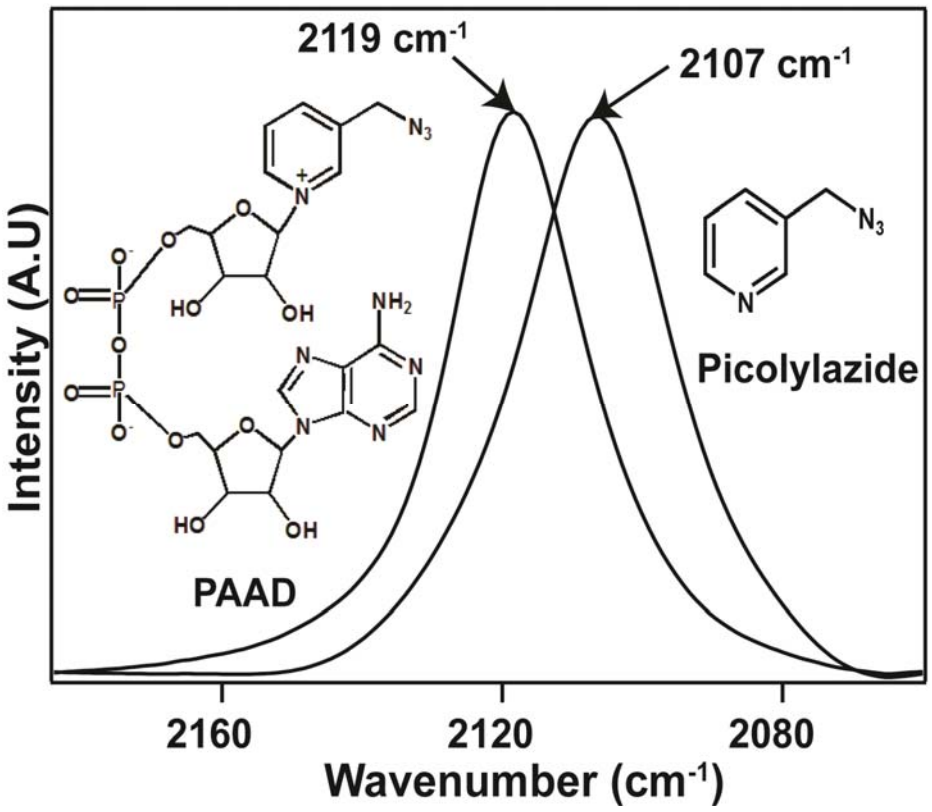

Figure 47 Infra-red spectrum of Picolyl azide(right) and PAAD (left)

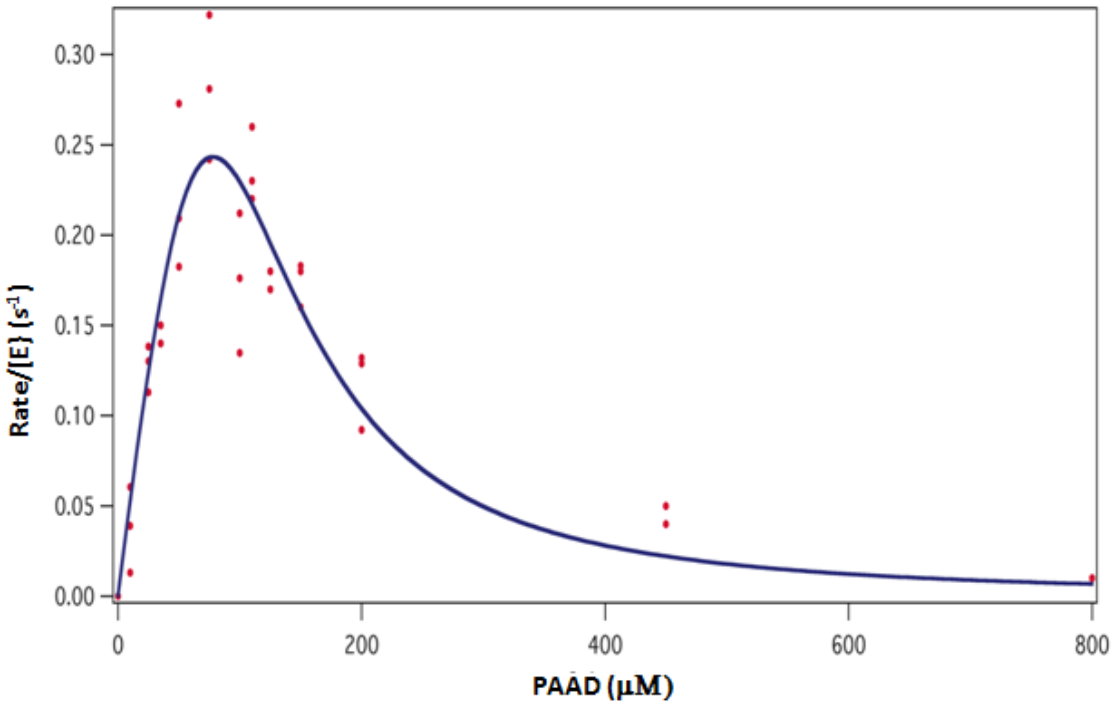

Figure 48 Initial velocity measurements of PAAD with FDH

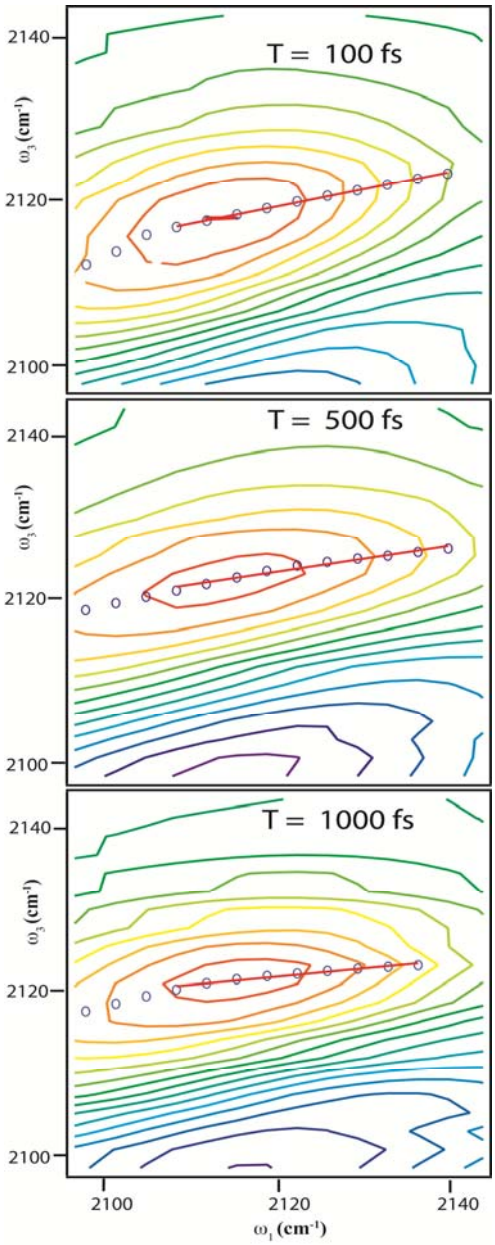

Figure 49 2D-IR plots of PAAD in water at different waiting times

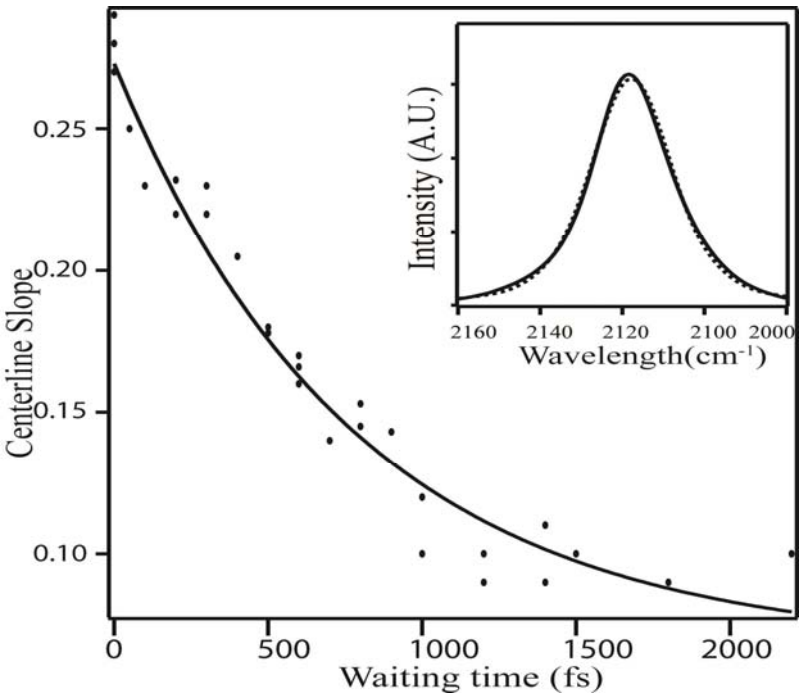

Figure 50 CLS decay of PAAD in water

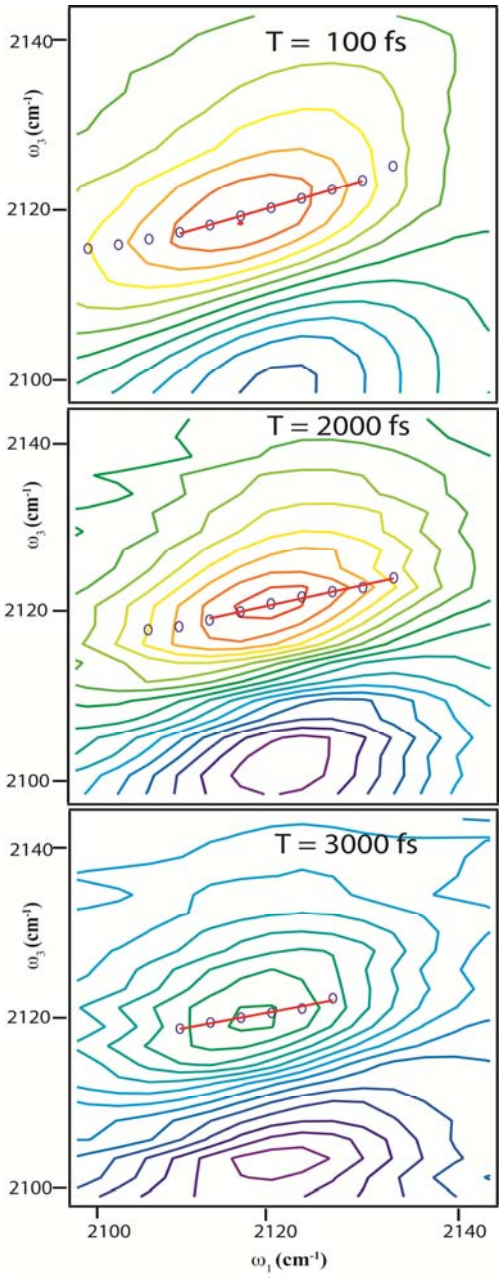

Figure 51 2D-IR of binary complex at different time slices

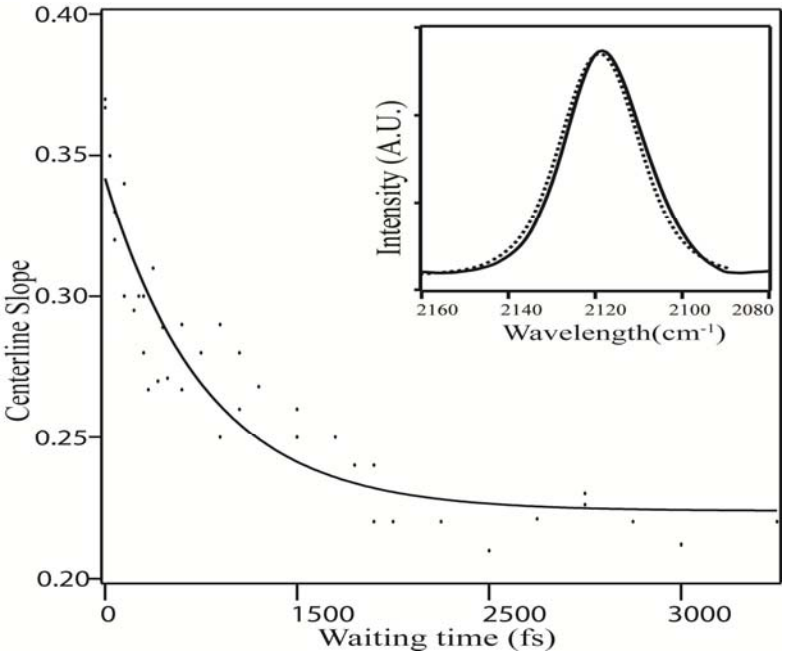

Figure 52 CLS decay of FDH-PAAD complex

CHAPTER 7

FUCTIONALLY RELEVANT DYNAMICS OF FORMATE DEHYDROGENASE AS PROBED BY PICOLYL AZIDO ADENINE DINUCLEOTIDE

7.1 Abstract

The active site of enzyme, Formate Dehydrogenase is probed by a new analog PAAD. The perturbation of the ternary complex FDH-PAAD-azide is investigated by probing the azide frequency in the complex. The FFCF for azide shows perturbation but overall this complex still represents the transitional-state configuration as it undergoes complete spectral diffusion. We complete FFCF decay for PAAD which points out that the active site is rigid in immediate vicinity.

7.2 Introduction

Enzyme motions are necessary for its functions.[21, 94] Experimental and theoretical studies suggest that enzyme motion at femtosecond to picosecond timescales is relevant to understand the importance of thermal fluctuations at enzyme active site. Evidence of fast motions at active sites is seen in many enzymes, which are involved in H-transfer reaction.[4, 69, 70, 127, 128] These enzymes show anomalous isotope kinetic effects, which is considered as a signature of quantum mechanical tunneling. An efficient quantum tunneling mechanism requires the nuclear wave functions of donor and acceptor potential wells should be close to each other and have degenerate energies. Protein motions at the active site can cause fluctuation in donor acceptor distance and can result in coupling of environmental dynamics to C-H bond activation. Theoretical Marcus-like models predict that the motions that influences the donor acceptor distance in a tunnel ready configurations of these enzymes are insensitive to thermal fluctuations. In this model, it is

predicated that slow large amplitude motions of the enzyme no longer modulate the donor acceptor distance in the tunnel ready configuration. Till recently, such motions at short time scales could only be studied though computer simulations but with the advent of 2D-IR, it is now possible to directly access the dynamics of the active site in femtosecond-picosecond time scales.[23, 64, 115, 116] To access the dynamics, we need mid-IR probes which can bind to the active site, have a strong transition at a suitable spectral region and cause minimal perturbation. Azide is an ideal mid-IR probe and transitional analog, for a model enzyme Formate Dehydrogenase, which satisfy all the above characteristics of a probe. We have studied extensively the active site dynamics with this probe of FDH with its binding partners NAD^+ and NADH. Indeed from these studies, we conclude that in accordance to Marcus like model, the transitional state defined by the ternary complexes FDH-azide-NAD and FDH-azide NADH, is insensitive to thermal fluctuations. These complexes have rigid active sites , which samples the environment completely within a couple of picoseconds . Though this result has enormous significance, it cannot be generalized. Natural mid-IR active transitional state analog like azide is rare in enzymes. Azide as a probe also lacks generality and will not bind to active site of most enzymes. As such we are limited in our observations of fast dynamics of other enzymes at the active site.

NAD is a ubiquitous cofactor, which binds close to the active site of numerous enzymes. Mid-IR active analogs of NAD^+ are therefore suitable candidates to be general probes to investigate enzyme dynamics. We have recently synthesized a mid-IR active analog, PAAD (Picolyl azido adenenine dinucleotide), which has similar binding characteristics as native NAD^+. This analog has the potential to be a general probe to investigate the active site

dynamics of NAD^+ dependent dehydrogenase. Though this synthesized molecule behaves similar to native NAD^+, it is necessary to understand nature of the dynamics it reports, the impact of its chemical modification compared to native NAD^+ on dynamics of the active site and its influence on its binding partners. Formate dehydrogenase provides a unique opportunity as it binds both azide and PAAD in its active site. In this report, we study the dynamic landscape at the active site as reported both by azide and PAAD by 2D-IR spectroscopy. These results is compared to ternary complexes of FDH with native NAD^+ using azide as a probe, which we have previously studied in our laboratory.

7.3 Result and Discussion

The preparation of PAAD is straightforward and yields the product in high purity as white powered. PAAD is soluble in water and acts as a substrate in FDH. So, instead of formate, we use azide, which happens is a transitional state inhibitor of FDH , with an inhibition constant constant of 40 nM as the third binding partner. The dissociation constant of the ternary complex determined by titrating PAAD with FDH-Azide complex is 4 μM , which is comparable to native NAD^+. Taken together with earlier reported kinetic parameters and the measured binding parameters in this work, suggests that PAAD binds to the active site in a similar way as native NAD^+ in FDH.

The ternary FDH-PAAD azide is an interesting complex as both the azido-stretching vibration (2119 cm^{-1}, FWHM 23 cm^{-1}) of PAAD as well as the azide anion antisymmetric stretch(2048 cm^{-1}, FWHM 24 cm^{-1}) can be accessed using 2D-IR spectroscopy. These two probes are far apart in frequency space that they can be individually monitored without spectral congestion.

Figure 53. shows 2D-IR spectra of PAAD as a reporter of active site dynamics in FDH-PAAD-azide complex. The red lobe implies 0-1 transition of the chromophore PAAD and represents stimulated emission whereas the blue lobes represent 1-2 transition corresponding to the excited state absorption. At early waiting times, there is a strong correlation between the frequency ω_1, measured before the waiting time, and the frequency ω_3, measured after the waiting time. At later waiting times, there is loss of correlation between the frequency during ω_1 and that during ω_3. This loss of correlation causes corresponding changes in peak shape from elongated lobes along the diagonal at early waiting times to be completely oval lobes at later times. Such changes reflect complete spectral diffusion resulting from the equilibrium environmental fluctuations. The FFCF (Frequency-frequency correlation function) is given by $<\delta\omega(t)\delta\omega(0)>$ and represents the time scales for the frequency fluctuations that report on the dynamics of the environment around PAAD. To extract the FFCF from the 2D IR data, we use the center line slope (CLS) analysis. In this method, we take vertical slices through the 2D spectrum at each value of ω_1 and locate the position of the maximum in ω_3. The resulting sequence of points is the center line, shown as the blue circles in Figure 1. The slope subtended by the line joining the blue circles is defined as the center line slope and is proportional to the FFCF for this value of T_W. The decay of CLS with T_W represented by Figure 54, quantify the time scales for the structural fluctuations in the environment of the chromophore. We fit the decay of the CLS to a sum of exponentials plus a constant offset retaining the minimum number of terms to accurately describe the decay. We use the relative amplitudes and time scales of the decay as input to fit the infrared absorption line shape, as seen in inset of Fig 54 , by varying the

overall amplitude of the FFCF. The fit parameters follows usual form of generalized Kubo line shape function.

$$C(t) = \Delta_1^2 e^{-t/\tau_1} + \Delta_2^2 e^{-t/\tau_2} + \Delta_3^2$$

where the Δ's reflect to the amplitude of the frequency fluctuations and the τ's indicate the time scales of the motions responsible for those fluctuations. For PAAD in the ternary complex (Fig 54), we fit the data to a single exponential, which in FFCF represents the parameters $\Delta = 1.13$ ps^{-1} and $\tau = 2.3$ ps.

The active site dynamics reported for ternary complex by azide at different waiting times by 2D-IR is presented in Figure 55. The data obtained is analyzed as described above. The decay of CLS vs Tw (Figure 56) is fitted to a biexponential. The inset on the panel in Figure 56, shows that the fits to the infrared absorption spectra using the fit decay parameters and adjusting the overall amplitude of the FFCF, are in good agreement. The parameters of this fits are $\Delta_1 = 0.62$ ps^{-1} , $\tau_1 = 0.111$ ps. $\Delta_2 = 0.9$ ps^{-1} and $\tau_2 = 7.4$ ps.

The azide anion transition frequency in the active site of FDH in FDH-azide-PAAD is sensitive to electric fields. Therefore, azide frequency fluctuations is sensitive to local and global structural changes in the enzyme pocket. The 2D-IR analysis of this ternary complex shows that the FFCF decay can span different time scales. Typically for any enzyme the dynamics unveils in three distinct time scales ; the first time scales ranges from motonally narrowed to 100's of femtoseconds, the second or the intermediate part usually lasts anywhere between couple of picoseconds to 20 picoseconds and the last or the slowest motions appear beyond 20 picoseconds as static contributing 20 -30% of overall FFCF decay. In ternary FDH-azide-PAAD, the azide probes similar feature except that there is no slow or static

component to the FFCF. The fast time constant is around 111 fs, the intermediate around 7.4 ps and third or the slowest component (static) is negligible and constitutes less than 5% of overall decay. These features are qualitatively similar to FFCF of FDH-azide-NAD. In FDH, the active-site structure is compact and is located between two similar structural motifs each a sandwich of α-helix, parallel β-sheet, and α-helix. From the crystal structure of FDH-azide- NAD from the organism *Pseudomonas* sp. 101 , which has high sequence homology to the *Candida boidinii* , we know that azide anion is bound to the active site via hydrogen bond partners, Arg-284 (using *Pseudomonas* numbering) , His-332 , Ile-122 and Asn-146. The motion of these highly conserved residues have a significant influence on the FFCF of the azide anion in this ternary complex. So any perturbation in the system will reflect on the decay characteristics of the FFCF. In light of this argument , we see that even though the ternary FDH-azide- NAD and FDH-azide-PAAD are qualitatively same yet they are quantitatively different. The intermediate slow time scales of FFCF of azide are 3.5 ps and 7.4 ps with NAD and PAAD respectively in FDH. This difference arises because the PAAD perturbs the system compared to native NAD^+. Compared to amide in the nicotinamide ring of NAD^+, the methelene azide linker in lieu of amide in PAAD complex is bulky and hydrophobic. PAAD is an analog of NAD^+. We have found from kinetic and binding measurements that this compound binds to the active site of FDH similar to native NAD^+ with minimal perturbation. Though this perturbation is not obvious in the kinetic studies, it cleary shows up in quantitative difference of the FFCF of azide. However, there remarkable is a remarkable similarity in dynamics both qualitatively and quantitatively at longer timescales. At longer times scales, there is no slow large amplitude motions that can modulate the azide anti symmetric stretch

irrespective of the binding partner NAD or PAAD. In either of the complexes, the environment is rigid with narrow distribution of conformers. All high frequency large amplitude motions are sample within a few picoseconds in both the complexes. Another important observation from our data is that the lifetime of azide anion in considerable enhanced compared to in FDH-azide-PAAD complex compared to FDH-azide-NAD. The azide might be more isolated in the active site due to the binding of non natural binding partner PAAD resulting in longer lifetime. This change in binding details of azide must be subtle as the qualitative spectral features are not different compared in presence of native NAD^+.

In FDH-PAAD-azide complex, the dynamical features of FFCF of PAAD is qualitatively similar to FDH-azide-NAD complex. Though the first timescales are not resolvable within our experimental measurements, we do see the intermediate time component of 2.3 ps and no static contribution. In contrast, we see fast fluctuation of local hydrogen bond of azide, which decays within 200 fs in FDH-azide-NAD complex, is absent FDH-azide-PAAD. This difference clearly shows that PAAD and azide are sense different regions within the same active site and unlike azide anion; the azido moiety of PAAD is perhaps not strongly bound by hydrogen bonds in the active site. It is also possible that the azido stretch is insensitive to local fluctuations as it is attached to flexible ring systems in its moiety. The FFCF decay of PAAD is represented by a single exponential with a decay lifetime 2.3 ps. The most important feature is that the FFCF has no static contribution.

The absence of static contribution when probed by either PAAD of azide is remarkable as this result removes the ambiguity about the rigidity of different parts within the active site. Unlike azide, PAAD is assumed to mimic the binding characteristic of native NAD^+, which binds in distinct

binding domains called the Rossmann fold. As such, PAAD reports fast dynamics of different part within the same active site. Within this distinct portion of the binding site, the FFCF of the probe PAAD undergoes complete spectral diffusion. This means that the rigidity of the active site is not constrained to moieties associated with azide but extends to other parts defined by the active site. It is true that the FFCF of azide and PAAD are quantitatively different but qualitatively the FFCF is same at early waiting times. However, at longer waiting time both the complexes are qualitatively and quantitatively similar. Irrespective of the probes, complete spectral diffusion occurs in the complex even though specific timescales are different. The FFCF azide anion in FDH-azide-NAD can be compared to FFCF of both the probes FDH-azide-PAAD. Even though the FFCF of azide anion in these complexes are quantitatively different but they have no static contribution beyond 10 picosecond. The quantitative difference arises because native NAD^+ in the system is replaced by PAAD perturbs the dynamic details of the active site. Nonetheless, there is certainly absence of static component in the ternary complexes beyond ten picoseconds. It is known that FDH-azide-NAD represents transitional state configuration of the enzyme and our earlier experiments showed that this complex is thermally insensitive and samples narrow distribution of configurations. Even though perturbed, FDH-azide-PAAD, can be assumed to represent similar transitional state configuration. Like FDH-azide NAD, the fluctuations at the active site are high-frequency, small-amplitude motions that are fully sampled within a few picoseconds. This might be a the collective behavior of the active site as both PAAD and azide which probes different portions of the moiety undergoes fully samples the structural fluctuations within our time window albeit with different time scales. This result clearly demonstrates that chemically removing amide in

the nicotinamide ring of NAD^+ and replacing it with a methelene azide do not move the configuration of the enzyme complex away from the tunnel ready configuration. This structure still is in a deep potential well, which encompasses a narrow structural distribution, resulting in the fluctuations about the equilibrium structure being sampled on short timescales. Inspite of the fact that both azide and PAAD experiences narrow distribution but it does is not to suggest that the whole protein is entirely rigid or to what extent the complex cannot undergo slow thermal motions. The rigidity might exists only in the vicinity of the active site particularly the residues that hold the azide and PAAD in the active site and is responsible for the enzyme-ligand-cofactor interactions that contributes to the lowering of the free energy barrier for the reaction.

The role of dynamics in picoseconds to femtosecond timescales at the active site is relatively unexplored. Understanding the relation between the dynamics observed using 2D-IR spectroscopy and molecular motions in the active site can resolve the conflict of the role of active site dynamics. It is unfortunate that there are only a handful of natural mid-IR probes that binds to the active site of the enzyme, have a transition in suitable region and minimally perturbs the system. PAAD is an analog of NAD^+, we synthesized as a general viable probe to investigate active site dynamics. Kinetic and bind studies of this analog with our model enzyme FDH shows that this analog closely represents the natural characteristics of native analog. Nonetheless, we expected the enzyme perturbed when bound to PAAD as it is chemically different from native NAD^+. In our studies, we clearly show that the FFCF decays completely in the complex FDH-azide-PAAD when probe either by azide and PAAD. In our previous experiments with FDH-azide-NAD, we have seen similar results in which the FFCF have no static contribution. This

result is interpreted as a representation of transition state structure of the catalyzed reaction. In this deep potential minimum, the active site is rigid and experiences a narrow configuration. Replacing NAD^+ with PAAD, still maintains this tunnel ready configuration as both azide and PAAD in the complex undergo complete spectral diffusion. Of course, there is perturbation in the system as evident from quantitative difference in the FFCF of azide anion depending on the ligand partner, whether it is native NAD or PAAD, but qualitatively both the systems represents transitional state of the catalyzed reaction. The subtle perturbation though qualitatively similar might modulate the binding pocket differently as is evident from enhanced lifetime of the azide chromophore with PAAD.

7.4 Conclusion

We report synthesis and characterization of an azido analog of NAD, as a general probe to investigate enzyme dynamics. Its binding and kinetic characteristics with our model enzyme FDH shows that this compound binds similarly as native NAD in the active site. We compared it dynamics with our previously well studied model, FDH-azide-NAD^+ and conclude that the new complex FDH-azide-PAAD also have similar characteristics. Like tunnel ready configuration of FDH-azide-NAD^+, the FDH-azide-PAAD complex also samples narrow distribution of configuration. The complete decay of FFCF of both azide and PAAD, shows that different parts of the active site are rigid and that this complex too perhaps represent transitional state.Further experiments, including kinetic isotope effects and determination of the crystal structure to understand the molecular origin of our spectral features are underway in our laboratory.

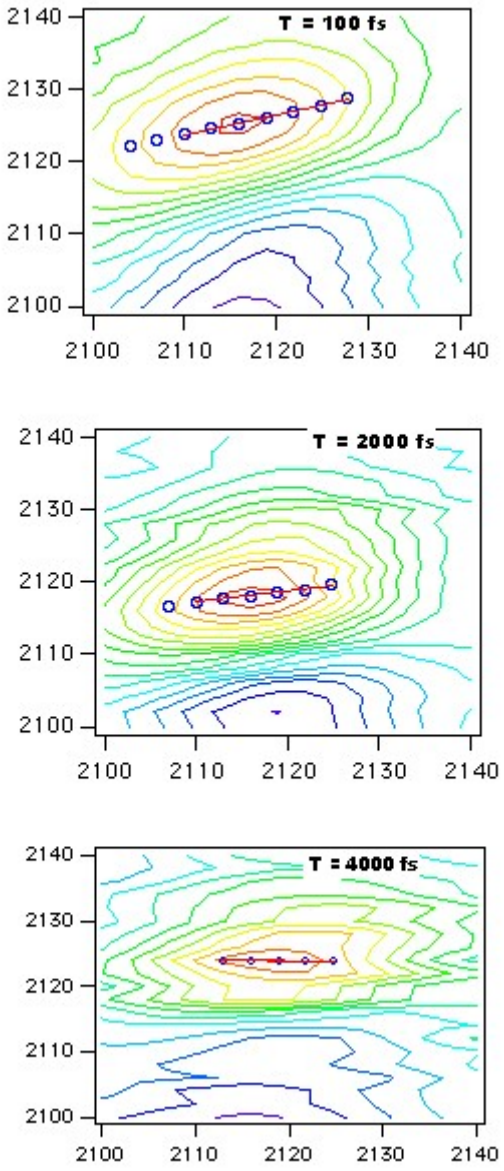

Figure 53 2D IR of PAAD in FDH-PAAD-azide complex at different waiting time

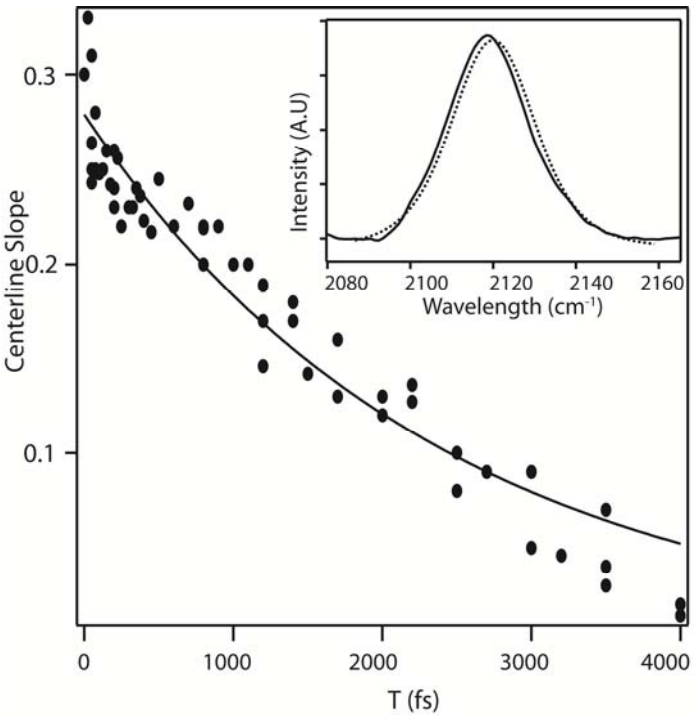

Figure 54 CLS decay of PAAD in FDH-PAAD-Azide complex

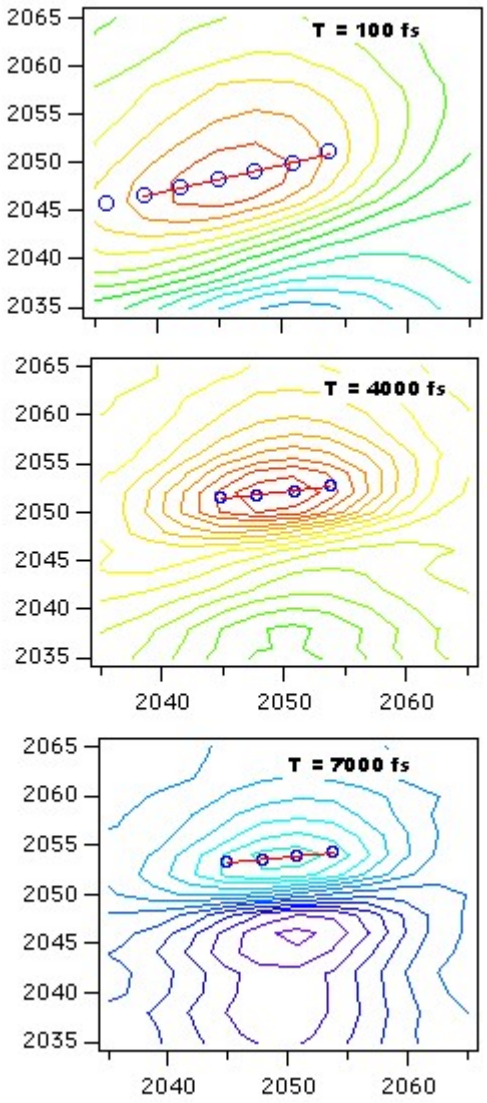

Figure 55 2D-IR of azide in FDH-Azide-PAAD complex

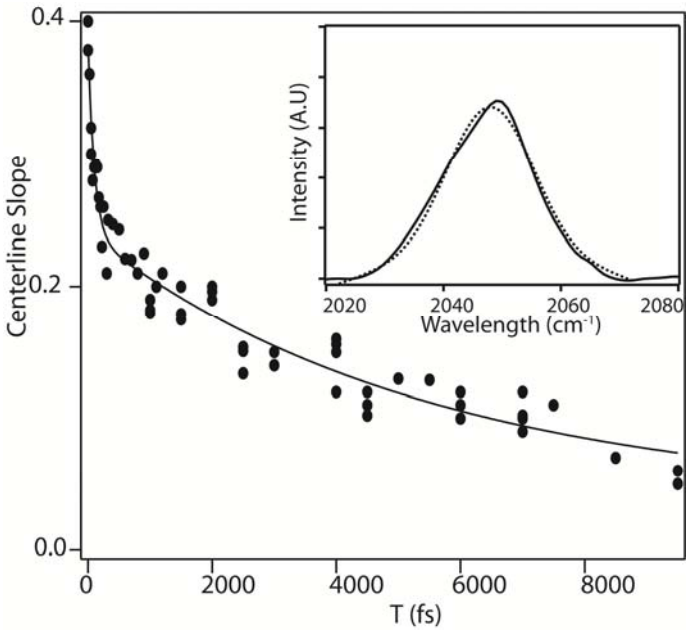

Figure 56 CLS decay of azide in FDH-PAAD-Azide complex

CHAPTER 8

SUMMARY,SCOPE AND FUTURE DIRECTIONS

We have investigated the dynamics of the active site of ternary complexes of FDH- with NAD and NADH using azide as probe. In FDH, azide is a potent inhibitor and represents transitional state dynamics of the complexes. Our 2D-IR measurements represent the dynamics of the active site, where structural motions have greatest influence over kinetic properties. The results indicate that azide samples the entire distribution in a few picoseconds in these ternary complexes. Such observation is unexpected because it is implies that long secondary structural motions do not influence the active site. The most likely explanation of these results is that the active site of the ternary complexes is rigid and samples a narrow conformational distribution. In contrast, the FFCF of binary FDH-Azide complex shows a significant static component. So, it appears that the absence of static component is a hallmark of transitional-state. The results are consistent with the Marcus like model, where it is predicted that in tunnel ready state the enzyme adopts an optimal balance between donor and acceptor, resulting in efficient tunneling that is insensitive to thermally induced fluctuations about the average donor acceptor distance. This behavior at tunnel ready configuration might me true for a large number of enzymes. However, it is difficult to investigate the dynamics of most enzymes due to the lack of proper spectroscopic probe that can bind to the active site, have strong transition in a suitable mid-IR region and minimally perturb the system. Apart from these, the complex should represent functionally relevant dynamics.

We have synthesized mid-IR active analogs of NAD, which is a coenzyme in numerous enzymes. These analogs, azido-NAD^+ and PAAD, are characterized and their interactions with various enzymes are recorded. Based on the results, we can conclude that these analogs binds to several NAD-dependent enzymes with an affinity that is similar to that for native NAD^+ and that the substitution of the azide at the amide position of the nicotinamide ring is a minor perturbation. 2D-IR studies of these analogs in water have demonstrated that it is an excellent probe of the dynamics of the water molecules that are solvating the azo moiety. In particular, PAAD is promising candidate as it has high molar absorvity and make it a viable general probes as this probe can even access the dynamics of enzymes with limited solubity.

We have probe the dynamics of FDH-Azide-PAAD complex, as a model case to understand the dynamical features of the active site with PAAD as a reporter and its perturbation to the enzyme active site. Our studies reveal that, PAAD do effect the FFCF of azide, which is an indication of perturbation in the system compared to FDH-Azide-NAD^+. However, both azide and PAAD, undergoes complete spectral diffusion in 10 ps , which means that FDH-Azide-PAAD still represents transitional state like FDH-Azide-NAD^+. This results also points out that the rigidity in the active site is not local by encompasses immediate vicinity of the active site. This conclusion is drawn from the fact that PAAD and azide are bound in different motifs within the active site and The FFCF of both have no static component.

The analogs, PAAD and azido-NAD, sets the ground work for exhaustive and intensive studies on enzyme dynamics. In FDH, itself several pertinent investigations have to be considered. The first measurements

should be KIEs with these analogs, which will indicate the extent of the hydrogen tunneling, and its temperature dependence will determine the change in the active site fluctuations and their effect on KIEs. We can then directly measure the change of dynamics of the active site at different temperature by 2D-IR, using a temperature controlled sample cell. As such, these two techniques will thus complement each other in establishing a connection between the kinetics, structure and dynamics.

The analogs will also allow us to understand the dynamical implication at the active site by introducing site-specific mutations. Such, mutation studies will help us understand the role of coupled networks that is invoked to understand the function of many enzymes. In addition, the subpicosecond contributions to the FFCF that we observe in each complex are of similar time scales and may reflect the kind of compressive active-site motions that is invoked in reactions where gating is necessary to modulate the donor-acceptor distance and that are believed to be present in the enzyme even if such motions do not influence the temperature dependence of the KIE, as is in these complexes. Such hypothesis can be tested by doing mutation. Another possibility is to systematically study the active site with PAAD or azido NAD^+ by binding the active site with various other binding partners in lieu of azide and look for any familiar trend in the active site. The introduction of analogs can be thought to be an external mutation of the enzyme. So, the effects of using different analogs in the same enzyme can help us to understand the dynamical characteristics of active site. PAAD also gives us a unique handle to understand the effect of dynamics by increasing the chain length of methelene linker connecting the azido moiety to nicotinamide ring. It is also possible to study the implication in dynamics of having different mid-IR probe substituted in place of the azido group in

PAAD or azido-NAD^+. Chromophores like thiocyanate can also extend our time window to observe dynamics. These experiments are not limited for FDH and can be easily extended to other NAD-dependent enzymes

An important aspect of these analogs is their generality to probe enzyme active site. We have shown that azido–NAD^+, can bind across several NAD- dependent enzymes. It can envisaged that PAAD should show similar trend. This means that we can possible accesses numerous NAD-dependent enzymes and understand the dynamical trends if any, both with ground and transitional state analogs. PAAD is particularly promising as it has high molar absorvity and can access enzymes which have low solubility. The synthetic procedure used to make these analogs can be used to synthesize similar NADP analogs. This will allow us to NADP- dependent enzymes specifically DHFR. A lot of computational, structural and experimental data has been accumulated on this enzyme. So, a direct measurement of active site dynamics by 2D-IR will help us to understand the connection between protein motions and its efficiency as a catalyst.

The role of NAD^+ is not restricted as a coenzyme. Recent observations show that NAD plays an important role in cellular signaling. So, using analogs of NAD^+ can serve as an IR marker to understand the intricate cell functions. With new imaging techniques, it will be possible to have a real-time analysis of biological systems using these analogs as a contrasting agent.

In conclusion, we have shown that analogs of NAD^+ can be potential candidates to understand the relatively unexplored femtosecond to picoseconds dynamics of enzyme active site. Studies of PAAD with model enzyme FDH, shows us interesting dynamics in the active site in timescales of few hundred femtoseconds to couple of picoseconds. As NAD^+ are

ubiquitous coenzymes, these studies can be extended to numerous NAD-dependent systems. Similar strategy to convert a cofactor to a suitable mid-IR probe can potentially be used to access the dynamics of other enzymes.

BIBLIOGRAPHY

1. Jencks, W. P., *Catalysis in Chemistry and Enzymology (McGraw-Hill Series in Advanced Chemistry)*. 1969; 644 pp.

2. Boehr, D. D.; McElheny, D.; Dyson, H. J.; Wright, P. E., The Dynamic Energy Landscape of Dihydrofolate Reductase Catalysis. *Science* **2006,** 313, (5793), 1638-1642.

3. Nagel, Z. D.; Klinman, J. P., Tunneling and Dynamics in Enzymatic Hydride Transfer. *Chemical Reviews* **2006,** 106, (8), 3095.

4. Kohen, A., Kinetic isotope effects as probes for hydrogen tunneling, coupled motion and dynamics contributions to enzyme catalysis. *Progress in Reaction Kinetics and Mechanism* **2003,** 28, (2), 119-156.

5. Kohen, A., Current issues in enzymatic hydrogen transfer from carbon: tunneling and coupled motion from kinetic isotope effect studies. *Hydrogen-Transfer React.* **2007,** 4, 1311-1340.

6. Henzler-Wildman, K. A.; Lei, M.; Thai, V.; Kerns, S. J.; Karplus, M.; Kern, D., A hierarchy of timescales in protein dynamics is linked to enzyme catalysis. *Nature* **2007,** 450, (7171), 913.

7. Hilt, W.; Pfleiderer, G.; Fortnagel, P., Glucose dehydrogenase from Bacillus subtilis expressed in Escherichia coli. I: Purification, characterization and comparison with glucose dehydrogenase from Bacillus megaterium. *Biochim. Biophys. Acta, Protein Struct. Mol. Enzymol.* **1991,** 1076, (2), 298-304.

8. Yahashiri, A.; Howell Elizabeth, E.; Kohen, A., Tuning of the H-transfer coordinate in primitive versus well-evolved enzymes. *Chemphyschem: a European journal of chemical physics and physical chemistry* **2008,** 9, (7), 980-2.

9. Koshland, D. E., Jr., Correlation Of Structure And Function In Enzyme Action. *Science (New York, N.Y.)* **1963,** 142, 1533-41.

10. Ringe, D.; Petsko, G. A., How enzymes work. *Science (Washington, DC, United States)* **2008,** 320, (5882), 1428-1429.

11. Fersht, A., *Enzymes: Structures and Reaction Mechanisms*. 1983; 350 pp.

12. McElheny, D.; Schnell, J. R.; Lansing, J. C.; Dyson, H. J.; Wright, P. E., Defining the role of active-site loop fluctuations in dihydrofolate reductase catalysis. *Proceedings of the National Academy of Sciences of the United States of America* **2005,** 102, (14), 5032-5037.

13. Hammes-Schiffer, S., Hydrogen tunneling and protein motion in enzyme reactions. *Accounts of Chemical Research* **2006,** 39, (2), 93-100.

14. Sen, A.; Kohen, A., Enzymatic tunneling and kinetic isotope effects: chemistry at the crossroads. *Journal of Physical Organic Chemistry* 23, (7), 613-619.

15. Sen, A.; Kohen, A., Quantum effects in enzyme kinetics. *Quantum Tunnelling in Enzyme-Catalysed Reactions* **2009**, 161-178.

16. Prakash, M. K.; Marcus, R. A., An interpretation of fluctuations in enzyme catalysis rate, spectral diffusion, and radiative component of lifetimes in terms of electric field fluctuations. *Proceedings of the National Academy of Sciences of the United States of America* **2007,** 104, (41), 15982-15987.

17. Marcus, R. A., Enzymatic catalysis and transfers in solution. I. Theory and computations, a unified view. *The Journal of chemical physics* **2006,** 125, (19), 194504.

18. Antoniou, D.; Schwartz, S. D., Internal Enzyme Motions as a Source of Catalytic Activity: Rate-Promoting Vibrations and Hydrogen Tunneling. *The Journal of Physical Chemistry B* **2001,** 105, (23), 5553.

19. Mincer, J. S.; Schwartz, S. D., A Computational Method to Identify Residues Important in Creating a Protein Promoting Vibration in Enzymes. *The Journal of Physical Chemistry B* **2002,** 107, (1), 366.

20. Schwartz, S. D., Vibrationally enhanced tunneling and kinetic isotope effects of enzymatic reactions. *Isotope Effects in Chemistry and Biology* **2006**, 475-498.

21. Agarwal, P. K., Role of Protein Dynamics in Reaction Rate Enhancement by Enzymes. *Journal of the American Chemical Society* **2005,** 127, (43), 15248.

22. Agarwal, P. K., Enzymes: an integrated view of structure, dynamics and function.*Microbial Cell Factories* **2006,** 5, 1-12.

23. Hunt, N. T., Ultrafast 2D-IR spectroscopy-method and applications. *Spectroscopy Europe* **2008,** 20, (2), 7-10.

24. Ge, N.-H.; Hochstrasser, R. M., Femtosecond two-dimensional infrared spectroscopy: IR-COSY and THIRSTY. *PhysChemComm [online computer file]* **2002**, 17-26.

25. Billington, R. A.; Bruzzone, S.; De Flora, A.; Genazzani, A. A.; Koch-Nolte, F.; Ziegler, M.; Zocchi, E., Emerging functions of extracellular pyridine nucleotides. *Molecular Medicine (Manhasset, NY, United States)* **2006,** 12, (11-12), 324-327.

26. Berger, F.; Lau, C.; Ziegler, M., Regulation of poly(ADP-ribose) polymerase 1 activity by the phosphorylation state of the nuclear NAD biosynthetic enzyme NMN adenylyltransferase 1. *Proceedings of the National Academy of Sciences of the United States of America* **2007,** 104, (10), 3765-3770.

27. Ziegler, M., New functions of a long-known molecule emerging roles of NAD in cellular signaling. *European Journal of Biochemistry* **2000,** 267, (6), 1550-1564.

28. Koch-Nolte, F.; Haag, F.; Guse Andreas, H.; Lund, F.; Ziegler, M., Emerging roles of NAD+ and its metabolites in cell signaling. *Science signaling* **2009,** 2, (57), mr1.

29. Woenckhaus, C.; Jeck, R.; Avramovic, O., Pyridine Nucleotide Coenzymes. *Coenzyme and cofactors* **1987,** II, 499-568.

30. Tonooka, S., Enzymatic-Synthesis Of Pyridine-Nucleotides - Structural Property Of Some New Nad-Analogs, And Base Conditions Available For The Analog Formation. *Bulletin Of The Chemical Society Of Japan* **1982,** 55, (5), 1531-1537.

31. Woenckhaus, C.; Jeck, R., Specific Modification Of Alcohol-Dehydrogenase By Nad Analogs. *Hoppe-Seylers Zeitschrift Fur Physiologische Chemie* **1976,** 357, (3), 287-287.

32. Winne, C. R.; Lepoivre, J. A.; Alderweireldt, F. C., Synthesis Of Nad+ Analogs.1. 3 - Benzoylpyridine Nucleoside. *Bulletin Des Societes Chimiques Belges* **1980,** 89, (1), 67-70.

33. Sawanishi, H.; Tajima, K.; Tsuchiya, T., Studies on diazepines. XXVIII. Syntheses of 5H-1,3-diazepines and 2H-1,4-diazepines from 3-azidopyridines. *Chem. Pharm. Bull.* **1987,** 35, (10), 4101-9.

34. Hixson, S. S.; Hixson, S. H., *Photochemistry and Photobiology* **1973,** 18, (2), 135-138.

35. Ziegenhorn, J.; Senn, M.; Buecher, T., Molar absorptivities of beta -NADH and beta -NADPH. *Clinical Chemistry (Washington, DC, United States)* **1976,** 22, (2), 151-60.

36. Plapp, B. V., Catalysis by alcohol dehydrogenases. *Isotope Effects in Chemistry and Biology* **2006**, 811-835.

37. Braenden, C. I.; Eklund, H.; Zeppezauer, E.; Samama, J. P.; Plapp, B., Structure and mechanism of alcohol dehydrogenase. *Proceedings of the FEBS Meeting* **1979,** 52, (Protein: Struct., Funct. Ind. Appl.), 15-23.

38. Jeck, R.; Scholze, M.; Tischlich, A.; Woenckhaus, C.; Zimmermann, J., New reactive coenzyme analogs for affinity labeling of NAD+ and NADP+ dependent dehydrogenases. *Zeitschrift fuer Naturforschung, C: Biosciences* **1995,** 50, (7/8), 476-86.

39. Schultz, R. M.; Groman, E. V.; Engel, L. L., 3(17)beta-Hydroxysteroid Dehydrogenase of Pseudomonas testosteroni. Ligand binding properties. *The Journal of biological chemistry* **1977,** 252, (11), 3784-90.

40. Neilands, J. B., Lactic dehydrogenase of heart. I. Purity, kinetics, and equilibria. *Journal of Biological Chemistry* **1952,** 199, 373-81.

41. Mueggler, P. A.; Wolfe, R. G., Malate dehydrogenase. Kinetic studies of substrate activation of supernatant enzyme by L-malate. *Biochemistry* **1978,** 17, (22), 4615-20.

42. Telegdi, M.; Wolfe, D. V.; Wolfe, R. G., Malate dehydrogenase. XII. Initial rate kinetic studies of substrate activation of porcine mitochondrial enzyme by malate. *Journal of Biological Chemistry* **1973,** 248, (18), 6484-9.

43. Wolfe, R. G.; Raval, D. N., Chemical and kinetic properties of pig heart mitochondrial malic dehydrogenase. *Mech. Action Dehydrogenases, Symp.* **1969**, 155-95.

44. Massey, V.; Gibson, Q. H., Reaction mechanism of lipoyl dehydrogenase employing rapid spectrophotometry. *Proceedings of the International Congress of Biochemistry* **1963,** 5, 157-73.

45. Veeger, C.; Massey, V., Reaction mechanism of lipoamide dehydrogenase. II. Modification by trace metals. *:Biochimica et Biophysica Acta* **1962,** 64, 83-100.

46. Klinman, J. P., Linking protein structure and dynamics to catalysis: the role of hydrogen tunnelling. *Philosophical Transactions of the Royal Society, B: Biological Sciences* **2006,** 361, (1472), 1323-1331.

47. Kohen, A.; Klinman, J. P., Hydrogen tunneling in enzymes: Linking the role of protein dynamics to catalysis. *Hydrogen tunneling in Biology* **1999**,6, 191-198.

48. Kohen, A., Kinetic isotope effects as probes for hydrogen tunneling in enzyme catalysis. *Isotope Effects in Chemistry and Biology* **2006**, 743-764.

49. Wang, L.; Goodey, N. M.; Benkovic, S. J.; Kohen, A., Coordinated effects of distal mutations on environmentally coupled tunneling in dihydrofolate reductase. *Proceedings of the National Academy of Sciences of the United States of America* **2006,** 103, (43), 15753-15758.

50. Wang, L.; Goodey, N. M.; Benkovic, S. J.; Kohen, A., The role of enzyme dynamics and tunnelling in catalysing hydride transfer: studies of distal mutants of dihydrofolate reductase. *Philosophical Transactions of the Royal Society, B: Biological Sciences* **2006,** 361, (1472), 1307-1315.

51. Wang, L.; Tharp, S.; Selzer, T.; Benkovic, S. J.; Kohen, A., Effects of a distal mutation on active site chemistry. *Biochemistry* **2006,** 45, (5), 1383-1392.

52. Mukamel, S., Principles of nonlinear optical spectroscopy. **1997**.

53. Hammes-Schiffer, S., Impact of enzyme motion on activity. *Biochemistry* **2002**, 45,13335-13345.

54. Roca, M.; Moliner, V.; Tunon, I.; Hynes, J. T., Coupling between Protein and Reaction Dynamics in Enzymatic Processes: Application of Grote-Hynes Theory to Catechol O-Methyltransferase*: Journal of the American Chemical Society* **2006,** 128, (18), 6186-6193.

55. Kim, Y. S.; Hochstrasser, R. M., Applications of 2D IR Spectroscopy to Peptides, Proteins, and Hydrogen-Bond Dynamicsâ€. *The Journal of Physical Chemistry B* **2009,** 113, (24), 8231.

56. Merchant, K. A.; Thompson, D. E.; Xu, Q.-H.; Williams, R. B.; Loring, R. F.; Fayer, M. D., Myoglobin-CO Conformational Substate Dynamics: 2D Vibrational Echoes and MD Simulations. *Biophysical Journal* **2002,** 82, (6), 3277.

57. Fang, C.; Bauman, J. D.; Das, K.; Remorino, A.; Arnold, E.; Hochstrasser, R. M., Two-dimensional infrared spectra reveal relaxation of the nonnucleoside inhibitor TMC278 complexed with HIV-1 reverse transcriptase. *Proceedings of the National Academy of Sciences* **2008,** 105, (5), 1472-1477.

58. Finkelstein, I. J.; Ishikawa, H.; Kim, S.; Massari, A. M.; Fayer, M. D., Substrate binding and protein conformational dynamics measured by 2D-IR vibrational echo spectroscopy. *Proceedings of the National Academy of Sciences* **2007,** 104, (8), 2637-2642.

59. Ishikawa, H.; Finkelstein, I. J.; Kim, S.; Kwak, K.; Chung, J. K.; Wakasugi, K.; Massari, A. M.; Fayer, M. D., Neuroglobin dynamics observed with ultrafast 2D-IR vibrational echo spectroscopy. *Proceedings of the National Academy of Sciences* **2007,** 104, (41), 16116-16121.

60. Ishikawa, H.; Kim, S.; Kwak, K.; Wakasugi, K.; Fayer, M. D., Disulfide bond influence on protein structural dynamics probed with 2D-IR vibrational echo spectroscopy. *Proceedings of the National Academy of Sciences* **2007,** 104, (49), 19309-19314.

61. Kwak, K.; Park, S.; Finkelstein, I. J.; Fayer, M. D., Frequency-frequency correlation functions and apodization in two-dimensional infrared vibrational echo spectroscopy: A new approach. *Journal Of Chemical Physics* **2007,** 127.

62. Hill, S. E.; Bandaria, J. N.; Fox, M.; Vanderah, E.; Kohen, A.; Cheatum, C. M., Exploring the Molecular Origins of Protein Dynamics in the Active Site of Human Carbonic Anhydrase II. *The Journal of Physical Chemistry B* **2009,** 113, (33), 11505.

63. Finkelstein, I. J.; Zheng, J. R.; Ishikawa, H.; Kim, S.; Kwak, K.; Fayer, M. D., Probing dynamics of complex molecular systems with ultrafast 2D IR vibrational echo spectroscopy. *Physical Chemistry Chemical Physics* **2007,** 9, (13), 1533-1549.

64. Finkelstein, I. J.; Zheng, J.; Ishikawa, H.; Kim, S.; Kwak, K.; Fayer, M. D., Probing dynamics of complex molecular systems with ultrafast 2D IR vibrational echo spectroscopy. *Phys. Chem. Chem. Phys.* **2007,** 9, (13), 1533-1549.

65. Watney, J. B.; Agarwal, P. K.; Hammes-Schiffer, S., Effect of Mutation on Enzyme Motion in Dihydrofolate Reductase. *Journal of the American Chemical Society* **2003,** 125, (13), 3745-3750.

66. Kohen, A.; Klinman, J. P., Enzyme Catalysis: Beyond Classical Paradigms. *Accounts of Chemical Research* **1998,** 31, (7), 397-404.

67. Stojkovic, V.; Kohen, A., Enzymatic H transfers: quantum tunneling and coupled motion from kinetic isotope effect studies. *Israel Journal of Chemistry* **2009,** 49, (2), 163-173.

68. Allemann, R. K.; Evans, R. M.; Loveridge, E. J., Probing coupled motions in enzymatic hydrogen tunnelling reactions. *Biochemical Society Transactions* **2009,** 037, (2), 349-353.

69. Cha, Y.; Murray, C. J.; Klinman, J. P., Hydrogen tunneling in enzyme reactions. *Science* **1989,** 243, (4896), 1325-1330.

70. Bruno, W. J.; Bialek, W., Vibrationally enhanced tunneling as a mechanism for enzymic hydrogen transfer. *Biophysical Journal.* **1992,** 63, (3), 689-99.

71. Bialek, W.; Bruno, W. J.; Joseph, J.; Onuchic, J. N., Quantum and classical dynamics in biochemical reactions. *Photosynthesis Research* **1989,** 22, (1), 15-27.

72. Zheng, J.; Kwak, K.; Fayer, M. D., Ultrafast 2D IR Vibrational Echo Spectroscopy. *Accounts of Chemical Research* **2006,** 40, (1), 75.

73. Woys, A. M.; Lin, Y.-S.; Reddy, A. S.; Xiong, W.; de Pablo, J. J.; Skinner, J. L.; Zanni, M. T., 2D IR Line Shapes Probe Ovispirin Peptide Conformation and Depth in Lipid Bilayers. *Journal of the American Chemical Society* 132, (8), 2832.

74. Kim, Y. S.; Liu, L.; Axelsen, P. H.; Hochstrasser, R. M., 2D IR provides evidence for mobile water molecules in Î²-amyloid fibrils. *Proceedings of the National Academy of Sciences* **2009,** 106, (42), 17751-17756.

75. Mukherjee, P.; Kass, I.; Arkin, I. T.; Zanni, M. T., Picosecond dynamics of a membrane protein revealed by 2D IR. *Proceedings of the National Academy of Sciences of the United States of America* **2006,** 103, (10), 3528-3533.

76. Bandaria, J. N.; Dutta, S.; Hill, S. E.; Kohen, A.; Cheatum, C. M., Fast Enzyme Dynamics at the Active Site of Formate Dehydrogenase. *Journal of the American Chemical Society* **2007,** 130, (1), 22.

77. Popov, V. O.; Lamzin, V. S., *Biochemistry Journal* 301(Pt 3). 625–643.

78. Tishkov, V. I.; Popov, V. O., Catalytic mechanism and application of formate dehydrogenase. *Biochemistry* **2004,** 69, (11), 1252-1267.

79. Pauly, H. E.; Pfleiderer, G., Conformational and functional aspects of the reversible dissociation and denaturation of glucose dehydrogenase. *Biochemistry* **1977,** 16, (21), 4599.

80. Mitamura, T.; Urabe, I.; Okada, H., Enzymic properties of isozymes and variants of glucose dehydrogenase from Bacillus megaterium. *European Journal of Biochemistry* **1989,** 186, (1-2), 389-93.

81. Telegdi, M.; Wolfe, D. V.; Wolfe, R. G., Malate Dehydrogenase. *Journal of Biological Chemistry* **1973,** 248, (18), 6484-6489.

82. Naraharisetty, S. R. G.; Kurochkin, D. V.; Rubtsov, I. V., C-D Modes as structural reporters via dual-frequency 2DIR spectroscopy. *Chemical Physics Letters* **2007,** 437, (4-6), 262.

83. Keizo, Y.; Toshihiro, N.; Yasutaka, M.; Itaru, U.; Hirosuke, O., Characterization of Mutant Glucose Dehydrogenases with Increasing Stability *Annals of the New York Academy of Sciences* **1990,** 613, (Enzyme Engineering 10), 362-365.

84. Bandaria, J. N.; Cheatum, C. M.; Kohen, A., Examination of Enzymatic H-Tunneling through Kinetics and Dynamics. *Journal of the American Chemical Society* **2009,** 131, (29), 10151-10155.

85. Oyeyemi, O. A.; Sours, K. M.; Lee, T.; Resing, K. A.; Ahn, N.; Klinman, J. P., Temperature dependence of protein motions in a thermophilic dihydrofolate reductase and its relationship to catalytic efficiency. *Proceedings of the National Academy of Sciences of the United States of America, Early Edition*, (May 13 2010), 1-6.

86. Hay, S.; Evans, R. M.; Levy, C.; Loveridge, E. J.; Wang, X.; Leys, D.; Allemann, R. K.; Scrutton, N. S., Are the catalytic properties of enzymes from piezophilic organisms pressure adapted? *ChemBioChem* **2009,** 10, (14), 2348-2353.

87. Pang, J.; Hay, S.; Scrutton, N. S.; Sutcliffe, M. J., Deep Tunneling Dominates the Biologically Important Hydride Transfer Reaction from NADH to FMN in Morphinone Reductase. *Journal of the American Chemical Society* **2008,** 130, (22), 7092-7097.

88. Dybala-Defratyka, A.; Paneth, P.; Truhlar, D. G., Quantum catalysis in enzymes. *Quantum Tunnelling Enzyme-Catal. React. Quantum Tunnelling in Enzyme-Catalysed Reactions* **2009**, 36-78.

89. Massari, A. M.; Finkelstein, I. J.; Fayer, M. D., Dynamics of Proteins Encapsulated in Silica Sol-Gel Glasses Studied with IR Vibrational Echo Spectroscopy. *Journal of the American Chemical Society* **2006,** 128, (12), 3990-3997.

90. Massari Aaron, M.; Finkelstein Ilya, J.; McClain Brian, L.; Goj, A.; Wen, X.; Bren Kara, L.; Loring Roger, F.; Fayer Michael, D., The influence of aqueous versus glassy solvents on protein dynamics: vibrational echo experiments and molecular dynamics simulations. *Journal of the American Chemical Society* **2005,** 127, (41), 14279-14289.

91. Tucker Matthew, J.; Getahun, Z.; Nanda, V.; DeGrado William, F.; Gai, F., A new method for determining the local environment and orientation of individual side chains of membrane-binding peptides. *Journal of the American Chemical Society* **2004,** 126, (16), 5078-9.

92. Getahun, Z.; Huang, C.-Y.; Wang, T.; De Leon, B.; DeGrado, W. F.; Gai, F., Using nitrile-derivatized amino acids as infrared probes of local environment. *Journal of the American Chemical Society* **2003,** 125, (2), 405-411.

93. Waegele, M. M.; Tucker, M. J.; Gai, F., 5-Cyanotryptophan as an infrared probe of local hydration status of proteins. *Chemical Physics Letters* **2009,** 478, (4-6), 249-253.

94. Jimenez, R.; Salazar, G.; Yin, J.; Joo, T.; Romesberg, F. E., Protein dynamics and the immunological evolution of molecular recognition. *Proceedings of the National Academy of Sciences of the United States of America* **2004,** 101, (11), 3803-3808.

95. Naraharisetty, S. R. G.; Kasyanenko, V. M.; Zimmermann, J.; Thielges, M. C.; Romesberg, F. E.; Rubtsov, I. V., C-D Modes of Deuterated Side Chain of Leucine as Structural Reporters via Dual-frequency Two-dimensional Infrared Spectroscopy. *Journal of Physical Chemistry B* **2009,** 113, (14), 4940-4946.

96. Kinnaman, C. S.; Cremeens, M. E.; Romesberg, F. E.; Corcelli, S. A., Infrared line shape of an alpha -carbon deuterium-labeled amino acid. *Journal of the American Chemical Society* **2006,** 128, (41), 13334-13335.

97. Zimmermann, J.; Gundogdu, K.; Cremeens, M. E.; Bandaria, J. N.; Hwang, G. T.; Thielges, M. C.; Cheatum, C. M.; Romesberg, F. E., Efforts toward Developing Probes of Protein Dynamics: Vibrational Dephasing and Relaxation of Carbon-Deuterium Stretching Modes in Deuterated Leucine. *Journal of Physical Chemistry B* **2009,** 113, (23), 7991-7994.

98. Elving, P. J.; Bresnahan, W. T.; Moiroux, J.; Samec, Z., NAD/NADH as a model redox system: Mechanism, mediation, modification by the environment. *Bioelectrochemistry and Bioenergetics* **1982,** 9, (3), 365.

99. Chaykin, S., Nicotinamide Coenzymes. *Annual Review of Biochemistry* **1967,** 36, (1), 149-170.

100. Anderson, B. M.; Anderson, C. D., Properties and applications of immobilized snake venom NAD glycohydrolase. *Analytical biochemistry* **1984,** 140, (1), 250-255.

101. Xu, G. Q.; Zou, C. G., Nad+ Analogs In Formation Of New Fluorophores On Ultraviolet-Irradiation With D-Glyceraldehyde-3-Phosphate Dehydrogenase. *Scientia Sinica Series B-Chemical Biological Agricultural Medical & Earth Sciences* **1982,** 25, (2), 152-159.

102. Niekamp, C. W.; Hinz, H. J.; Jaenicke, R.; Woenckhaus, C., Thermal Interactions Of Lactate-Dehydrogenase With Nad Analogs. *Hoppe-Seylers Zeitschrift Fur Physiologische Chemie* **1977,** 358, (3), 284-284.

103. Samama, J. P.; Marchalrosenheimer, N.; Biellmann, J. F.; Rossmann, M. G., An Investigation Of The Active-Site Of Lactate-Dehydrogenase With Nad+ Analogs. *European Journal Of Biochemistry* **1981,** 120, (3), 563-569.

104. Gruber, B. A.; Leonard, N. J., Dynamic and static quenching of 1,N6-ethenoadenine fluorescence in nicotinamide 1,N6-ethenoadenine dinucleotide and in 1,N6-etheno-9-(3-(indol-3-yl) propyl) adenine. *Proceedings of the National Academy of Sciences of the United States of America* **1975,** 72, (10), 3966-3969.

105. Hingorani, V. N.; Chang, L. F. H.; Ho, Y. K., Chemical modification of bovine transducin: probing the GTP-binding site with affinity analogs. *Biochemistry* **1989,** 28, (18), 7424-32.

106. Kim, H.; Haley, B. E., Synthesis and properties of 2-azido-NAD+. A study of interaction with glutamate dehydrogenase. *The Journal of biological chemistry* **1990,** 265, (7), 3636-41.

107. Kwak, K.; Zheng, J. R.; Cang, H.; Fayer, M. D., Ultrafast two-dimensional infrared vibrational echo chemical exchange experiments and theory. *Journal Of Physical Chemistry B* **2006,** 110, (40), 19998-20013.

108. Li, S.; Schmidt, J. R.; Skinner, J. L., Vibrational energy relaxation of azide in water. *Journal of Chemical Physics* **2006,** 125, (24), 244507/1-244507/8.

109. Li, S.; Schmidt, J. R.; Piryatinski, A.; Lawrence, C. P.; Skinner, J. L., Vibrational Spectral Diffusion of Azide in Water. *Journal of Physical Chemistry B* **2006,** 110, (38), 18933-18938.

110. Wade-Jardetzky, N. G.; Jardetzsky, O., The Conformation of Pyridine Dinucleotide in Solution. *The Journal of Biological Chemistry* **1966,** 241, (1), 85-91.

111. Benkovic, S. J.; Hammes-Schiffer, S., Enzyme motions inside and out. *Science (Washington, DC, U. S.)* **2006,** 312, (5771), 208-209.

112. Hammes-Schiffer, S.; Benkovic, S. J., Relating protein motion to catalysis. *Annu. Rev. Biochem.* **2006,** 75, 519-541.

113. Hammes-Schiffer, S.; Watney, J. B., Hydride transfer catalysed by Escherichia coli and Bacillus subtilis dihydrofolate reductase: coupled motions and distal mutations. *Philosophical Transactions of the Royal Society, B: Biological Sciences* **2006,** 361, (1472), 1365-1373.

114. Park, S.; Kwak, K.; Fayer, M. D., Ultrafast 2D-IR vibrational echo spectroscopy: a probe of molecular dynamics. *Laser Physics Letters* **2007,** 4, 704-718.

115. Hunt, N. T., 2D-IR spectroscopy: ultrafast insights into biomolecule structure and function. *Chemical Society Reviews* **2009,** 38, (7), 1837-1848.

116. Zheng, J.; Kwak, K.; Fayer, M. D., Ultrafast 2D IR vibrational echo spectroscopy. *Accounts Of Chemical Research* **2007,** 40, (1), 75-83.

117. Fayer, M. D., Dynamics of Liquids, Molecules, and Proteins Measured with Ultrafast 2D IR Vibrational Echo Chemical Exchange Spectroscopy. *Annual Review Of Physical Chemistry* **2009,** 60, 21-38.

118. Bandaria, J. N.; Dutta, S.; Hill, S. E.; Kohen, A.; Cheatum, C. M., Fast Enzyme Dynamics at the Active Site of Formate Dehydrogenase. *Journal of the American Chemical Society* **2008,** 130, (1), 22-23.

119. Walter, P., Preparation And Properties Of Methyl And Amino Nicotinamide Substituted Nad Analogs. *Federation Proceedings* **1962,** 21, (2), 240.

120. Pietta, P. G.; Mauri, P. L.; Pace, M.; Agnellini, D., Monitoring The Preparation Of Nad Analogs By Reversed-Phase High-Performance Liquid-Chromatography. *Chromatographia* **1988,** 25, (6), 543-544.

121. Golovatsky, I. D.; Grivnak, L. M.; Gashpar, E. D., The Activity Of Lactate-Dehydrogenase In The Presence Of Certain Structural Analogs Of The Nad Nicotinamide Fragment. *Ukrainskii Biokhimicheskii Zhurnal* **1982,** 54, (1), 21-25.

122. Freyne, E. J.; Esmans, E. L.; Lepoivre, J. A.; Alderweireldt, F. C., Studies On Nad+ Analogs.1. Synthesis And Conformation Of 3-Ac-5-Alkylpyad+. *Journal Of Carbohydrates-Nucleosides-Nucleotides* **1981,** 8, (6), 481-494.

123. Freyne, E. J.; Esmans, E. L.; Vanosselaer, T. O.; Lepoivre, J. A.; Alderweireldt, F. C., Studies On Nad+ Analogs.2. Purification By Hplc And Enzymatic-Activity Of 3-Ac-5-Alkylpyad+. *Journal Of Carbohydrates-Nucleosides-Nucleotides* **1981,** 8, (6), 537-545.

124. Windman, I., 3-Acetyl Pyridine Analog Of Nad In Bcnu-Treated Ehrlich Ascites Tumor-Cells. *Israel Journal Of Medical Sciences* **1981,** 17, (6), 485-485.

125. Dutta, S.; Cook, R. J.; Amnon., K.; Cheatum, C., Characterization of azo-NAD+ to assess its potential as a 2D IR probe of enzyme dynamics. *Analytical biochemistry* **2010**.

126. Goldstein, B. M.; Colby, T. D., Conformational constraints in NAD analogs: implications for dehydrogenase binding and specificity. *Advances in Enzyme Regulation* **2000,** 40, (1), 405.

127. Nagel, Z. D.; Klinman, J. P., A 21st century revisionist's view at a turning point in enzymology. *Nature Chemical Biology* **2009,** 5, (8), 543-550.

128. Benkovic, S. J.; Hammes-Schiffer, S., Dihydrofolate reductase: hydrogen tunneling and protein motion. *Hydrogen-Transfer Reactions* **2007,** 4, 1439-1454.